Lectures on Bound states*

Paul Hoyer
Department of Physics, POB 64, FIN-00014 University of Helsinki, Finland

Even a first approximation of bound states requires contributions of all powers in the coupling. This means that the concept of "lowest order bound state" needs to be defined. In these lectures I discuss the "Born" (no loop, lowest order in $\hbar$) approximation. Born level states are bound by gauge fields which satisfy the classical field equations.

As a check of the method, Positronium states of any momentum are determined as eigenstates of the QED Hamiltonian, quantized at equal time. Analogously, states bound by a strong external field $A^\mu(\boldsymbol{x})$ are found as eigenstates of the Dirac Hamiltonian. Their Fock states have dynamically created e^+e^- pairs, whose distribution is determined by the Dirac wave function. The linear potential of $D = 1 + 1$ dimensions confines electrons but repels positrons. As a result, the mass spectrum is continuous and the wave functions have features of both bound states and plane waves.

The classical solutions of Gauss' law are explored for hadrons in QCD. A non-vanishing boundary condition at spatial infinity generates a constant $\mathcal{O}\left(\alpha_s^0\right)$ color electric field between quarks of specific colors. Poincaré invariance limits the spectrum to color singlet $q\bar{q}$ and qqq states, which do not generate an external color field. This restricts the $\mathcal{O}\left(\alpha_s^0\right)$ interactions between hadrons to string breaking dynamics as in dual diagrams. Light mesons lie on linear Regge and parallel daughter trajectories. There are massless states which may be significant for chiral symmetry breaking. Since the bound states are defined at equal time in all frames they have a non-trivial Lorentz covariance.

arXiv:1605.01532v1 [hep-ph] 5 May 2016

Contents

I. Introduction and Summary 3

1. Basics of bound state perturbation theory 3
2. Bound state Born term 5
3. Positronium bound by its classical gauge field 6
4. Dirac states 7
5. Application to hadrons in QCD 7
6. Hadrons at tree level 8

II. Positronium at Born level 8

1. State definition 8
2. Classical Gauge Field 10
3. The Hamiltonian 10
4. Schrödinger Equation for Positronium in motion 11

III. Dirac states 12

A. General analysis 12

1. Dirac equation and wave function 13
2. Dirac states [18] 13
3. The vacuum state 15

B. Dirac states in $D = 1 + 1$ dimensions 16

1. Wave function 16

* Based on lectures presented during 2014-15 at NIKHEF, Amsterdam; IPhT Saclay; CP^3, Odense; GSI, Darmstadt; Bloomington, IN and Subatech, Nantes.

2. Continuous spectrum 17
3. Relative amount of valence and sea 18
4. The electron and positron distributions 19
5. Case of $m = 0$ 21

IV. Features of hadrons 22
1. General remarks 22
2. Perturbative aspects of the hadron spectrum 22
3. Duality 24
4. $\alpha_s(Q^2)$ at low scales Q 25

V. QCD Bound States in the rest frame 26
A. The meson and baryon states 26
B. Symmetries: Poincaré, Parity and Charge Conjugation for Mesons 26
1. Space translations 26
2. Rotations 27
3. Parity 28
4. Charge conjugation 28
C. The confining field $\mathcal{A}^\mu$ 29
1. Requirements on a viable solution 29
2. Field energy of the meson component (5.36) 30
3. Field energy of the baryon component (5.37) 31
D. The bound state equations ($\boldsymbol{P} = 0$) 32
1. The meson confining potential 32
2. The baryon confining potential 32
3. Meson bound state equation 33
4. Baryon bound state equation 33

VI. Rest frame meson wave functions 34
A. $D = 1 + 1$ dimensions 34
1. Analytic solution 34
2. Non-relativistic and relativistic limits 35
3. Discrete spectrum 36
4. Duality 37
B. Mesons in $D = 2 + 1$ dimensions 40
1. Bound state equation 40
2. Wave function in the $r \to \infty$ limit 41
3. Spectrum in $D = 2 + 1$ 41
C. Mesons in $D = 3 + 1$ dimensions 43
1. Quantum numbers 43
2. π trajectory 43

3. a_1 trajectory 44
4. ρ trajectory 45
D. Chiral symmetry 47
1. Chiral transformations 47
2. Chiral properties of the bound state solutions 47
3. Massless bound states 49

VII. Frame dependence 50
A. Mesons with $\boldsymbol{P} \neq 0$ in $D = 1 + 1$ dimensions 51
1. QED_2 bound states with $A^1 = 0$ 51
2. QED_2 bound states with a boosted classical gauge field 52
B. Mesons with $\boldsymbol{P} \neq 0$ in $D = 2 + 1$ and $D = 3 + 1$ dimensions 54
1. The bound state equation 54
2. An ansatz for the boost property of meson wave functions 54

VIII. What's new – and what's next? 56
1. QED bound states of lowest order in $\hbar$ 56
2. Dirac states vs. wave functions 56
3. Confinement from an $\mathcal{O}\left(\alpha_s^0\right)$ classical gluon field 56
4. Hadron spectra 57
5. Boost covariance 57
6. String breaking and hadron loops 57
7. Scattering amplitudes 57

Acknowledgments 58

References 58

I. INTRODUCTION AND SUMMARY

Perturbation theory is a central tool in studies of the Standard Model of particle physics. Basic principles, *e.g.*, analyticity and the factorization of hard QCD subprocesses, are supported by generic properties of Feynman diagrams. Scattering amplitudes are generally well approximated by contributions of low order in the coupling.

Bound states are different: No Feynman diagram has a bound state pole. Bound states are generated by the *divergence* of the perturbative expansion.

1. Basics of bound state perturbation theory

Introductory Quantum Mechanics describes the Hydrogen atom by postulating the Schrödinger equation with the classical potential $V(r)$,

$$V(r) = -\alpha/r \qquad \Phi_0(r) = N \exp(-\alpha\, m\, r) \tag{1.1}$$

The wave function $\Phi_0(r)$ is exponential in α, whereas Feynman diagrams are of fixed order in α. It is important to understand how the QM description of bound states emerges from the underlying Quantum Field Theory (QED) [1].

Why does the perturbative expansion diverge for bound states – no matter how small is α? The typical momentum transfer between the atomic constituents is of the order of the inverse atomic radius, $p \sim \alpha m$. This Bohr momentum scale brings powers of α into the denominators of electron and photon propagators. They can balance the powers of α from the vertices.

It is straightforward to verify[1] that in the $e^+e^- \to e^+e^-$ amplitude the powers of α balance for the "ladder" diagrams in Fig. 1 (and only for them). As indicated, the sum can be expressed as a convolution between single photon exchange and the amplitude itself. This is called a "Dyson-Schwinger equation".

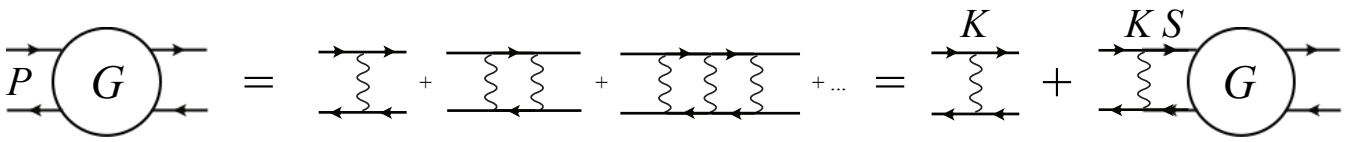

FIG. 1: For momentum transfers $p = \mathcal{O}(\alpha m)$ the leading contribution to the $e^+e^- \to e^+e^-$ scattering amplitude (left) comes from ladder diagrams (middle). Their sum can be expressed as a convolution between single photon exchange and the scattering amplitude itself (right). This gives the "Dyson-Schwinger equation" (1.3) for the $e^+e^- \to e^+e^-$ amplitude.

The loop integrals in the ladder diagrams range over all momenta p. Only loop momenta $p \sim \alpha m$ contribute at leading order. The intermediate e^+e^- propagators may then be treated as being on-shell. This reduces the ladder sum to a geometric sum of single photon exchange amplitudes, analogous to the familiar

$$G(x) = x + x^2 + x^3 + \ldots = x + xG(x) \qquad \Longrightarrow \qquad G(x) = \frac{x}{1-x} \tag{1.2}$$

The pole of $G(x)$ at $x = 1$ is analogous to a bound state pole. More precisely, let $G(P)$ be the Green function of total momentum P with external propagators removed, K the similarly truncated single photon exchange amplitude and S the two-particle (e^+e^-) propagator. Then the Dyson-Schwinger equation of Fig. 1 is

$$G(P) = K + KS\,K + KS\,KSK + \ldots = K + K\,S\,G(P) \tag{1.3}$$

Each product denotes a convolution integral over the relative momentum between the e^+ and the e^-. Let $G(P)$ have a bound state pole at $P^0 = E_n$, where $E_n = \sqrt{M_n^2 + \boldsymbol{P}^2}$ is the energy of the bound state. On general grounds the residue of the pole is the product of the bound state wave functions Φ_n for the initial and final states. Because neither K nor S have bound state poles the Dyson-Schwinger relation (1.3) implies a "Bethe-Salpeter" equation for the wave function shown in Fig. 2(b),

$$G(P) = \frac{\Phi_n \Phi_n^\dagger}{P^0 - E_n} + \ldots \qquad \Longrightarrow \qquad \Phi_n = K\,S\,\Phi_n \tag{1.4}$$

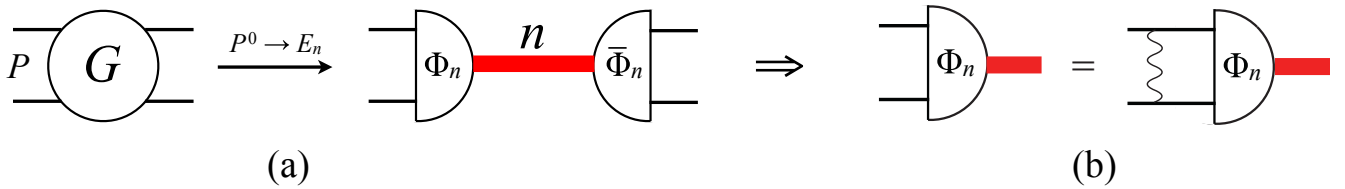

FIG. 2: (a) The residue of a bound state pole in a scattering amplitude G factorizes into a product of wave functions for the initial and final state. (b) The Dyson-Schwinger relation in Fig. 1 implies a "Bethe-Salpeter equation" for the wave function.

The Bethe-Salpeter equation is based on Feynman diagrams and thus explicitly Lorentz covariant. In the rest frame it reduces to the Schrödinger equation in the limit $\alpha \to 0$. Loop corrections to the single photon exchange kernel K and to the two-particle propagator S can be added perturbatively. In this way the Bethe-Salpeter equation provides an in principle exact, Lorentz-covariant framework for field theory calculations of bound states. Many topical studies of QCD and hadron physics are based on the Dyson-Schwinger equations [3].

---

[1] See, for example, section II A of my previous lecture notes [2]. Those notes give more details also on other issues mentioned here.

Explicit Lorentz covariance is very helpful in evaluating scattering amplitudes, but has turned out to complicate bound state calculations. In the bound state rest frame the momentum transfers are $|\boldsymbol{p}| \sim \alpha\, m$ and $p^0 \sim \alpha^2 m$. The photon propagator $\sim 1/p^2 \simeq -1/\boldsymbol{p}^2$ is thus independent of p^0 at lowest order: The interaction is instantaneous in time. This simplification is specific to the rest frame, in a general frame $p^0 \sim |\boldsymbol{p}| \propto \alpha\, m$. In a Lorentz covariant formulation we must therefore keep the p^0 dependence of the propagator. This makes the equation hard to solve – in fact no analytic solution of the Bethe-Salpeter equation is known, even for a single photon exchange kernel. The calculation of higher order corrections is progressively more difficult [4].

For reasons such as this the Bethe-Salpeter framework is impractical in precision calculations of atomic structure. The preferred method is Non-Relativistic QED (NRQED), which is an effective field theory based on expanding the QED action in powers of $|\boldsymbol{p}|/m$ [5]. At lowest order this gives the Schrödinger equation of Introductory QM. NRQED is applicable only in the rest frame of the bound state, but this is sufficient to determine energy levels. Positronium hyperfine structure at $\mathcal{O}\left(\alpha^7 \log \alpha\right)$ provides one of the most stringent tests of the Standard Model [6].

2. Bound state Born term

We have seen that already the first approximation of a bound state wave function (1.1) requires all powers of α. The higher order corrections are also expressed as powers of α. This makes the choice of the first approximation ambiguous. We can apparently rearrange the infinite series by moving some of the "higher order corrections" into the "lowest order", or *vice versa*. We already saw a hint of this in the handling of the p^0 dependence of the single photon exchange kernel.

It turns out that the Dyson-Schwinger equation can be formulated in many equivalent ways [1]. In its exact version the equation contains power series in α for both the kernel K and the two-particle propagator S. Either of the expansions can be freely chosen, then the other one is fixed by the known expansion of the Green function G.

In considering this ambiguity it is helpful to recall a more familiar situation where the perturbative expansion diverges even more dramatically than for Positronium: Classical E &M. Phenomena well described by classical electromagnetic fields involve very low momentum transfers, $|\boldsymbol{p}| \ll \alpha\, m$. In this regime the relevant degrees of freedom are not individual photons but their collective fields, which obey Maxwell's equations. The classical dynamics is unambiguous.

Classical field theory emerges in the $\hbar \to 0$ limit of the quantum theory. The Green function of a scalar field is in the functional integral formulation given by

$$G(x_1, \ldots, x_n) = \int [d\varphi]\, \exp\left(iS[\varphi]/\hbar\right) \varphi(x_1) \ldots \varphi(x_n) \tag{1.5}$$

The main contribution to the functional integral in the $\hbar \to 0$ limit is from classical field configurations for which the action is stationary, $\delta S[\varphi]/\delta\varphi = 0$. Fluctuations of the field φ around the classical configurations are suppressed by powers of $\hbar$. They correspond to loop corrections in the perturbative expansion.

The $\hbar$ expansion seems equivalent to the expansion in α: Each loop correction brings one power of $\hbar$ and one of α [7]. However, the $\hbar$ and α powers do not match in the lowest order (Born) term. Tree-level Feynman diagrams have no loops, whereas their power of α depends on the number of external legs. A bound state is built from repeated scattering and thus has an unlimited number of external legs. The geometric sum of single photon exchange amplitudes in Fig. 1 is equivalent to a sum of $\mathcal{O}\left(\hbar^0\right)$ tree diagrams, it has no loop contributions but all powers of α. A loop correction to the ladder diagrams does bring a factor $\hbar\alpha$.

The functional integral (1.5) provides a physically motivated definition of "lowest order" bound states: They are of lowest order in $\hbar$, not in α. Born-level bound states are characterized by interactions mediated by a classical gauge field. This is regarded as evident in Introductory QM, where the classical potential (1.1) of Hydrogen is adopted.

Perturbation theory expands around free fields. The infinite sum of ladder diagrams builds the classical potential. Consider the expression for the S-matrix,

$$S_{fi} = {}_{out}\langle f,\, t \to \infty| \left\{ \mathrm{T} \exp\Big[-i \int_{-\infty}^{\infty} dt\, H_I(t) \Big] \right\} |i,\, t \to -\infty\rangle_{in} \tag{1.6}$$

The interaction Hamiltonian is proportional to the coupling constant, in QED

$$H_I = e \int d\boldsymbol{x}\, \bar{\psi}\, e\not{A}\, \psi \tag{1.7}$$

Feynman diagrams of $\mathcal{O}(e^n)$ are given by an nth order expansion of the time-ordered exponential. The $|\ \rangle_{in}$ and ${}_{out}\langle\ |$ states are $\mathcal{O}\left(e^0\right)$ *free* states at asymptotic times. Thus the charged particles in $|e^+e^-\rangle_{in} = b^\dagger\, d^\dagger\, |0\rangle$ have no associated photon field. This violates the classical field equations. If the electron is at $\boldsymbol{x} = \boldsymbol{x}_1$ and the positron at $\boldsymbol{x}_2$ Gauss' law for A^0 requires

$$-\boldsymbol{\nabla}^2 A^0(\boldsymbol{x}) = e\big[\delta(\boldsymbol{x}-\boldsymbol{x}_1) - \delta(\boldsymbol{x}-\boldsymbol{x}_2)\big] \tag{1.8}$$

Nevertheless, the expression (1.6) for the S-matrix is formally exact since the free $|e^+e^-\rangle_{in}$ state at $t \to -\infty$ has an unlimited time to relax to the physical $|e^+e^-\rangle$ state, via repeated interactions specified by H_I. Building the classical gauge field requires an infinite number of interactions, hence the need for the infinite sum of ladder diagrams in Fig. 1.

The classical gauge field provides the binding potential in bound states. In "hard" QED interactions, $|\boldsymbol{p}| \gg \alpha m$, the classical field is of secondary importance. Nevertheless, its absence in the *in* and *out* states manifests itself in the appearance of infrared singularities in the perturbative expansion. The soft photons decouple from neutral atoms at momenta corresponding to the atomic radius, $|\boldsymbol{p}| \sim \alpha m$. This gives rise to $\log\alpha$ contributions in bound state perturbation theory.

In conclusion, describing Positronium in terms of Feynman diagrams requires a divergent sum to generate the classical $-\alpha/r$ potential. The $\hbar$ expansion provides a physically motivated first approximation. The gauge field operator in the Hamiltonian takes the value of the classical field, given by the equations of motion (1.8). Loop corrections to the Born level bound states may be evaluated by using them as *in* and *out* states in the expression (1.6) of the S-matrix.

3. Positronium bound by its classical gauge field

In section II I determine the Positronium state and binding energy at Born level according to the above principles. The state (2.3) is expressed in terms of the electron and positron field operators taken at equal time and with a spatial distribution described by a c-numbered (4×4) wave function Φ. The requirement (2.1) that this state be stationary in time, *i.e.*, be an eigenstate of the QED Hamiltonian, determines the bound state equation for Φ. Each Fock state $|e^-(\boldsymbol{x}_1)e^+(\boldsymbol{x}_2)\rangle$ generates a specific classical field. The Positronium state reduces to (2.8) in the limit of weak binding, $\alpha \to 0$.

The use of the classical gauge field A^μ in the interaction Hamiltonian (1.7) merits some remarks. In the Positronium rest frame ($\boldsymbol{P}$=0) the A^0 field dominates and is given by Gauss' law (1.8),

$$A^0(\boldsymbol{x}) = \frac{e}{4\pi}\left(\frac{1}{|\boldsymbol{x}-\boldsymbol{x}_1|} - \frac{1}{|\boldsymbol{x}-\boldsymbol{x}_2|}\right) \tag{1.9}$$

Note that:

1. The $e^\mp$ positions $\boldsymbol{x}_1, \boldsymbol{x}_2$ determine $A^0(\boldsymbol{x})$ for all $\boldsymbol{x}$ at each instant of time.
2. Each position $\boldsymbol{x}_1, \boldsymbol{x}_2$ is associated with a distinct $A^0(\boldsymbol{x})$ field.
3. The potential energy of the electron is
$$eA^0(\boldsymbol{x}_1) = -\frac{\alpha}{|\boldsymbol{x}_1-\boldsymbol{x}_2|} \tag{1.10}$$
plus an infinite "self-energy" $\alpha/0$. The latter is independent of $\boldsymbol{x}_1, \boldsymbol{x}_2$ and can be subtracted.
4. The potential energy of the positron equals that of the electron,
$$-eA^0(\boldsymbol{x}_2) = -\frac{\alpha}{|\boldsymbol{x}_1-\boldsymbol{x}_2|} \tag{1.11}$$
5. The field energy calculated from (1.9) is
$$\frac{1}{4}\int d^3\boldsymbol{x} F_{\mu\nu}(\boldsymbol{x})F^{\mu\nu}(\boldsymbol{x}) = \frac{\alpha}{|\boldsymbol{x}_1-\boldsymbol{x}_2|} \tag{1.12}$$
The sum of (1.10) – (1.12) gives the Positronium potential $V(r)$ in (1.1).

Each order of the $\hbar$ expansion is Poincaré invariant. In section II 4 I determine how the Positronium wave function and energy depend on its momentum $\boldsymbol{P}$ by Lorentz transforming the classical gauge field as in (2.12). The outcome confirms expectations: $E = \sqrt{\boldsymbol{P}^2 + M^2}$ and the wave function Lorentz contracts as in classical relativity. The same result was found using the Bethe-Salpeter equation [8].

4. Dirac states

The Born level Positronium state (2.8) consists of a single e^+e^- pair and its associated classical gauge field. The situation is different for a relativistic electron bound in an external field, described by the Dirac equation. Relativistic dynamics involves virtual pairs created by the field (*cf.* Fig. 3b), as first demonstrated by the Klein Paradox [9]. This obscures the relation between the ostensibly single-particle Dirac wave function and the multiparticle state. I consider the structure of Dirac states in section III.

A Dirac state (3.4) can be expressed in terms of the electron field $\psi(t, \boldsymbol{x})$ operating on a non-trivial ground state $|\Omega\rangle$. The Dirac wave function specifies the spatial distribution of the $e^\pm$ creation and annihilation operators. The ground state (3.14) is a superposition of e^+e^- pairs, determined by the complete set of Dirac wave functions.

In section III B I apply the general expressions to the case of Dirac states in $D = 1+1$ dimensions, where the classical external field $eA^0(x) = V'|x|$ is linear and $A^1 = 0$. The analytic solution (3.34) has features of both bound and scattering states: The energy spectrum is continuous and the norm of the wave function approaches a constant value as $|x| \to \infty$. These features are generic for power potentials $V(r) \propto r^{\pm n}$ in all dimensions – with the exception of the $1/r$ potential in $D = 3 + 1$ [10].

The linear potential $eA^0(x) = V'|x|$ confines electrons but repels positrons. Thus the electron and positron in an e^+e^- pair are distributed asymmetrically, with the e^- at small and the e^+ at large $|x|$. In particular, the constant norm of the wave function as $|x| \to \infty$ is due only to the positrons. The kinetic energy of a positron grows with $|x|$, due to its increasingly negative potential.

For a sizeable electron mass m (in units of $\sqrt{V'}$) the Dirac spectrum is similar to the quantized Schrödinger spectrum for nearly all values of the parameter β in the solution (3.34). The continuous part of the Dirac spectrum is limited to states with wave functions that are suppressed at small $|x|$. The full set of Dirac states is complete and orthonormal, with δ-function normalization as for plane waves.

5. Application to hadrons in QCD

Hadrons are very different from atoms – which makes their similarities surprising. The fact that most hadrons can be classified as $q\bar{q}$ and qqq states is indicative of a perturbative coupling. The likeness of the quarkonium and atomic spectra makes this rather compelling. I review these and other phenomenological aspects of hadron physics in section IV.

In the perturbative approach to QED bound states described here the emphasis is on a proper definition of the lowest order contribution. For bound states this must be understood as lowest order in $\hbar$, not in α. At Born level the binding is due to a classical gauge field. In the Positronium rest frame the instantaneity of A^0 avoids issues of retardation. The state can be boosted by Lorentz transforming the classical gauge field.

This approach may apply also to hadrons in QCD. The classical gauge field then needs to cause confinement and chiral symmetry breaking. The solution of Gauss' law is unique up to homogeneous solutions, specified by the boundary condition at spatial infinity. A non-vanishing gauge field for $\boldsymbol{x} \to \infty$ generally breaks Poincaré invariance. In section V C 1 I list the arguments which point to a single acceptable solution. It allows bound states only in the form of color singlet mesons (5.36) and baryons (5.37). It is characterized by one dimensionful parameter Λ related to the strength of the classical field. The homogeneous solution is of $\mathcal{O}\left(\alpha_s^0\right)$, *i.e.*, independent of the QCD coupling.

In analogy to the QED case (1.9) there is a specific color field for each quark configuration of the hadron. Since the overall state is a singlet under (global) gauge transformations the gluon field vanishes when summed over the quark colors in mesons (5.45) as well as in baryons (5.55). Hence the classical field is invisible to external observers (such as other hadrons). The only $\mathcal{O}\left(\alpha_s^0\right)$ interactions between hadrons occur through quark overlap: the creation/annihilation of $q\bar{q}$ pairs. The dynamics resembles that described by dual diagrams [11, 12], such as Fig. 11.

The classical field results in a linear potential (5.59) for mesons. The baryon potential (5.61) agrees with the meson one when two of the quarks are at the same position. The two color components $a = 3, 8$ confine along $\boldsymbol{x}_1 - \boldsymbol{x}_2$ and $\boldsymbol{x}_1 + \boldsymbol{x}_2 - 2\boldsymbol{x}_3$ respectively, as seen from (5.48). There is no analogous solution for states with more than three quarks.

The classical field is non-perturbative in the sense that a comparable solution cannot be found for single quarks or gluons – only color singlet states are physical, in analogy to QED_2 [13]. Perturbative corrections are expected to be calculable using the standard S-matrix expression (1.6), with the $\mathcal{O}\left(\alpha_s^0\right)$ mesons and baryons as *in* and *out* states. The strong coupling $\alpha_s(Q^2)$ will freeze as $Q^2 \to 0$ if the $\hbar$ expansion is relevant (loop corrections are suppressed).

The indications that α_s does freeze are briefly discussed in section IV 4.

Since $\hbar$ is a fundamental parameter the full symmetries of the exact result, as well as unitarity, must be realized at each order of the expansion. Poincaré invariance is addressed in sections V B and VII, and a non-trivial example of gauge invariance given in section VII A. Unitarity is an infinite set of non-linear relations between bound state scattering amplitudes that can only be satisfied order by order in an expansion. The solution appears to be analogous to the familiar one based on Feynman diagrams. The tree approximation (discussed further below) implies calculable hadron loop corrections, corresponding to squaring the dual diagram in Fig. 11. The hadron loop expansion is equivalent to an expansion in $1/N_c$. Unitarity may be satisfied at each order of $1/N_c$.

6. Hadrons at tree level

Two distinct levels of approximation for hadrons emerge. The first one ignores perturbative effects of $\mathcal{O}(\alpha_s)$. In the $\mathcal{O}(\alpha_s^0)$ sector there is what might be called a tree level, where string breaking caused by contributions such as Fig. 11 (and the associated hadron loops) are neglected. Tree level results are straightforward to calculate. The first task is then to study whether they provide a reasonable first approximation to hadron physics, motivating further studies.

In section VI A I discuss the spectrum and wave functions of mesons in $D = 1 + 1$ dimensions. The solutions are similar to those of the Dirac equation in section III B, but there is an important difference. Some components of the 2×2 meson wave functions are generally singular at $M = V(x)$, where M is the bound state mass and $V(x)$ the linear potential (see (6.4)). Taking the quark mass $m \to \infty$ shows that requiring the relativistic wave function to be regular at $M = V$ is analogous to requiring normalizability of the non-relativistic Schrödinger wave function. At finite m the wave functions are regular only for specific values of the bound state mass M (section VI A 3). The meson spectrum is thus discrete, in contrast to the continuous Dirac spectrum.

The completeness and orthonormality of the Dirac states relies on a δ-function normalization, as appropriate for a continuous spectrum. The discrete meson states are not complete and orthogonal, since two meson states have a non-vanishing overlap with a single one through string-breaking as in Fig. 11. Unitarity and completeness can emerge only when hadron loop effects are included.

The tree level meson states can approximate physical phenomena via duality between bound and scattering states. As previously mentioned, the Dirac wave functions have aspects of both bound and plane wave states: The linear potential confines electrons but repels positrons. In section VI A 4 I discuss how meson states reduce to plane wave quark states in certain limits, as in the parton model. Specifically, the wave functions accomodate the duality illustrated in Fig. 13.

Meson states in $D = 3 + 1$ dimensions can be classified according to their spin, parity and charge conjugation (section VI C, (6.66)). For vanishing quark mass ($m = 0$) the spectrum resembles that of dual models [14, 15], with straight Regge and daughter trajectories.

Aspects of chiral symmetry are discussed in section VI D. For $m = 0$ the action has exact chiral invariance. Since the ground state is chirally symmetric each meson should have a partner with the same mass but opposite parity. This is also seen in the solutions. However, in some cases the condition that the wave function be regular is incompatible with chiral invariance. Then there is no parity degeneracy.

There are states with zero mass M that have a regular wave function at $M - V(r) = V'r = 0$. String breaking effects may be particularly important for them, since the whole wave function is in the classically forbidden domain $V(r) > M$. Nevertheless, these solutions may be relevant for chiral symmetry breaking. In particular, the $M = 0$, $J^{PC} = 0^{++}$ meson can mix with the chirally symmetric ground state without breaking Poincaré invariance. Then also the massless $J^{PC} = 0^{-+}$ pion couples to the axial current. The existence of massless bound states is intriguing, and their relevance for chiral symmetry breaking in QCD merits further study.

II. POSITRONIUM AT BORN LEVEL

1. State definition

The first step in our quest is the derivation of a Positronium state n at Born level directly from the QED action. Bound states are stationary in time and thus by definition eigenstates of the Hamiltonian,

$$H\,|n, \boldsymbol{P}\rangle = E\,|n, \boldsymbol{P}\rangle \tag{2.1}$$

The operator fields of the QED Hamiltonian H are taken at the same instant of time t as the Positronium state $|n, \boldsymbol{P}\rangle$. The Poincaré invariance of the QED action ensures that the energy eigenvalue has the proper dependence on the momentum $\boldsymbol{P}$ of the state,

$$E = \sqrt{M^2 + \boldsymbol{P}^2} \tag{2.2}$$

This is not explicit in (2.1) since the concept of equal time is frame dependent. The Hamiltonian transforms under boosts, and so do the states. Since we may consider $\hbar$ to be a free parameter the correct energy dependence must hold at each order of $\hbar$, and so also for the Born contribution. Eq. (2.2) provides a non-trivial check that the Born state is correctly evaluated.

Due to the non-relativistic internal dynamics Fock states with more than one e^+e^- pair do not contribute, so the state should have the structure

$$|n, \boldsymbol{P}\rangle = \int d\boldsymbol{x}_1 d\boldsymbol{x}_2 \, e^{i\boldsymbol{P}\cdot(\boldsymbol{x}_1+\boldsymbol{x}_2)/2} \bar{\psi}_\alpha(\boldsymbol{x}_1) \Phi_{\alpha\beta}(\boldsymbol{x}_1 - \boldsymbol{x}_2) \psi_\beta(\boldsymbol{x}_2) \, |0\rangle \tag{2.3}$$

Remarks:

- Each state $|e^-(\boldsymbol{x}_1)e^+(\boldsymbol{x}_2)\rangle$ is associated with a classical gauge field $A^\mu(\boldsymbol{x}; \boldsymbol{x}_1, \boldsymbol{x}_2)$. The gauge field operator in the Hamiltonian takes the value of the classical field when imposing (2.1) at Born level (section I 3).

- The operator valued electron field satisfies the canonical anticommutation relation

$$\left\{\psi^\dagger_\alpha(t, \boldsymbol{x}), \psi_\beta(t, \boldsymbol{y})\right\} = \delta_{\alpha,\beta} \, \delta^3(\boldsymbol{x} - \boldsymbol{y}) \tag{2.4}$$

  and may be expanded in the free state basis,

$$\psi_\alpha(t = 0, \boldsymbol{x}) \;=\; \int \frac{d\boldsymbol{k}}{(2\pi)^3 2E_k} \sum_\lambda \left[u_\alpha(\boldsymbol{k}, \lambda) e^{i\boldsymbol{k}\cdot\boldsymbol{x}} b_{\boldsymbol{k},\lambda} + v_\alpha(\boldsymbol{k}, \lambda) e^{-i\boldsymbol{k}\cdot\boldsymbol{x}} d^\dagger_{\boldsymbol{k},\lambda} \right] \tag{2.5}$$

$$\left\{ b_{\boldsymbol{p},\lambda}, b^\dagger_{\boldsymbol{q},\lambda'} \right\} \;=\; \left\{ d_{\boldsymbol{p},\lambda}, d^\dagger_{\boldsymbol{q},\lambda'} \right\} = 2E_p \, (2\pi)^3 \delta^3(\boldsymbol{p} - \boldsymbol{q}) \delta_{\lambda,\lambda'} \tag{2.6}$$

- The time t is implicit in (2.3) and may be take to be $t = 0$. Time evolution gives the state a phase $\exp(-iEt)$ and shifts the electron fields to t.

- The c-numbered wave function $\Phi_{\alpha\beta}(\boldsymbol{x}_1 - \boldsymbol{x}_2)$ depends implicitly on $\boldsymbol{P}$ and on the quantum numbers n of the Positronium state. Its 4×4 Dirac matrix structure simplifies for non-relativistic internal dynamics. The momentum space ansatz

$$\Phi_{\alpha\beta}(\boldsymbol{x}) = \int \frac{d\boldsymbol{k}}{(2\pi)^3} \, e^{i\boldsymbol{k}\cdot\boldsymbol{x}} \, {}_\alpha\Big[\gamma^0 u(\tfrac{1}{2}\boldsymbol{P} + \boldsymbol{k}, \lambda)\Big] \Big[\bar{v}(\tfrac{1}{2}\boldsymbol{P} - \boldsymbol{k}, \lambda')\gamma^0\Big]_\beta \, \phi_P(\boldsymbol{k}) \tag{2.7}$$

  where the scalar wave function $\phi_P(\boldsymbol{k})$ is helicity independent, gives in (2.3)

$$|n, \boldsymbol{P}\rangle = \int \frac{d\boldsymbol{k}}{(2\pi)^3} \, \phi_P(\boldsymbol{k}) \, b^\dagger(\tfrac{1}{2}\boldsymbol{P} + \boldsymbol{k}, \lambda) \, d^\dagger(\tfrac{1}{2}\boldsymbol{P} - \boldsymbol{k}, \lambda') \, |0\rangle \tag{2.8}$$

  We shall see that this state solves (2.1) for Positronium.

- In a space translation $\boldsymbol{x}_i \to \boldsymbol{x}_i + \boldsymbol{a}$ $(i = 1, 2)$ the integrand of (2.3) picks up the phase $\exp(i\boldsymbol{P}\cdot\boldsymbol{a})$, implying that the state has overall momentum $\boldsymbol{P}$. More directly, (2.3) is an eigenstate of the momentum operator (see section V B),

$$\boldsymbol{\mathcal{P}} = -i \int d\boldsymbol{x} \, \psi^\dagger(\boldsymbol{x}) \boldsymbol{\nabla} \psi(\boldsymbol{x}) \tag{2.9}$$

  with eigenvalue $\boldsymbol{P}$. Similarly, the symmetry of H under rotations ensures that the wave function $\Phi(\boldsymbol{x}_1 - \boldsymbol{x}_2)$ transforms according to the angular momentum representation of n in the rest frame, $\boldsymbol{P} = 0$.

2. Classical Gauge Field

Maxwell's equations specify the classical electromagnetic field in the presence of charges,

$$\partial_\mu F^{\mu\nu}(x) = j^\nu(x) \tag{2.10}$$

In the rest frame of Positronium ($\boldsymbol{P} = 0$) its electron and positron constituents move non-relativistically, $v \simeq \alpha \ll 1$. Hence the vector field $\boldsymbol{A}$ is of $\mathcal{O}(\alpha)$ compared to the Coulomb field A^0 (up to gauge transformations). Once we know the field in the rest frame we can boost it to a frame where $\boldsymbol{P} \neq 0$.

For $\boldsymbol{A} = 0$ (2.10) gives Gauss' law (1.8), which determines the expression (1.9) for A^0. I recall some features of this solution, which were already mentioned in section I 3 and are due to the instantaneous nature of A^0:

(*i*) Each component $|e^-(\boldsymbol{x}_1, \lambda)e^+(\boldsymbol{x}_2, \lambda')\rangle$ of the Positronium state carries a specific classical field.

(*ii*) The value of $A^0(\boldsymbol{x})$ is determined instantaneously for all $\boldsymbol{x}$.

The gauge field may be boosted in the usual way. For a boost ξ in the z-direction

$$P = (M\cosh\xi, 0, 0, M\sinh\xi) \tag{2.11}$$

$$\begin{aligned} A^0(\boldsymbol{x}) &= \cosh\xi\, A^0_R(\boldsymbol{x}_R; \boldsymbol{x}_{1R}, \boldsymbol{x}_{2R}) \\ A^1(\boldsymbol{x}) &= A^2(\boldsymbol{x}) = 0 \\ A^3(\boldsymbol{x}) &= \sinh\xi\, A^0_R(\boldsymbol{x}_R; \boldsymbol{x}_{1R}, \boldsymbol{x}_{2R}) \end{aligned} \tag{2.12}$$

where the rest frame quantities are marked by R. Since the distances are measured at equal time they are Lorentz contracted in the direction of the boost. Conversely, the rest frame coordinates in terms of the boosted ones are

$$\boldsymbol{x}_R = (x, y, z)_R = (x, y, z\,\cosh\xi) \equiv (\boldsymbol{x}_\perp, x_\parallel\,\cosh\xi) \tag{2.13}$$

The boosted field, expressed in the coordinates of the moving frame, is determined by A^0 (1.9) in the rest frame,

$$\begin{pmatrix} A^0(\boldsymbol{x}) \\ A^3(\boldsymbol{x}) \end{pmatrix} = \begin{pmatrix} \cosh\xi \\ \sinh\xi \end{pmatrix} \times \frac{e}{4\pi}\left[\frac{1}{\sqrt{(\boldsymbol{x}-\boldsymbol{x}_1)^2_\perp + (x-x_1)^2_\parallel \cosh^2\xi}} - \frac{1}{\sqrt{(\boldsymbol{x}-\boldsymbol{x}_2)^2_\perp + (x-x_2)^2_\parallel \cosh^2\xi}}\right] \tag{2.14}$$

In terms of the rest frame coordinates (2.13) this may be expressed as

$$\not{A} = \frac{\not{P}}{M}\,\frac{e}{4\pi}\left[\frac{1}{|\boldsymbol{x}-\boldsymbol{x}_1|_R} - \frac{1}{|\boldsymbol{x}-\boldsymbol{x}_2|_R}\right] \tag{2.15}$$

3. The Hamiltonian

It is convenient to divide the Hamiltonian into a kinetic and interaction part,

$$H = H_0 + H_I \tag{2.16}$$

In the absence of physical, transverse photons only the fermions contribute to the kinetic energy,

$$H_0 = \int d\boldsymbol{x}\,\bar\psi(\boldsymbol{x})\big(i\not\partial - m\big)\psi(\boldsymbol{x}) = \int \frac{d\boldsymbol{p}}{(2\pi)^3\,2E_p}\,E_p \sum_\lambda \left[b^\dagger_{\boldsymbol{p},\lambda} b_{\boldsymbol{p},\lambda} + d^\dagger_{\boldsymbol{p},\lambda} d_{\boldsymbol{p},\lambda}\right] \tag{2.17}$$

The classical field contributes to the energy through the terms $\frac{1}{4}F_{\mu\nu}F^{\mu\nu}$ and $\bar\psi\, e\not{A}\psi$ of the Hamiltonian density (their signs are opposite compared to the Lagrangian). In the rest frame, using (1.8),

$$\tfrac{1}{4}\int d\boldsymbol{x}\,F_{\mu\nu}F^{\mu\nu} = -\tfrac{1}{2}\int d\boldsymbol{x}\,\boldsymbol{\nabla}A^0\cdot\boldsymbol{\nabla}A^0 = \tfrac{1}{2}\int d\boldsymbol{x}\,A^0\cdot\boldsymbol{\nabla}^2 A^0 = -\tfrac{1}{2}e\left[A^0(\boldsymbol{x}_1) - A^0(\boldsymbol{x}_1)\right] = \frac{e^2}{4\pi|\boldsymbol{x}_1-\boldsymbol{x}_2|} \tag{2.18}$$

In the last equality I discarded the infinite "self-energies" $\propto \alpha/0$, which are independent of $\boldsymbol{x}_1, \boldsymbol{x}_2$ and thus irrelevant. The result has the same form as the Coulomb potential $-\alpha/r$ but is of opposite sign. It removes the double counting otherwise arising from the electron feeling the positron field and *vice versa*, *cf.* (1.10) – (1.12).

The contribution (2.18) is conveniently taken into account using the equation of motion for the gauge field operators,

$$\partial_\mu F^{\mu\nu}(x) = e\bar{\psi}(x)\gamma^\nu\psi(x) \tag{2.19}$$

In the absence of time dependent (propagating) gauge fields we can partially integrate in the expression for the field energy (now regarded as an operator expression),

$$\tfrac{1}{4}\int d\boldsymbol{x}\, F_{\mu\nu}F^{\mu\nu} = -\tfrac{1}{2}\int d\boldsymbol{x}\, A_\nu\partial_\mu F^{\mu\nu} = -\tfrac{1}{2}\int d\boldsymbol{x}\,\bar{\psi}\, e\not{A}\psi \tag{2.20}$$

This removes half of the fermion interaction term, so that the total interaction Hamiltonian becomes

$$H_I = \tfrac{1}{2}\int d\boldsymbol{x}\,\bar{\psi}\, e\not{A}\psi \tag{2.21}$$

4. Schrödinger Equation for Positronium in motion

I determine the bound state equation by imposing (2.1) in the general frame (2.12). Thus we find the bound state equation for Positronium in motion. The present Hamiltonian formulation with a classical gauge field is equivalent to the approach in [8], which used a time-ordered Bethe-Salpeter equation.

The kinetic energy is given by applying H_0 (2.17) to the Positronium state (2.8),

$$H_0\,|n,\boldsymbol{P}\rangle = \int \frac{d\boldsymbol{k}}{(2\pi)^3}\,\phi_P(\boldsymbol{k})(E_+ + E_-)\,b^\dagger(\tfrac{1}{2}\boldsymbol{P}+\boldsymbol{k},\lambda)\,d^\dagger(\tfrac{1}{2}\boldsymbol{P}-\boldsymbol{k},\lambda')\,|0\rangle \qquad E_\pm \equiv \sqrt{(\tfrac{1}{2}\boldsymbol{P}\pm\boldsymbol{k})^2+m^2} \tag{2.22}$$

The binding energy E_b is defined as the difference between the bound state mass M and twice the electron mass m,

$$M = 2m + E_b \tag{2.23}$$

Expanding the energy eigenvalue E in powers of the $\mathcal{O}\left(\alpha^2\right)$ E_b gives

$$E = \sqrt{\boldsymbol{P}^2+(2m+E_b)^2} \simeq \mathcal{E} + \frac{2mE_b}{\mathcal{E}} \qquad\qquad \mathcal{E}\equiv\sqrt{\boldsymbol{P}^2+4m^2} \tag{2.24}$$

Expressing $E(\boldsymbol{P})$ in this form implies that the bound state equation should give a $\boldsymbol{P}$-independent result for E_b. Expanding the fermion energies $E_\pm$ in powers of the $\mathcal{O}\left(\alpha\right)$ relative momentum $\boldsymbol{k}$ gives at $\mathcal{O}\left(\alpha^2\right)$,

$$E_\pm \simeq \tfrac{1}{2}\mathcal{E} + \frac{\pm\boldsymbol{P}\cdot\boldsymbol{k}+\boldsymbol{k}^2}{\mathcal{E}} - \frac{(\boldsymbol{P}\cdot\boldsymbol{k})^2}{\mathcal{E}^3} \tag{2.25}$$

I denote the component of $\boldsymbol{k}$ along $\boldsymbol{P}$ by $k_\parallel$ and the orthogonal components by $\boldsymbol{k}_\perp$. The difference between the total energy E and the $e^\pm$ kinetic energies is of $\mathcal{O}\left(\alpha^2\right)$ as it should be

$$E - E_+ - E_- \simeq \frac{1}{\cosh\xi}\Big[E_b - \frac{1}{m}\Big(\boldsymbol{k}_\perp^2 + \frac{k_\parallel^2}{\cosh^2\xi}\Big)\Big] = \frac{1}{\cosh\xi}\Big(E_b - \frac{\boldsymbol{k}_R^2}{m}\Big) \tag{2.26}$$

where the rest frame momentum is conjugate to $\boldsymbol{x}_R$ in (2.13),

$$\boldsymbol{k}_R = \Big(\boldsymbol{k}_\perp, \frac{k_\parallel}{\cosh\xi}\Big) \qquad\qquad \boldsymbol{k}_R\cdot\boldsymbol{x}_R = \boldsymbol{k}\cdot\boldsymbol{x} \tag{2.27}$$

I brought the boost ξ into (2.26) through the approximation

$$\cosh\xi = \frac{\sqrt{\boldsymbol{P}^2+(2m+E_b)^2}}{2m+E_b} \simeq \frac{\mathcal{E}}{2m} \tag{2.28}$$

which is allowed since (2.26) is already of $\mathcal{O}\left(\alpha^2\right)$, the accuracy of this calculation. Thus

$$(H_0-E)\,|n,\boldsymbol{P}\rangle = \frac{1}{\cosh\xi}\int\frac{d\boldsymbol{k}}{(2\pi)^3}\Big[\frac{1}{m}\Big(\boldsymbol{k}_\perp^2+\frac{k_\parallel^2}{\cosh^2\xi}\Big)-E_b\Big]\phi_P(\boldsymbol{k})\,b^\dagger(\tfrac{1}{2}\boldsymbol{P}+\boldsymbol{k},\lambda)\,d^\dagger(\tfrac{1}{2}\boldsymbol{P}-\boldsymbol{k},\lambda')\,|0\rangle \tag{2.29}$$

As H_I (2.21) acts on the bound state (2.3) we get contributions only for its commutation with the fermion operators since pair production effects may be neglected,

$$\big[H_I,\bar\psi(\boldsymbol{x}_1)\big]=\tfrac12 e\,\bar\psi(\boldsymbol{x}_1)\not{A}(\boldsymbol{x}_1)\gamma^0 \qquad\qquad [H_I,\psi(\boldsymbol{x}_2)]=-\tfrac12 e\,\gamma^0\not{A}(\boldsymbol{x}_2)\bar\psi(\boldsymbol{x}_1) \tag{2.30}$$

Up to the $\boldsymbol{x}_1,\boldsymbol{x}_2$-independent self-energies $\propto\alpha/0$ (2.15) gives

$$e\not{A}(\boldsymbol{x}_1)=-e\not{A}(\boldsymbol{x}_2)=\frac{\not{P}}{M}\,\frac{-\alpha}{|\boldsymbol{x}_1-\boldsymbol{x}_2|_R}\equiv\frac{\not{P}}{M}\,V(\boldsymbol{x}_{1R}-\boldsymbol{x}_{2R}) \tag{2.31}$$

Hence

$$H_I\,|n,\boldsymbol{P}\rangle=\frac{1}{2M}\int d\boldsymbol{x}_1 d\boldsymbol{x}_2\,e^{i\boldsymbol{P}\cdot(\boldsymbol{x}_1+\boldsymbol{x}_2)/2}\,\bar\psi(\boldsymbol{x}_1)\big[\not{P}\gamma^0\Phi(\boldsymbol{x}_1-\boldsymbol{x}_2)+\Phi(\boldsymbol{x}_1-\boldsymbol{x}_2)\gamma^0\not{P}\big]V(\boldsymbol{x}_{1R}-\boldsymbol{x}_{2R})\psi(\boldsymbol{x}_2)\,|0\rangle \tag{2.32}$$

Since this contribution is of $\mathcal{O}\left(\alpha^2\right)$ we may neglect the $\mathcal{O}\left(\alpha\right)$ $\boldsymbol{k}$-dependence of the u- and $\bar v$-spinors in the expression (2.7) of the wave function,

$$\Phi_{\alpha\beta}(\boldsymbol{x}_1-\boldsymbol{x}_2)=\Big[\gamma^0 u(\tfrac12\boldsymbol{P},\lambda)\Big]_\alpha\,\Big[\bar v(\tfrac12\boldsymbol{P},\lambda')\gamma^0\Big]_\beta\,\phi_P(\boldsymbol{x}_1-\boldsymbol{x}_2)\big[1+\mathcal{O}\left(\alpha\right)\big] \tag{2.33}$$

where $\phi_P(\boldsymbol{x})$ is the Fourier transform of $\phi_P(\boldsymbol{k})$. The Dirac structure in (2.32) is then explicit,

$$\begin{aligned}\not{P}\gamma^0\Phi(\boldsymbol{x}) &= 2m\,u(\tfrac12\boldsymbol{P},\lambda)\,\bar v(\tfrac12\boldsymbol{P},\lambda')\,\phi_P(\boldsymbol{x})\\ \Phi(\boldsymbol{x})\gamma^0\not{P} &= -2m\,\gamma^0 u(\tfrac12\boldsymbol{P},\lambda)\,\bar v(\tfrac12\boldsymbol{P},\lambda')\,\phi_P(\boldsymbol{x})\end{aligned} \tag{2.34}$$

To combine $H_I\,|n,\boldsymbol{P}\rangle$ with $(H_0-E)\,|n,\boldsymbol{P}\rangle$ I express (2.29) in coordinate space. Expanding the fermion fields as in (2.5) it is readily seen that

$$(H_0-E)\,|n,\boldsymbol{P}\rangle=\frac12\int d\boldsymbol{x}_1 d\boldsymbol{x}_2\,e^{i\boldsymbol{P}\cdot(\boldsymbol{x}_1+\boldsymbol{x}_2)/2}\,\bar\psi(\boldsymbol{x}_1)\Big[-\frac1m\Big(\boldsymbol{\partial}^2_{1\perp}+\frac{\partial^2_{1\|}}{\cosh^2\xi}\Big)-E_b\Big]\big[\gamma^0\Phi(\boldsymbol{x}_1-\boldsymbol{x}_2)-\Phi(\boldsymbol{x}_1-\boldsymbol{x}_2)\gamma^0\big]\psi(\boldsymbol{x}_2)\,|0\rangle \tag{2.35}$$

is equivalent to (2.29) (the γ^0's cause the factor $1/\cosh\xi$). Together with (2.32), using also (2.33), the bound station condition becomes

$$\begin{aligned}(H_0-E+H_I)\,|n,\boldsymbol{P}\rangle &= \frac12\int d\boldsymbol{x}_1 d\boldsymbol{x}_2\,e^{i\boldsymbol{P}\cdot(\boldsymbol{x}_1+\boldsymbol{x}_2)/2}\,\bar\psi(\boldsymbol{x}_1)\Big[-\frac1m\Big(\boldsymbol{\partial}^2_{1\perp}+\frac{\partial^2_{1\|}}{\cosh^2\xi}\Big)+V(\boldsymbol{x}_{1R}-\boldsymbol{x}_{2R})-E_b\Big]\phi_P(\boldsymbol{x}_1-\boldsymbol{x}_2)\\ &\times\ \big[u(\tfrac12\boldsymbol{P},\lambda)\,\bar v(\tfrac12\boldsymbol{P},\lambda')\gamma^0-\gamma^0 u(\tfrac12\boldsymbol{P},\lambda)\,\bar v(\tfrac12\boldsymbol{P},\lambda')\big]\psi(\boldsymbol{x}_2)\,|0\rangle=0\end{aligned} \tag{2.36}$$

The bound state equation is thus

$$\Big(-\frac{\boldsymbol{\nabla}^2_R}{m}-\frac{\alpha}{|\boldsymbol{x}_R|}\Big)\phi_P(\boldsymbol{x})=E_b\,\phi_P(\boldsymbol{x}) \tag{2.37}$$

which implies that the scalar wave function $\phi_P(\boldsymbol{x})$ defined by (2.8) for a bound state with momentum $\boldsymbol{P}$ is given by the Lorentz contracted rest frame Schrödinger wave function ϕ,

$$\phi_P(\boldsymbol{x})=\phi(\boldsymbol{x}_R) \tag{2.38}$$

The relation between $\boldsymbol{x}$ and $\boldsymbol{x}_R$ is given in (2.13). The fact that E_b is independent of $\boldsymbol{P}$ ensures that the bound state energy (2.24) is Lorentz covariant. This is a dynamical (not explicit) feature of Hamiltonian formulations, and provides a non-trivial check that the evaluation is complete at leading order.

III. DIRAC STATES

A. General analysis

In the previous section I discussed the frame dependence of a non-relativistic bound state (Positronium) governed by the Schrödinger equation. Strongly coupled states cannot be addressed within perturbative QED. For the binding

energy $-\frac{1}{4}m\alpha^2$ to be commensurate with the electron mass m the coupling α must be of $\mathcal{O}(1)$ – but then a perturbative treatment is no longer meaningful. Our understanding of relativistic bound states is consequently model dependent.

The Dirac equation provides a familiar model for relativistic binding. It describes the bound states of an electron in a strong external gauge field $A^\mu(\boldsymbol{x})$, which I take to be independent of time. The essential simplifications compared to full QED are:

(i) $A^\mu(\boldsymbol{x})$ is a fixed classical field, unaffected by the electron.

(ii) The electron interacts only with the external field. Loop corrections are neglected.

The $\boldsymbol{x}$-dependence of A^μ means that space translation invariance is lost, so there is no conserved momentum nor boost covariance. Binding energies are well defined since a static field preserves time translation invariance.

1. *Dirac equation and wave function*

It is useful to consider separately the Dirac (4-spinor) wave functions Φ_n with positive eigenvalues $E_n > 0$, and wave functions $\bar{\Phi}_n$ with negative eigenvalues $-\bar{E}_n < 0$. The corresponding Dirac equations are

$$\big(-i\boldsymbol{\nabla}\cdot\boldsymbol{\gamma} + m + e\not{A}\big)\Phi_n(\boldsymbol{x}) \;=\; E_n\gamma^0\Phi_n(\boldsymbol{x}) \tag{3.1}$$

$$\big(-i\boldsymbol{\nabla}\cdot\boldsymbol{\gamma} + m + e\not{A}\big)\bar{\Phi}_n(\boldsymbol{x}) \;=\; -\bar{E}_n\gamma^0\bar{\Phi}_n(\boldsymbol{x}) \tag{3.2}$$

The Positronium states in e^+e^- scattering are at lowest order described by the sum of ladder diagrams in Fig. 1. Dirac states with a Coulomb (A^0) potential can be analogously obtained from the scattering of an electron on a heavy particle at rest [16]. As indicated in Fig. 3(a) also crossed photon diagrams must then be included. In the limit of infinite target mass only instantaneous Coulomb photons are exchanged. When time-ordered, the crossed photon diagram in (a) takes the appearance of Fig. 3(b): at an intermediate time the electron is accompanied by an e^+e^- pair. For N photon exchanges $N!$ diagrams contribute, with up to $N-1$ simultaneous e^+e^- pairs.

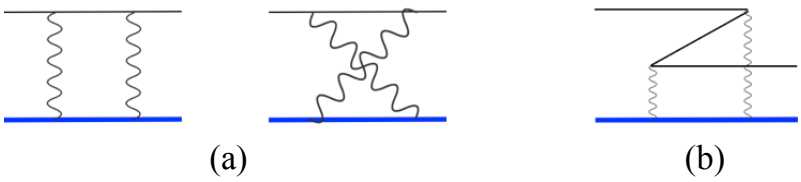

FIG. 3: (a) Feynman diagrams contributing to the Dirac states in the limit where the mass of the lower particle (thick blue line) tends to infinity. In the rest frame of the heavy particle the wavy lines represent instantaneous Coulomb photons. (b) When the crossed-photon diagram in (a) is time-ordered it reveals the creation and subsequent annihilation of an e^+e^- pair.

Soon after Dirac proposed his equation it was realized that the wave function cannot be a single particle probability amplitude in the same sense as the Schrödinger wave function. In electron scattering on potentials $V \gtrsim m$ the Dirac wave function does not conserve probability density, a phenomenon that is known as "Klein's paradox" [9]. The paradox is related to the e^+e^- pairs in the Dirac state. A proper description requires the methods of quantum field theory as explained, *e.g.*, in [17].

Dirac bound states provide a model for the dynamics of relativistic binding which is relevant also for hadrons. Like hadrons, Dirac states have Fock components with any number of constituents, yet their quantum numbers reflect only the "valence" electron. How does the ostensibly single particle wave function $\Phi(\boldsymbol{x})$ in (3.1) specify the higher Fock states? The Hamiltonian formalism I used for Positronium in Section II is helpful in answering this question.

2. *Dirac states* [18]

The Dirac Hamiltonian has the same appearance as the fermion Hamiltonian of QED,

$$H_D = \int d\boldsymbol{x}\,\bar{\psi}(\boldsymbol{x})\big[-i\boldsymbol{\nabla}\cdot\boldsymbol{\gamma} + m + e\not{A}\big]\psi(\boldsymbol{x}) \tag{3.3}$$

However, now the field A^μ is a fixed classical background field. There are no physical (propagating) photons. Since the Hamiltonian is quadratic in the fermion operator fields it can be diagonalized [19].

The positive (3.1) and negative (3.2) energy Dirac wave functions determine e^- and e^+ bound states defined as

$$\begin{aligned} |n\rangle &= \int d\boldsymbol{x}\, \psi^\dagger_\alpha(\boldsymbol{x})\Phi_{n\,\alpha}(\boldsymbol{x})\,|\Omega\rangle \equiv c^\dagger_n\,|\Omega\rangle \\ |\bar{n}\rangle &= \int d\boldsymbol{x}\, \bar{\Phi}^\dagger_{n\,\alpha}(\boldsymbol{x})\psi_\alpha(\boldsymbol{x})\,|\Omega\rangle \equiv \bar{c}^\dagger_n\,|\Omega\rangle \end{aligned} \tag{3.4}$$

where $\psi(\boldsymbol{x})$ is the electron field operator (2.5) and there is a sum over the Dirac index α. The vacuum state $|\Omega\rangle$ is an eigenstate of the Hamiltonian with eigenvalue taken to be zero,

$$H_D\,|\Omega\rangle = 0 \tag{3.5}$$

Two equivalent expressions for $|\Omega\rangle$ are given in Eqs. (3.14) and (3.17) below. Using

$$\big[H_D, \psi^\dagger(\boldsymbol{x})\big] = \psi^\dagger(\boldsymbol{x})\gamma^0(i\overleftarrow{\boldsymbol{\nabla}}\cdot\boldsymbol{\gamma} + m + e\not{A}) \qquad\qquad [H_D, \psi(\boldsymbol{x})] = -\gamma^0(-i\vec{\boldsymbol{\nabla}}\cdot\boldsymbol{\gamma} + m + e\not{A})\psi(\boldsymbol{x}) \tag{3.6}$$

we see that the states (3.4) are eigenstates of the Dirac Hamiltonian with *positive* eigenvalues,

$$\begin{aligned} H_D\,|n\rangle &= E_n\,|n\rangle \qquad E_n > 0 \\ H_D\,|\bar{n}\rangle &= \bar{E}_n\,|\bar{n}\rangle \qquad \bar{E}_n > 0 \end{aligned} \tag{3.7}$$

In terms of the wave functions in momentum space,

$$\Phi_n(\boldsymbol{x}) = \int \frac{d\boldsymbol{p}}{(2\pi)^3}\,\Phi_n(\boldsymbol{p})e^{i\boldsymbol{p}\cdot\boldsymbol{x}} \qquad\qquad \bar{\Phi}_n(\boldsymbol{x}) = \int \frac{d\boldsymbol{p}}{(2\pi)^3}\,\bar{\Phi}_n(\boldsymbol{p})e^{i\boldsymbol{p}\cdot\boldsymbol{x}} \tag{3.8}$$

the eigenstate operators defined in (3.4) can be expressed as

$$c_n = \sum_{\boldsymbol{p}} \Phi^\dagger_n(\boldsymbol{p})\big[u(\boldsymbol{p},\lambda)b_{\boldsymbol{p},\lambda} + v(-\boldsymbol{p},\lambda)d^\dagger_{-\boldsymbol{p},\lambda}\big] \equiv B_{np}b_p + D_{np}d^\dagger_p \tag{3.9}$$

$$\sum_{\boldsymbol{p}} \equiv \int \frac{d\boldsymbol{p}}{(2\pi)^3 2E_p}\sum_\lambda$$

$$\bar{c}_n = \sum_{\boldsymbol{p}} \big[b^\dagger_{\boldsymbol{p},\lambda}u^\dagger(\boldsymbol{p},\lambda) + d_{-\boldsymbol{p},\lambda}v^\dagger(-\boldsymbol{p},\lambda)\big]\bar{\Phi}_n(\boldsymbol{p}) \equiv \bar{B}_{np}b^\dagger_p + \bar{D}_{np}d_p \tag{3.10}$$

In the second expressions on the rhs. a sum over the repeated index $p \equiv (\boldsymbol{p},\lambda)$ is implied. In the weak binding limit ($|\boldsymbol{p}| \ll m$) the positive energy wave function Φ_n has only upper Dirac components, whereas $\bar{\Phi}_n$ has only lower Dirac components. Then $|n\rangle$ is a single electron state, whereas $|\bar{n}\rangle$ is a single positron state.

The operators c_n and $\bar{c}_n$ are related to b, d via a Bogoliubov transformation. Using the commutation relations (2.6) and the orthonormality of the Dirac wave functions we see that they obey standard anticommutation relations,

$$\begin{aligned} \big\{c_m, c^\dagger_n\big\} &= \sum_{\boldsymbol{p}} \Phi^\dagger_{m,\alpha}(\boldsymbol{p})\big[u_\alpha(\boldsymbol{p},\lambda)u^\dagger_\beta(\boldsymbol{p},\lambda) + v_\alpha(-\boldsymbol{p},\lambda)v^\dagger_\beta(-\boldsymbol{p},\lambda)\big]\Phi_{n,\beta}(\boldsymbol{p}) = \int \frac{d\boldsymbol{p}}{(2\pi)^3}\Phi^\dagger_{m,\alpha}(\boldsymbol{p})\Phi_{n,\alpha}(\boldsymbol{p}) = \delta_{mn} \\ \big\{\bar{c}_m, c^\dagger_n\big\} &= 0 \\ \big\{\bar{c}_m, \bar{c}^\dagger_n\big\} &= \int \frac{d\boldsymbol{p}}{(2\pi)^3}\bar{\Phi}^\dagger_{m,\alpha}(\boldsymbol{p})\bar{\Phi}_{n,\alpha}(\boldsymbol{p}) = \delta_{mn} \end{aligned} \tag{3.11}$$

Inserting the completeness condition for the Dirac wave functions,

$$\sum_n \big[\Phi_{n,\alpha}(\boldsymbol{x})\Phi^\dagger_{n,\beta}(\boldsymbol{y}) + \bar{\Phi}_{n,\alpha}(\boldsymbol{x})\bar{\Phi}^\dagger_{n,\beta}(\boldsymbol{y})\big] = \delta_{\alpha\beta}\delta^3(\boldsymbol{x}-\boldsymbol{y}) \tag{3.12}$$

into the Dirac Hamiltonian (3.3) we find, recalling that the wave functions satisfy (3.1) and (3.2),

$$\begin{aligned} H_D &= \int d\boldsymbol{x}\, d\boldsymbol{y}\, \bar\psi_{\alpha'}(\boldsymbol{x})\big[-i\boldsymbol{\nabla}_{\boldsymbol{x}}\cdot\boldsymbol{\gamma}+m+e\not{A}(\boldsymbol{x})\big]_{\alpha'\alpha}\sum_n\big[\Phi_{n,\alpha}(\boldsymbol{x})\Phi^\dagger_{n,\beta}(\boldsymbol{y})+\bar\Phi_{n,\alpha}(\boldsymbol{x})\bar\Phi^\dagger_{n,\beta}(\boldsymbol{y})\big]\psi_\beta(\boldsymbol{y}) \\ &= \sum_n\int d\boldsymbol{x}\, d\boldsymbol{y}\,\psi^\dagger_\alpha(\boldsymbol{x})\big[E_n\Phi_{n,\alpha}(\boldsymbol{x})\Phi^\dagger_{n,\beta}(\boldsymbol{y})-\bar E_n\bar\Phi_{n,\alpha}(\boldsymbol{x})\bar\Phi^\dagger_{n,\beta}(\boldsymbol{y})\big]\psi_\beta(\boldsymbol{y}) \\ &= \sum_n\big[E_nc^\dagger_nc_n-\bar E_n\bar c_n\bar c^\dagger_n\big]\to\sum_n\big[E_nc^\dagger_nc_n+\bar E_n\bar c^\dagger_n\bar c_n\big] \end{aligned} \tag{3.13}$$

In the last step I normal-ordered the operators, neglecting the zero-point energies according to (3.5).

3. The vacuum state

The expression for the vacuum state may be found using the methods in [19]. In terms of the coefficients defined in (3.9),

$$|\Omega\rangle = N_0\exp\Big[-b^\dagger_q\big(B^{-1}\big)_{qm}D_{mr}d^\dagger_r\Big]\,|0\rangle \tag{3.14}$$

Sums over the repeated indices q,m,r are implied in the exponent, and the normalization factor N_0 ensures that $\langle\Omega|\Omega\rangle=1$. The vacuum state may alternatively be expressed in terms of $\bar B,\bar D$ using the relation

$$B_{mp}\bar B_{np}+D_{mp}\bar D_{np}=\sum_{\boldsymbol{p}}\Phi^\dagger_{m,\alpha}(\boldsymbol{p})\big[u_\alpha(\boldsymbol{p},\lambda)u^\dagger_\beta(\boldsymbol{p},\lambda)+v_\alpha(-\boldsymbol{p},\lambda)v^\dagger_\beta(-\boldsymbol{p},\lambda)\big]\bar\Phi_{n,\beta}(\boldsymbol{p})=\int\frac{d\boldsymbol{p}}{(2\pi)^3}\Phi^\dagger_{m,\alpha}(\boldsymbol{p})\bar\Phi_{n,\alpha}(\boldsymbol{p})=0 \tag{3.15}$$

Multiplying by $(B^{-1})_{qm}(\bar D^{-1})_{rn}$ and summing over m,n gives

$$-(B^{-1})_{qm}D_{mr}=(\bar D^{-1})_{rn}\bar B_{nq} \tag{3.16}$$

Using also $b^\dagger_qd^\dagger_r=-d^\dagger_rb^\dagger_q$ we find the form of the vacuum equivalent to (3.14),

$$|\Omega\rangle = N_0\exp\Big[-d^\dagger_r\big(\bar D^{-1}\big)_{rn}\bar B_{nq}b^\dagger_q\Big]\,|0\rangle \tag{3.17}$$

In order to verify that $c_n\,|\Omega\rangle=0$ we note that since b_p essentially differentiates the exponent in (3.14),

$$B_{nq}b_q\,|\Omega\rangle=-B_{nq}\big(B^{-1}\big)_{qm}D_{mr}d^\dagger_r\,|\Omega\rangle=-D_{nr}d^\dagger_r\,|\Omega\rangle \tag{3.18}$$

This cancels the contribution of the second term in the definition (3.9) of c_n. The demonstration that $\bar c_n$ annihilates the vacuum is simular. Thus

$$c_n\,|\Omega\rangle=\bar c_n\,|\Omega\rangle=H\,|\Omega\rangle=0 \tag{3.19}$$

According to (3.9) the e^- bound state takes the form,

$$c^\dagger_n\,|\Omega\rangle\equiv\big[b^\dagger_rB_{rn}+d_rD_{rn}\big]\,|\Omega\rangle \tag{3.20}$$

which also serves to define the coefficients B_{rn} and D_{rn}. The "sea" contribution $\propto d_r$ is

$$d_rD_{rn}N_0\exp\Big[-b^\dagger_q\big(B^{-1}\big)_{qm}D_{mr}d^\dagger_r\Big]\,|0\rangle=b^\dagger_q\big(B^{-1}\big)_{qm}D_{mr}D_{rn}\,|\Omega\rangle \tag{3.21}$$

Similarly as in (3.15) we have

$$\sum_{\boldsymbol{p}}(B_{mp}\,B_{pn}+D_{mp}\,D_{pn})=\int\frac{d\boldsymbol{p}}{(2\pi)^3}\Phi^\dagger_m(\boldsymbol{p})\,\Phi_n(\boldsymbol{p})=\delta_{mn} \tag{3.22}$$

Using this in (3.21) gives

$$d_rD_{rn}\,|\Omega\rangle=\big[b^\dagger_q(B^{-1})_{qn}-b^\dagger_rB_{rn}\big]\,|\Omega\rangle \tag{3.23}$$

Hence the fermion state (3.20) can be alternatively expressed as

$$c_n^\dagger\,|\Omega\rangle = b_p^\dagger (B^{-1})_{pn}\,|\Omega\rangle \tag{3.24}$$

The vacuum state $|\Omega\rangle$ (3.14) describes the distribution of the e^+e^- pairs that appear in the bound state through perturbative diagrams such as Fig. 3(b). It is a formal expression, involving a sum over all states m and the inverted matrix $\left(B^{-1}\right)_{qm}$. In the weak binding limit $D_{np} \to 0$ and $|\Omega\rangle \to |0\rangle$. Then (3.22) ensures that $(B^{-1})_{pn} = B_{np}$.

The coefficient B_{pn} describes the "valence" electron momentum distribution in the bound state (3.20). For a confining potential it is expected to be limited to low $|\boldsymbol{p}|$. In the next section I verify this for a linear potential in $D = 1+1$ dimensions. This presumably also holds for the valence + sea electron distribution described by $\left(B^{-1}\right)_{pn}$ of (3.24).

B. Dirac states in $D = 1+1$ dimensions

Physics in $D = 1+1$ dimensions is often used as a model for confinement since the QED potential is linear. The Dirac equation can be solved analytically in terms of Confluent Hypergeometric functions. These turn out to have quite different properties compared to the Airy-function solutions of the Schrödinger equation with a linear potential. The difference stems from the e^+e^- pairs that contribute to relativistic dynamics.

1. Wave function

The Dirac wave function for a linear potential in $D = 1+1$ is known since a long time [20]. The following discussion uses the notation and results of [21], as well as the relation between the wave function and the states presented in section III A 2.

Denoting the (positive or negative) eigenvalues by M the Dirac equation in $D = 1+1$ with $A^1 = 0$ is

$$\left[-i\gamma^0\gamma^1\partial_x + \gamma^0 m + eA^0\right]\Phi(M,x) = M\Phi(M,x) \tag{3.25}$$

The Dirac matrices can be represented in terms of Pauli matrices,

$$\gamma^0 = \sigma_3 \qquad \gamma^1 = i\sigma_2 \qquad \gamma^0\gamma^1 = \sigma_1 \tag{3.26}$$

The energy scale is set by the coupling $e = 1$ and the potential is linear as in QED_2,

$$V(x) \equiv eA^0(x) = V'|x| = \tfrac{1}{2}e^2|x| \equiv \tfrac{1}{2}|x| \tag{3.27}$$

Let

$$\Phi(M,x) = \begin{bmatrix} \varphi(x) \\ \chi(x) \end{bmatrix} \qquad \sigma(x) = (M-V)^2 \qquad \partial_x = \varepsilon(-x)(M-V)\partial_\sigma \tag{3.28}$$

where $\varepsilon(x) = x/|x|$ is the sign function. The equations for the two components of the Dirac wave function are

$$\begin{aligned} -i\partial_x\chi &= (M-V-m)\varphi, \\ -i\partial_x\varphi &= (M-V+m)\chi. \end{aligned} \tag{3.29}$$

They depend on M and x only in the combination $M-V$, motivating the introduction of σ in (3.28). The 2nd order equation for $\varphi(x)$ is

$$\partial_x^2\varphi(x) + \frac{\varepsilon(x)}{2(M-V+m)}\,\partial_x\varphi(x) + \left[(M-V)^2 - m^2\right]\varphi(x) = 0 \tag{3.30}$$

Let $\varphi(x=0)$ be real and $\chi(x=0)$ imaginary. This reduces the four real parameters of the general solution to two real parameters. The differential equations (3.29) ensure that the phases imposed at $x = 0$ hold at all x,

$$\varphi^*(x) = \varphi(x) \qquad\qquad \chi^*(x) = -\chi(x) \tag{3.31}$$

For states of definite parity $\eta = \pm 1$ it suffices to find the wave function for $x \geq 0$ since

$$\varphi(-x) = \eta\varphi(x) \qquad\qquad \chi(-x) = -\eta\chi(x) \tag{3.32}$$

Continuity at $x = 0$ requires that $\chi(0) = 0$ for $\eta = +1$, while $\varphi(0) = 0$ for $\eta = -1$.

The solution of the differential equations (3.29) are conveniently expressed in terms of the functions

$$\begin{aligned} f(x) &\equiv [\varphi(x) + \chi(x)]e^{i\sigma} \\ g(x) &\equiv [\varphi(x) - \chi(x)]e^{i\sigma} \end{aligned} \tag{3.33}$$

Then for $x > 0$,

$$\begin{aligned} f(x) &= N_M\Big[e^{i\beta}\,{}_1F_1(-i\tfrac{1}{2}m^2, \tfrac{1}{2}, 2i\sigma) + 2ime^{-i\beta}(M-V)\,{}_1F_1(\tfrac{1}{2} - i\tfrac{1}{2}m^2, \tfrac{3}{2}, 2i\sigma)\Big] \\ g(x) &= N_M\Big[e^{-i\beta}\,{}_1F_1(\tfrac{1}{2} - i\tfrac{1}{2}m^2, \tfrac{1}{2}, 2i\sigma) - 2ime^{i\beta}(M-V)\,{}_1F_1(1 - i\tfrac{1}{2}m^2, \tfrac{3}{2}, 2i\sigma)\Big] \end{aligned} \tag{3.34}$$

The real normalization constant $N_M > 0$ and the phase β are defined in terms of the real constants a, b of Eq. (2.15) in [21] through $a + ib = N_M\, e^{i\beta}$. Since $\beta \to \beta + \pi$ only gives an overall sign change we may restrict the phase to $-\pi/2 \leq \beta < \pi/2$.

2. Continuous spectrum

The continuity condition at $x = 0$ determines M as a function of β. Since β is a continuous variable also the eigenvalues M take a *continuous range* of (positive and negative) values. This is in stark contrast to the discrete spectrum of the Schrödinger equation in $D = 1 + 1$ with a linear potential. Already in the 1930's Plesset [10] noted that the Dirac spectrum is continuous for positive and negative power-law potentials in any dimension. The only exception is the $1/r$ potential in $D = 3 + 1$ dimensions.

The expression (3.20) for the electron bound state has Fock components with any number of e^+e^- pairs due to the structure (3.14) of the vacuum $|\Omega\rangle$. The linear potential (3.27) confines electrons but *repulses positrons*: the e^+ potential is *negative*, $-V(x) = -\frac{1}{2}|x|$. A positron can appear at any x provided the sum of its kinetic and potential energies $E_p - V(x)$ is commensurate with the energy eigenvalue M of the state (hence $|p| \simeq \frac{1}{2}|x|$ at large distances). This condition can be satisfied for any M, allowing a continuous spectrum.

The analytic solution (3.34) bears out these intuitive expectations. The parameter β determines the relative amount of "valence" e^- and "sea" e^+e^- contributions. For finite fermion mass m there is a specific value $\beta = \beta_{min}$ which corresponds to a minimal sea. This minimum is exponentially damped in m^2, similarly as the Schwinger pair production rate in a constant electric field [22]. Conversely, there is a value of β that minimizes the valence e^- contribution.

The large x behavior of the wave functions in (3.34) is, with $\sigma \simeq \frac{1}{4}x^2 - M|x|$,

$$\frac{1}{N_M}\lim_{x\to\infty} e^{-i\sigma}f(x) = C_M\, e^{-i\sigma}(2\sigma)^{im^2/2} - \frac{m}{2\sqrt{\sigma}}C_M^*\, e^{i\sigma}(2\sigma)^{-im^2/2} + \mathcal{O}\left(x^{-2}\right) \tag{3.35}$$

where

$$C_M = e^{i(\beta-\delta)}\frac{\Gamma(1 - im^2/2)}{m\sqrt{2\pi}}e^{3\pi m^2/4}\sqrt{1 - e^{-\pi m^2}}\Big[\sqrt{1 + e^{-\pi m^2}} + e^{i(\delta - 2\beta - \pi/4)}\sqrt{1 - e^{-\pi m^2}}\Big] \tag{3.36}$$

$$\delta = \arg\left[\frac{\Gamma(1 - i\frac{1}{2}m^2)}{\Gamma(\frac{1}{2} - i\frac{1}{2}m^2)}\right] \overset{m\to\infty}{\to} -\frac{\pi}{4} \tag{3.37}$$

The corresponding result for the g-function is obtained from the relation $e^{-i\sigma}g(x) = \left[e^{-i\sigma}f(x)\right]^*$, which follows from (3.33) and the phase choice (3.31). The wave functions (3.34) thus have constant asymptotic magnitude,

$$\lim_{x\to\infty}|f(x)| = \lim_{x\to\infty}|g(x)| = N_M\,|C_M| \tag{3.38}$$

The continuous spectrum means that the orthonormality relation (3.22) involves a Dirac δ-function,

$$\int_{-\infty}^{\infty} dx\, \Phi_\eta^\dagger(M, x)\Phi_{\eta'}(M', x) = \delta_{\eta\eta'}\delta(M - M') \tag{3.39}$$

where η, η' denote parities. As for plane waves the δ-function must arise from the infinite range of the x-integral. For arbitrarily large Λ,

$$\int_\Lambda^\infty dx\, \Phi_\eta^\dagger(M,x)\Phi_\eta(M',x) = \tfrac{1}{2}\delta(M-M') + \dots \tag{3.40}$$

where $\dots$ represents Λ-dependent finite contributions. Recalling that $\varphi(x)$ is real and $\chi(x)$ is imaginary, as well as the definition (3.33) of $f(x)$, (3.40) requires

$$\int_\Lambda^\infty dx \left[\varphi_M(x)\varphi_{M'}(x) - \chi_M(x)\chi_{M'}(x)\right] = \mathrm{Re}\int_\Lambda^\infty dx \left[e^{-i\sigma} f_M(x)\right]\left[e^{-i\sigma'} f_{M'}(x)\right]^* = \tfrac{1}{2}\delta(M-M') + \dots \tag{3.41}$$

Using the asymptotic expression (3.35) allows to determine the normalization constant,

$$N_M = \frac{1}{\sqrt{2\pi}\,|C_M|} \tag{3.42}$$

According to (3.38) this implies that $|f(x\to\infty)| = 1/\sqrt{2\pi}$ is independent of β and M. The normalization (3.42) also gives the correct $\delta(x-y)$-function in the completeness condition (3.12).

3. Relative amount of valence and sea

Let us now consider how the parameter β determines the relative amount of "valence" (small $|x|$) and "sea" (large $|x|$) contributions. Since $|f(x\to\infty)|$ is β-independent it suffices to consider the wave function in the region of small $|x|$. The comparison is most meaningful for large m, since the $V(x) \lesssim 2m$ region is classically forbidden for the sea.

At large m the dynamics is non-relativistic at small $|x|$. The Schrödinger equation with the linear potential (3.27) is

$$-\frac{1}{2m}\partial_x^2\rho(x) + \frac{1}{2}|x|\rho(x) = E_b\rho(x), \tag{3.43}$$

where $E_b = M - m$ is the binding energy. Both the coordinate and binding energy scale as $x, E_b \propto m^{-1/3}$. The normalizable solutions are given by the Airy function,

$$\rho(x) = N\,\mathrm{Ai}[m^{1/3}(x-2E_b)] \qquad (x>0), \tag{3.44}$$

with $\rho(x) = \pm\rho(-x)$.

The non-relativistic limit of the wave function $f(x)$ in (3.34) is given in Eq. (2.21) of [21], and the derivation is detailed in App. B of [2],

$$\lim_{\substack{m\to\infty \\ m^{1/3}x \text{ fixed}}} e^{-i\sigma} f(x) = \sqrt{2\pi}N_M(\cos\beta + \sin\beta)m^{1/3}e^{\pi m^2/2}\mathrm{Ai}[m^{1/3}(x-2E_b)] \tag{3.45}$$

The result agrees (up to the normalization) with the Schrödinger Airy-function solution. Determining N_M from (3.42) and (3.36), with $\delta = -\frac{1}{4}\pi$ as in (3.37), we get

$$\lim_{\substack{m\to\infty \\ m^{1/3}x \text{ fixed}}} e^{-i\sigma} f(x) = \frac{1}{\sqrt{2}}\,\frac{(\cos\beta+\sin\beta)m^{1/3}\mathrm{Ai}[m^{1/3}(x-2E_b)]}{\left|\cos\left(\beta+\frac{\pi}{4}\right) + \frac{i}{2}e^{-\pi m^2}\sin\left(\beta+\frac{\pi}{4}\right)\right|} \tag{3.46}$$

The value $\beta = -\frac{1}{4}\pi$ minimizes the "valence" wave function at low $|x|$. Conversely, $\beta = +\frac{1}{4}\pi$ suppresses the (relative) amount of sea by a factor $\exp(-\pi m^2)$, corresponding to the tunnelling rate from the classically forbidden region. As in the Schwinger mechanism [22], there are always some virtual pairs in a non-vanishing electric field.

Fig. 4 illustrates the β-dependence of the positive parity ground state wave function when $m = 1$. In (a) $\beta = \beta_{min} = \frac{1}{2}\delta + \frac{3}{8}\pi$, the value which minimizes C_M (3.36) and thus maximizes $\varphi(0)$. The relative magnitude of the oscillations at large x are indeed seen to be smaller in (a) than in (b), where $\beta = 0$. In both cases $\varphi(x)$ agrees in shape with the Schrödinger wave function $\rho(x)$ at low x.

Fig. 5 compares the five first eigenvalues M for the Dirac solutions with $\beta = \beta_{min}$ and $\beta = 0$ with the Schrödinger values. The three solutions give nearly the same masses for the lowest excitations. Values of M that differ widely

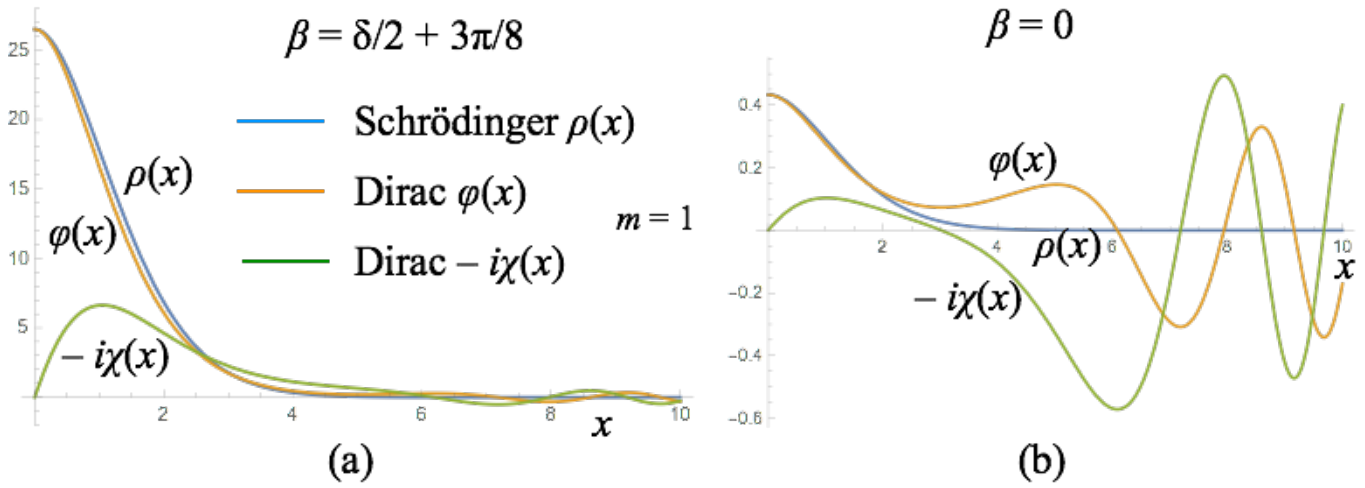

FIG. 4: The ground state Schrödinger wave function $\rho(x)$ for $m = 1$ compared with the upper and lower components of the Dirac wave function (3.28) for (a) $\beta = \beta_{min} = 0.925$ and (b) $\beta = 0$. For ease of comparison the Schrödinger wave function is arbitrarily normalized by $\rho(0) = \varphi(0)$.

Dirac and Schrödinger Eigenvalues M (m=1, η = +1)

n	1	2	3	4	5
Dirac $\beta = \beta_{min}$	1.5234	2.4554	3.0671	3.5644	3.9954
Dirac $\beta = 0$	1.5100	2.4490	3.0621	3.5602	3.9917
Schrödinger $M = m + E_b$	1.5094	2.6241	3.4100	4.0816	4.6861

FIG. 5: The eigenvalues M (in units of the electron charge e) of the five lowest (positive parity) states calculated from the Schrödinger and Dirac equations. In the Dirac case the fermion mass $m = 1$, $\beta = 0.925$ and $\beta = 0$.

from the Schrödinger ones occur only in a restricted range of $\beta \simeq -\frac{1}{4}\pi$, where the valence contribution is suppressed according to (3.46). That range moreover narrows quickly as m increases. For the Dirac as well as the Schrödinger equation the quantization of M is determined by the valence electron at low $|x|$. M can therefore take a continuous range of values in the Dirac equation only when the valence contribution is suppressed.

The reduction of the Dirac wave function to the Schrödinger one is usually demonstrated by taking $m \to \infty$ with $x \propto m^{-1/3}$. From (3.46) we see that this is not quite adequate in the case of a linear potential, since the relative size of the large x oscillations decrease with m only when $\beta = \beta_{min}$. A more proper limit is thus $m \to \infty$ with $\beta = \beta_{min}$.

4. The electron and positron distributions

I have been rather loosely referring to the low and high $|x|$ regions as "valence" and "sea", respectively. The analysis in section III A 2 allows to specify the $e^{\pm}$ distributions more precisely. The $M > 0$ electron state (3.20) is

$$|M\rangle = c_M^\dagger\,|\Omega\rangle = \int_{-\infty}^{\infty} \frac{dp}{2\pi\,2E_p}\left[b_p^\dagger u^\dagger(p) + d_{-p}v^\dagger(-p)\right]\Phi_M(p)\,|\Omega\rangle \equiv \int_{-\infty}^{\infty} \frac{dp}{\sqrt{2\pi\,2E_p}}\left[b_p^\dagger \widetilde{B}_{pM} + d_p \widetilde{D}_{pM}\right]|\Omega\rangle \qquad (3.47)$$

The $\widetilde{B}, \widetilde{D}$ matrices are defined to absorb the convention-dependent factor $1/\sqrt{2\pi\, 2E_p}$ arising from the definition of the Fourier transform and the u, v-spinors,

$$\widetilde{B}_{pM} = \frac{1}{\sqrt{2\pi\, 2E_p}}\, u^\dagger(p)\Phi_M(p) \qquad u(p) = \frac{1}{\sqrt{E_p+m}}\begin{pmatrix} E_p+m \\ p \end{pmatrix} \tag{3.48}$$

$$\widetilde{D}_{pM} = \frac{1}{\sqrt{2\pi\, 2E_p}}\, v^\dagger(p)\Phi_M(-p) \qquad v(p) = \frac{1}{\sqrt{E_p+m}}\begin{pmatrix} p \\ E_p+m \end{pmatrix} \tag{3.49}$$

The p-depdendence of $\widetilde{B}_{pM}$ determines at what momenta an e^- is added to the vacuum (3.14), whereas $\widetilde{D}_{pM}$ determines the p-distribution of the e^+ in the vacuum that is annihilated by d_p.

In terms of the solutions (3.34) of the Dirac equation, for $M > 0$ positive parity states,

$$\widetilde{B}^{\eta=+}_{pM} = \frac{1}{\sqrt{2\pi\, 2E_p(E_p+m)}}\,\mathrm{Re}\int_0^\infty dx\, e^{-i\sigma} f(x)\big[(E_p+p+m)e^{-ipx} + (E_p-p+m)e^{ipx}\big] = \widetilde{B}^{\eta=+}_{-p,M}$$

$$\widetilde{D}^{\eta=+}_{pM} = \frac{-1}{\sqrt{2\pi\, 2E_p(E_p+m)}}\,\mathrm{Re}\int_0^\infty dx\, e^{-i\sigma} f(x)\big[(E_p-p+m)e^{-ipx} - (E_p+p+m)e^{ipx}\big] = -\widetilde{D}_{-p,M} \tag{3.50}$$

For $p \to \infty$ the rapidly oscillating phases $\exp(\pm ipx)$ allows to approximate the x-integrals in (3.50) using the stationary phase method,

$$\int_{-\infty}^{\infty} dx F(x) e^{i\varphi(x)} \simeq e^{\varepsilon(\varphi''(x_s))i\pi/4}\sqrt{\frac{2\pi}{|\varphi''(x_s)|}}F(x_s)e^{i\varphi(x_s)} \tag{3.51}$$

where $\varepsilon(x)$ is the sign function and $\varphi(x) \simeq \varphi(x_s) + \frac{1}{2}\varphi''(x_s)(x-x_s)^2$ is a rapidly varying phase. The condition for the stationary phase is that $\partial_x\varphi(x_s) = 0$.

As $x \to \infty$ the phase of the leading term in $e^{-i\sigma}f(x)$ (3.35) varies rapidly (the phase change of the power is subleading),

$$\arg\big[\lim_{x\to\infty} e^{-i\sigma}f(x)\big] = -\sigma = -M^2 + Mx - \tfrac{1}{4}x^2 \tag{3.52}$$

Due to the $p \to -p$ symmetries in (3.50) we need only consider $p \to +\infty$. Then (3.52) can give a stationary phase at $x = x_s$ only with the Fourier phase $\exp(ipx)$ in (3.50),

$$\frac{d}{dx}(-\sigma+px)\Big|_{x=x_s} = M - \tfrac{1}{2}x_s + p = 0 \qquad \begin{cases} p - V(x_s) = -M \\ \sigma(x_s) = p^2 \\ px_s - \sigma(x_s) = p(p+2M) \end{cases} \tag{3.53}$$

In (3.50) the factor multiplying $\exp(ipx)$ is of $\mathcal{O}\left(p^{-1}\right)$ for B_{Mp} and of $\mathcal{O}\left(p^0\right)$ for D_{Mp}. Hence the oscillations of the wave function in Fig. 4 at large x are due to positrons, not electrons. The positron kinetic energy $E_p \simeq p$ and potential energy $-V(x_s)$ sum to $-M$. The sea electron forming the pair with the positron is confined by the potential to low x, together with the valence electron created by $b_p^\dagger \widetilde{B}_{pM}$. According to Fig. 4 the electrons are distributed similarly to the Schrödinger wave function. The two of them thus contribute $2M$ to the energy, so that the total energy of the $e^-(e^+e^-)$ Fock state adds up to the bound state energy M.

The next-to-leading term in the asymptotic expansion (3.35) of $f(x)$ is suppressed by $\mathcal{O}\left(\sigma^{-1/2}\right) = \mathcal{O}\left(p^{-1}\right)$ when $x \propto p$. It gives a stationary phase with the $\exp(-ipx)$ term in (3.50), whose coefficient in $\widetilde{B}_{pM}$ is of $\mathcal{O}\left(p^0\right)$. This contribution is of the same $\mathcal{O}\left(p^{-1}\right)$ as the one from the $\exp(ipx)$ term in $\widetilde{B}_{pM}$. The two contributions cancel,

$$\exp(ipx): \qquad \frac{m\sqrt{2}}{p}\, N_M\, \mathrm{Re}\Big[C_M(2p^2)^{im^2/2}\, e^{-i\pi/4}e^{ip(p+2M)}\Big]$$

$$\exp(-ipx): \qquad -\frac{m\sqrt{2}}{p}\, N_M\, \mathrm{Re}\Big[C_M^*(2p^2)^{-im^2/2}\, e^{i\pi/4}e^{-ip(p+2M)}\Big] \tag{3.54}$$

since the real part of a complex number and its conjugate are equal. Consequently

$$\lim_{p\to\infty} \widetilde{B}^+_{pM} \lesssim \mathcal{O}\left(p^{-2}\right) \tag{3.55}$$

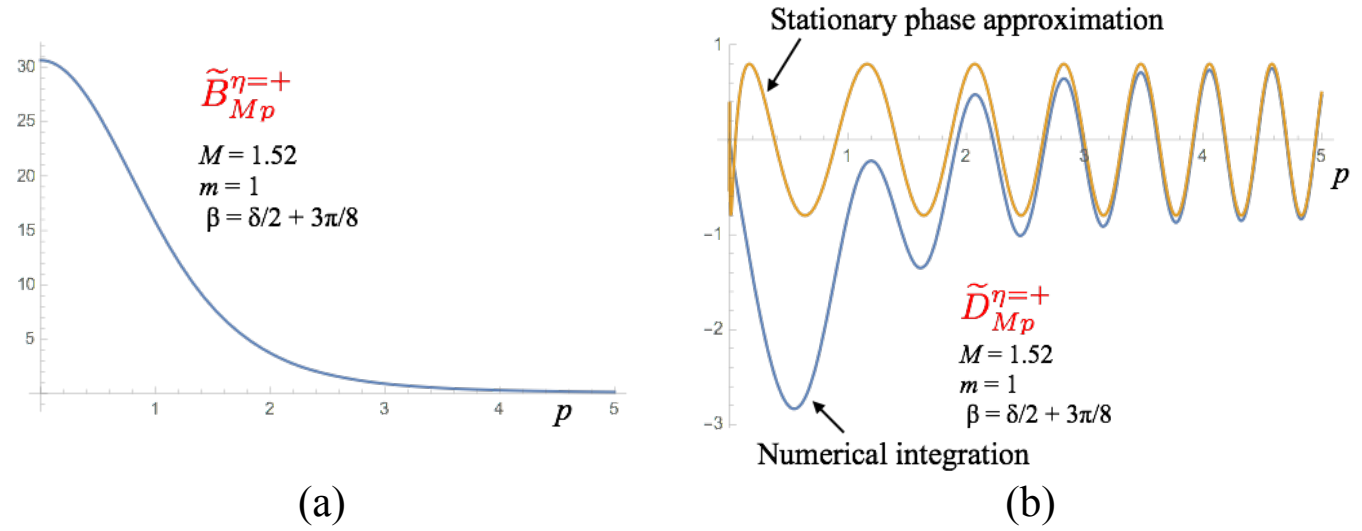

FIG. 6: Numerical results for the momentum dependence of the (a) $\widetilde{B}^{\eta=+}_{pM}$ and (b) $\widetilde{D}^{\eta=+}_{pM}$ matrices (3.50) of the ground state, for $m = 1$ and $\beta = \beta_{min}$. The stationary phase approximation for $\widetilde{D}^{\eta=+}_{pM}$ is indicated in (b).

5. *Case of* $m = 0$

The expressions of the previous section simplify considerably when the fermion mass $m = 0$. Using

$$ {}_1F_1(0, \tfrac{1}{2}, 2i\sigma) = 1 \qquad\qquad {}_1F_1(\tfrac{1}{2}, \tfrac{1}{2}, 2i\sigma) = e^{2i\sigma} \tag{3.56}$$

and the parity η convention (3.32) the components $\varphi_\eta(x), \chi_\eta(x)$ of Dirac wave function $\Phi(M, x)$ (3.28) are for any x,

$$\begin{aligned} \varphi_+(x) &= \frac{1}{\sqrt{2\pi}} \cos\left[x(M - \tfrac{1}{4}|x|)\right] \qquad & \varphi_-(x) &= \frac{1}{\sqrt{2\pi}} \sin\left[x(M - \tfrac{1}{4}|x|)\right] \\ \chi_+(x) &= \frac{i}{\sqrt{2\pi}} \sin\left[x(M - \tfrac{1}{4}|x|)\right] \qquad & \chi_-(x) &= -\frac{i}{\sqrt{2\pi}} \cos\left[x(M - \tfrac{1}{4}|x|)\right] \end{aligned} \tag{3.57}$$

where M can be any real number. The relation between β and M is

$$\beta = M^2 - n\pi \quad (\eta = +1) \qquad\qquad \beta = M^2 - \frac{\pi}{2} - n\pi \quad (\eta = -1) \tag{3.58}$$

with the integer n chosen so that $-\pi/2 \le \beta < \pi/2$.

The simple form (3.57) of the wave function allows orthonormality and completeness to be explicitly verified,

$$\int_{-\infty}^{\infty} dx\, \Phi^\dagger_\eta(M, x)\Phi_{\eta'}(M', x) = \delta_{\eta\eta'}\delta(M - M') \tag{3.59}$$

$$\sum_{\eta=\pm} \int_{-\infty}^{\infty} dM\, \Phi_\eta(M, x)\Phi^\dagger_\eta(M, y) = \sum_\eta \int_{-\infty}^{\infty} dM \begin{pmatrix} \varphi_\eta(x)\varphi_\eta(y) & -\varphi_\eta(x)\chi_\eta(y) \\ \chi_\eta(x)\varphi_\eta(y) & -\chi_\eta(x)\chi_\eta(y) \end{pmatrix} = \delta(x - y) \begin{pmatrix} 1 & 0 \\ 0 & 1 \end{pmatrix} \tag{3.60}$$

With $m = 0$ the matrix elements of the operators in the electron state (3.47) are, for $M > 0$ and $p > 0$,

$$\begin{aligned} \widetilde{B}^{\eta=+}_{p>0,M} &= \frac{1}{\pi\sqrt{2}} \int_0^\infty dx\, \cos\left[x(M - p) - \tfrac{1}{4}x^2\right] \\ \widetilde{D}^{\eta=+}_{p>0,M} &= \frac{1}{\pi\sqrt{2}} \int_0^\infty dx\, \cos\left[x(M + p) - \tfrac{1}{4}x^2\right] \end{aligned} \tag{3.61}$$

The "valence" electron distribution decreases with momentum as $1/p^3$,

$$\lim_{p\to\infty} \widetilde{B}^{\eta=+}_{pM} = \frac{1}{\pi\, 2\sqrt{2}}\, \frac{1}{(p-M)^3}\left[1+\mathcal{O}\left(p^{-1}\right)\right] \tag{3.62}$$

while the stationary phase contribution to $\widetilde{D}^{\eta=+}_{pM}$ is of $\mathcal{O}\left(p^0\right)$,

$$\lim_{p\to\infty} \widetilde{D}^{\eta=+}_{pM} = \frac{\sqrt{2}}{\sqrt{\pi}}\, \cos\left[(p+M)^2 - \tfrac{1}{4}\pi\right] \tag{3.63}$$

IV. FEATURES OF HADRONS

1. General remarks

Quantum Chromodynamics accurately describes hard scattering using perturbation theory and universal parton distributions. Numerical lattice calculations support the correctness of QCD also for soft processes. Comparisons of QCD-inspired models with data have given a general understanding of hadron dynamics [23]. Color confinement implies that the constituents of hadrons (quarks and gluons) do not exist as free states. This is related to their relativistic binding energy, which enables pair production. The dynamical breaking of chiral symmetry leads, among other things, to the observed small mass of the pion. The vast literature on QCD is summarized in [24].

Analytic approaches to soft hadron processes complement numerical evaluations. This has only been possible at the expense of additional assumptions, outside the QCD field theory framework. It is desirable to derive from QCD those model features which successfully describe data.

Perturbation theory is the main analytic, first-principles approach to QED and QCD. The perturbative characteristics of soft QCD dynamics has been underlined by Dokshitzer [25–27]. It is not completely straightforward to apply perturbation theory even to QED bound states. Already the first approximation of a bound state requires summing an infinite number of Feynman diagrams. Reorderings of the perturbative expansion lead to different, and in principle equivalent formulations [1, 28]. The $\hbar$ expansion motivates a specific "Born term" for bound states characterized by the absence of loops: Only gauge fields which satisfy the classical field equations contribute.

In section II I derived the Born term for Positronium. In the rest frame it yields the standard Schrödinger equation with the classical potential $-\alpha/r$. It gives the correct dependence of the the Positronium energy on its momentum $\boldsymbol{P}$, and a wave function that Lorentz contracts as in classical physics. Higher order (loop) corrections are expected to be calculable from the S-matrix (1.6), with the Born term used in the *in* and *out* states.

The loop expansion is a power series in $\hbar\alpha$ and as such converges only for small (perturbative) couplings. The binding energy $E_b = -\frac{1}{4}m_e\alpha^2$ of Positronium if of $\mathcal{O}\left(m_e\right)$ only for $\alpha \gtrsim 1$. Hence strongly bound (relativistic) states cannot be accessed within perturbative QED. The situation for QCD may be different because the confining potential can cause relativistic binding even at small α_s. This is the scenario that will be explored below.

In section III I discussed some properties of strongly bound states in the familiar setting of the Dirac equation, which describes the binding of an electron in a strong external field. Dirac states include virtual e^+e^- pairs whose distributions are given by the negative energy components of the Dirac wave function. A potential which confines electrons repulses positrons, giving dramatic effects on the spectrum and wave functions.

In the rest of these lectures I consider whether the concept of Born term could be applicable to hadrons. The novel features of color confinement and chiral symmetry breaking then need to appear as a consequence of the classical gluon field and ground state. I begin by recalling some phenomenological features of hadron dynamics which hint at a perturbative framework.

2. Perturbative aspects of the hadron spectrum

The spectra of heavy quarkonia have features that are remarkably similar to the Positronium spectrum (Fig. 7). The $J^{PC} = 1^{--}$ charmonium state J/ψ was dubbed the "Hydrogen atom of QCD" because it was thought to provide the key to the deciphering of hadron structure. The quarkonium spectra are in fact well described [29] by the Schrödinger

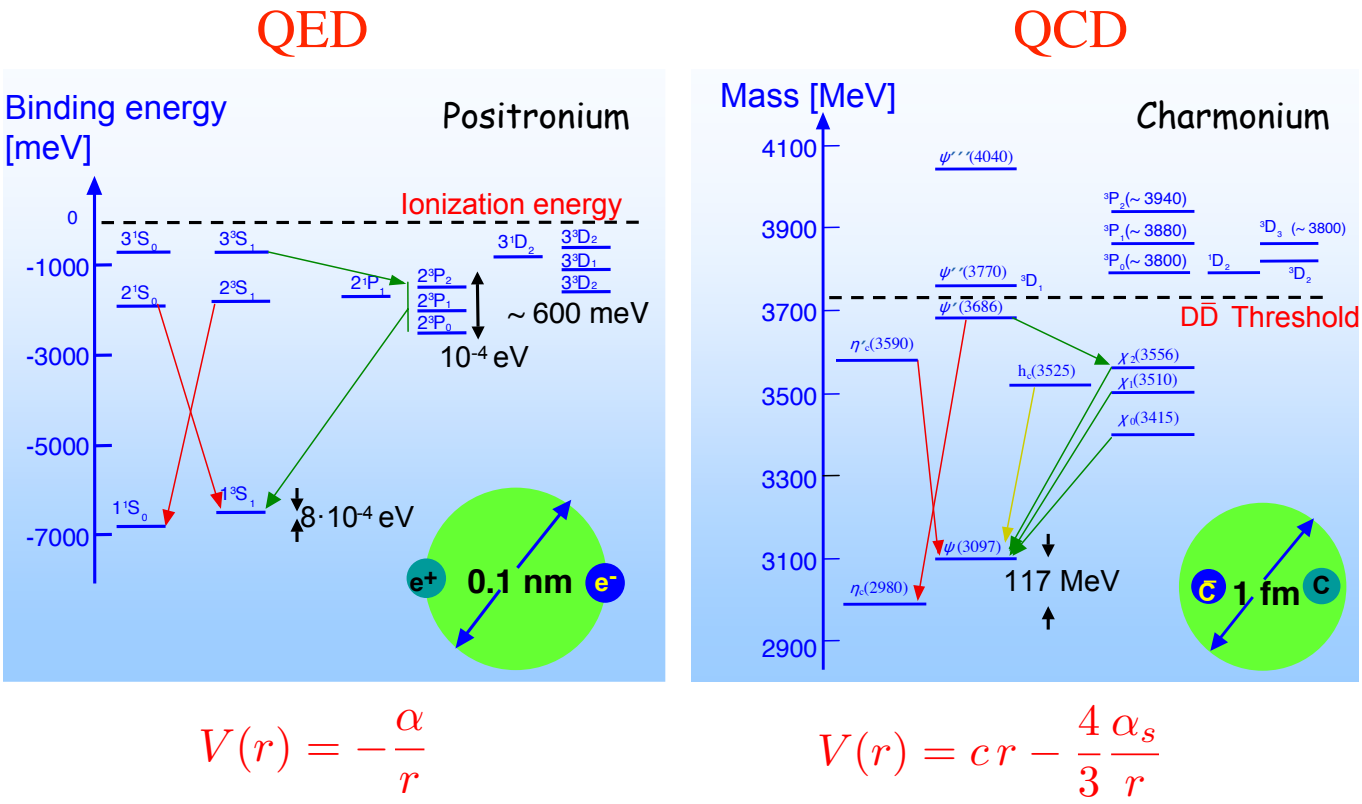

$$V(r) = -\frac{\alpha}{r} \qquad\qquad V(r) = cr - \frac{4}{3}\frac{\alpha_s}{r}$$

FIG. 7: Comparison of the Positronium and charmonium spectra. The overall features are surprisingly similar, considering that the hyperfine splittings differ by a factor $\gtrsim 10^{11}$ and that QCD is a confining, non-abelian theory.

equation, provided a linear term is added to the single gluon exchange potential,

$$V_{QED}(r) = -\frac{\alpha}{r} \qquad\qquad V_{QCD}(r) = V'r - \frac{4}{3}\frac{\alpha_s}{r} \tag{4.1}$$

The fine and hyperfine splittings agree with the perturbative corrections to the Schrödinger result. This hint from Nature merits serious consideration. It suggests that the Born approximation of atoms discussed in section II is applicable also in QCD. The QCD action has no dimensionful parameter corresponding to the slope V' of the linear potential in (4.1). In the absence of loops (renormalization) V' can only arise via a *boundary condition* in the solution of the classical gauge field equations.

The linear potential leads to color confinement and strong binding regardless of the size of α_s. The ionization threshold of QED becomes a threshold for open charm $(D, \Lambda_c, \ldots)$ pair production in QCD. Charmonium resonances of high mass are indeed observed to decay mainly into open charm states. In recent years narrow "XYZ" states have been discovered, often close to particle production thresholds [30]. As in QED, narrow widths and closeness to thresholds indicates weak coupling. The new states may be characterized as "hadron molecules" [31], but a quantitative description awaits a better understanding of hadron dynamics.

Hadrons composed of light quarks (u, d, s) have quantum numbers that allow them to be classified as $q\bar{q}$ and qqq states with specific values of quark spins and angular momenta. The bound state masses and couplings can be qualitatively modelled [32, 33]. The success of the quark description encourages a perturbative approach, since the degrees of freedom of strongly interacting constituents generally are not reflected in the spectrum. For example, the spectrum of QED in $D = 1 + 1$ dimensions (the "massive Schwinger model") has the features of e^+e^- "atomic" bound states only at weak coupling, $e/m \ll 1$. When the interaction is strong $(e/m \gg 1)$ loops dominate and the spectrum has the characteristics of weakly bound scalars [13].

The binding energies (or mass splittings) of light hadrons are of the same order as the hadron masses. Hence the internal dynamics must be ultrarelativistic, in stark contrast to atoms. One would expect to see the degrees of freedom also of gluon constituents in the hadron spectrum. Searches for "hybrid" and "glueball" states, some of which would stand out because of their quantum numbers, have not led to definite results. Physical gluons appear mainly as radiative corrections to hard interactions. The gluon distribution in the proton is large at high Q^2 and low x, but

strongly scale-dependent. At $Q \sim 1$ GeV the gluon distribution is insignificant, whereas the sea quark contribution persists at low x [34].

3. *Duality*

Hadrons couple selectively to each other. An extreme example is the X(3872) (molecular?) charmonium state, whose total width $\Gamma_{tot} < 1.2$ MeV is minimal despite apparently allowed, wide open decay channels. Light hadron dynamics is selective as well. Already at the dawn of the quark model Zweig [11] found it remarkable that the $\phi(1020)$ perfers to decay into $K\bar{K}$ (82% of the time), even though kinematics favors $\pi\pi\pi$. Fig. 8 illustrates Zweig's rule, which he formulated in terms of dual diagrams: The "connected" quark diagram (a) dominates the "disconnected" one in (b). This rule is applicable to other processes as well and today is known as the OZI rule, after Okuba, Zweig and Iizuka [35]. A review of the status of the OZI rule may be found in [36].

As indicated in Fig. 8(b) the $\phi(1020) \to \pi\pi\pi$ decay can be mediated by three (or more) gluons. The observed suppression of this process indicates that gluon exchange contributions are subleading in soft dynamics. This is consistent with the notion that the coupling α_s remains perturbative at low scales.

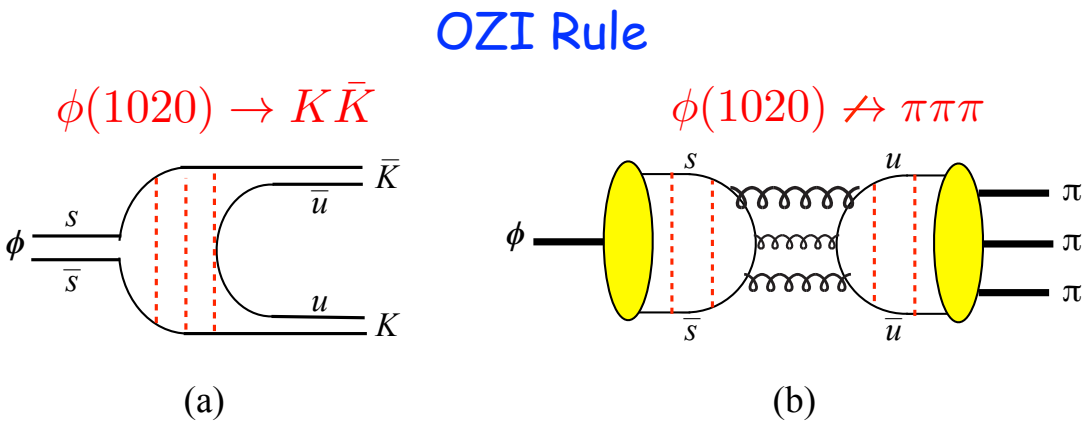

FIG. 8: According to the OZI rule, the connected quark diagram (a) dominates over the disconnected one in (b). In today's perspective the dashed lines in (a) represent the confining color field (the linear potential of (4.1)). The $u\bar{u}$ pair is created by this field ("string breaking"). In (b) there is no confining field after the $s\bar{s}$ annihilates, and the transition can be mediated only by gluon exchange.

Quark diagrams like those of Fig. 8(a) illustrate the remarkable phenomenon of "duality" in hadron dynamics [12]. Phenomenological studies show that $2 \to 2$ hadron scattering amplitudes are described *either* by the resonances in the direct (s-) channel *or* by particle exchange in the crossed (t-) channel – not by their sum. Resonances of different spins and masses must contribute in a coherent manner for them to mimic particle exchange. One aspect of this is that resonances are found to lie on approximately linear Regge trajectories [33]. A good illustration of duality is provided by the dual amplitude for $\pi^+\pi^- \to \pi^+\pi^-$ [15].

Another aspect of duality was observed by Bloom and Gilman in deep inelastic lepton scattering, $eN \to eX$ [37]. Quite unexpectedly, the x_{Bj}-dependence of the N^* contributions to the inclusive system X agree (on average) with the quark distribution of the target proton. A review of recent experimental results may be found in [38]. A further apparition is Local Parton Hadron Duality, which relates the perturbatively calculated inclusive *parton* production to the measured *hadron* distributions in high energy processes [26].

Duality is a pervasive and as yet poorly understood feature of hadron dynamics. It allows the average contribution of resonances to be described by a smoothly distributed scattering amplitude. A hint of how bound state and scattering features can mix is given by the Dirac bound states in D=1+1, discussed in section III B. The wave functions of hadrons found below have dual features such as indicated in Fig. 13.

4. $\alpha_s(Q^2)$ at low scales Q

A perturbative description of hadrons in QCD requires that the coupling $\alpha_s(Q^2)$ be of moderate size at low Q. Our knowledge [39] of the perturbative coupling α_s is summarized in Fig. 9. At the lowest perturbative scale $\alpha_s^{\overline{MS}}(m_\tau^2) = 0.334 \pm 0.014$ [40].

The coupling α_s is not directly measurable, and meaningful only in the context of a theoretical framework. Several analyses raise the possibility that $\alpha_s(Q^2)$ freezes around $Q \simeq 1$ GeV, at a value $\alpha_s^{\overline{MS}} \simeq 0.5$. In Gribov's picture of confinement [26, 41] there is, in QCD as well as in QED, a critical value of the coupling where the vacuum changes character and new features emerge,

$$\begin{aligned} \alpha^{crit}(QED) &= \pi\left(1-\sqrt{\frac{2}{3}}\right) \simeq 0.58 \quad \gg \frac{1}{137} \\ \alpha_s^{crit}(QCD) &= \frac{\pi}{C_F}\left(1-\sqrt{\frac{2}{3}}\right) \simeq 0.43 \quad \gtrsim \alpha_s(m_\tau^2) \end{aligned} \tag{4.2}$$

As indicated in Fig. 9 the running QCD coupling reaches Gribov's critical value at $Q \simeq 1$ GeV. The value of the critical coupling is small enough that a an expansion in $\alpha_s^{crit}/\pi \simeq 0.14$ may be relevant.

Fig. 10(a) shows estimates based on event shapes of the QCD coupling $\alpha_0(\mu_I)$, averaged over $0 \le Q \le \mu_I = 2$ GeV [42]. A similar analysis of event shapes in e^+e^- annihilation using NNLO perturbative QCD gave $\alpha_0(2\text{ GeV}) = 0.5132 \pm 0.0115\,(\text{exp}) \pm 0.0381\,(\text{th})$ [43]. Fig. 10(b) shows the result of an analysis using the pinch technique [44], in which the low scale coupling was estimated as $\alpha_{PT}(0) = 0.7 \pm 0.3$. Further studies of the behaviour of the QCD coupling at low scales may be found in Refs. [45].

The running of α_s originates from the renormalization of divergent loop integrals. The coupling does not run at the Born (no loop) level. If the Born approximation is adequate at low values of Q the coupling necessarily freezes.

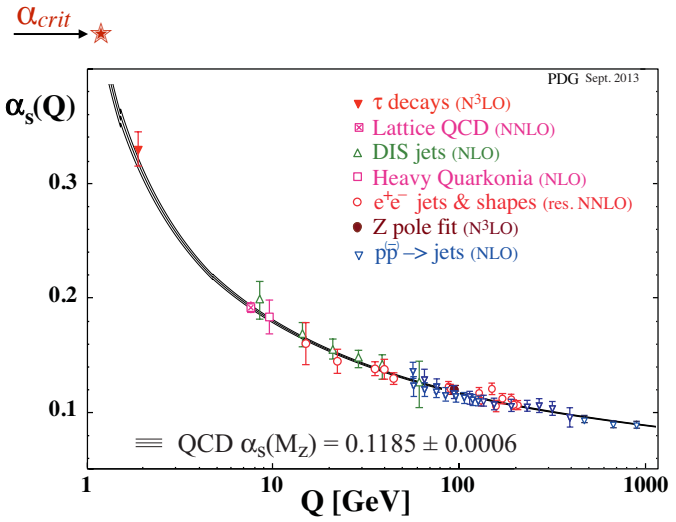

FIG. 9: The QCD coupling α_s, as measured in several processes and calculated using lattice QCD [39]. The point "α_{crit}" refers to Eq. (4.2).

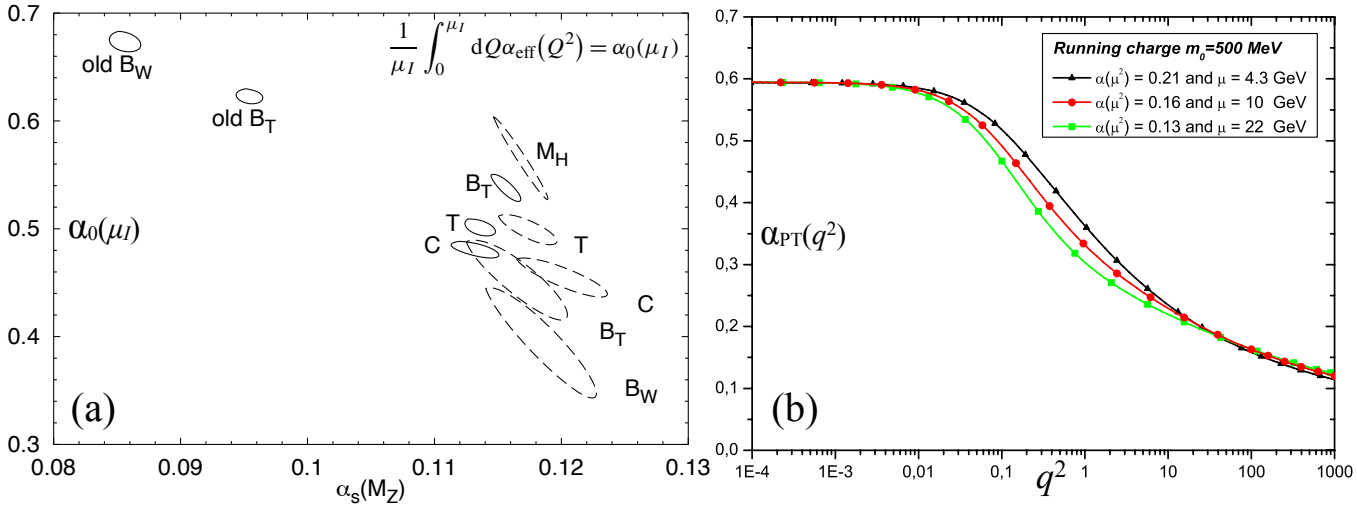

FIG. 10: (a) The average value of α_s for $Q \le \mu_I = 2$ GeV based on several measures of event shapes [42]. (b) The effective coupling of the Pinch Technique, using Schwinger-Dyson equations [44].

V. QCD BOUND STATES IN THE REST FRAME

A. The meson and baryon states

Based on the previous study of Positronium (2.3) and Dirac (3.4) states I express the meson ($\mathcal{M}$) and baryon ($\mathcal{B}$) Born level states of QCD in the rest frame ($\boldsymbol{P}=0$) as

$$|\mathcal{M};M,\boldsymbol{P}=0\rangle \;=\; \int d\boldsymbol{x}_1\,d\boldsymbol{x}_2\,\bar\psi_A(\boldsymbol{x}_1)\Phi^{AB}_{\mathcal{M}}(\boldsymbol{x}_1-\boldsymbol{x}_2)\psi_B(\boldsymbol{x}_2)\,|0\rangle \tag{5.1}$$

$$|\mathcal{B};M,\boldsymbol{P}=0\rangle \;=\; \int d\boldsymbol{x}_1\,d\boldsymbol{x}_2\,d\boldsymbol{x}_3\,\psi^\dagger_A(\boldsymbol{x}_1)\psi^\dagger_B(\boldsymbol{x}_2)\psi^\dagger_C(\boldsymbol{x}_3)\Phi^{ABC}_{\mathcal{B}}(\boldsymbol{x}_1,\boldsymbol{x}_2,\boldsymbol{x}_3)\,|0\rangle \tag{5.2}$$

The states and fields are all evaluated at a common time t (not shown). A sum over the repeated quark color indices (A,B,C) is understood, and Dirac indices suppressed. The baryon wave function needs to be translation invariant,

$$\Phi^{ABC}_{\mathcal{B}}(\boldsymbol{x}_1,\boldsymbol{x}_2,\boldsymbol{x}_3)=\Phi^{ABC}_{\mathcal{B}}(\boldsymbol{x}_1+\boldsymbol{a},\boldsymbol{x}_2+\boldsymbol{a},\boldsymbol{x}_3+\boldsymbol{a}) \tag{5.3}$$

for the state to carry momentum $\boldsymbol{P}=0$.

Similarly as for Positronium, there are no gauge links connecting the fields. The meson state is invariant under a local gauge transformation $U(\boldsymbol{x})$ provided the wave function transforms accordingly,

$$\psi(\boldsymbol{x})\to U(\boldsymbol{x})\psi(\boldsymbol{x}) \qquad\qquad \Phi_{\mathcal{M}}(\boldsymbol{x}_1-\boldsymbol{x}_2)\to U^\dagger(\boldsymbol{x}_1)\Phi_{\mathcal{M}}(\boldsymbol{x}_1-\boldsymbol{x}_2)U(\boldsymbol{x}_2) \tag{5.4}$$

The baryon wave function $\Phi_{\mathcal{B}}$ is similarly gauge dependent. The usual "color singlet" wave functions,

$$\Phi^{AB}_{\mathcal{M}}(\boldsymbol{x}_1-\boldsymbol{x}_2) \;=\; \frac{1}{\sqrt{N_C}}\delta^{AB}\Phi_{\mathcal{M}}(\boldsymbol{x}_1-\boldsymbol{x}_2) \tag{5.5}$$

$$(N_C=3)$$

$$\Phi^{ABC}_{\mathcal{B}}(\boldsymbol{x}_1,\boldsymbol{x}_2,\boldsymbol{x}_3) \;=\; \frac{1}{\sqrt{N_C!}}\epsilon^{ABC}\Phi_{\mathcal{B}}(\boldsymbol{x}_1,\boldsymbol{x}_2,\boldsymbol{x}_3) \tag{5.6}$$

are in fact invariant only under global gauge transformations.

B. Symmetries: Poincaré, Parity and Charge Conjugation for Mesons

The QCD action is invariant under Poincaré transformations (time and space translations, rotations and boosts) as well as under the discrete parity and charge conjugation transformations. The "kinetic" transformations (space translations, rotations, parity and charge conjugation) do not change the time coordinate of the field operators. The transformation of the states under kinetic transformations is explicitly determined by the representation of the corresponding subgroup to which the wave function belongs.

Time translations are generated by the Hamiltonian, which includes the interaction terms of the action. Consequently this is called a "dynamic" transformation. In order that a state be an eigenstate of the Hamiltonian its wave function should satisfy the bound state equation (section V D). Also boosts are dynamical, and moreover change the definition of simultaneity. Equal-time states in one frame are non-trivially related to equal-time states in another frame. In section II 4 we found the frame dependence of the Positronium wave function. In section VII I discuss how relativistic, Born level bound states transform under boosts.

1. Space translations

Under space translations $\boldsymbol{x}\to\boldsymbol{x}+\boldsymbol{a}$ the quark fields are transformed by the operator

$$U(\boldsymbol{a})=\exp[-i\boldsymbol{a}\cdot\boldsymbol{\mathcal{P}}] \qquad \text{where} \qquad \boldsymbol{\mathcal{P}}=\int d\boldsymbol{x}\,\psi^\dagger(\boldsymbol{x})(-i\boldsymbol{\nabla})\psi(\boldsymbol{x}) \tag{5.7}$$

(I suppress the common time t in all operators). The momentum operator satisfies

$$[\boldsymbol{\mathcal{P}},\psi(\boldsymbol{x})]=i\boldsymbol{\nabla}\psi(\boldsymbol{x}) \qquad\qquad \left[\boldsymbol{\mathcal{P}},\bar\psi(\boldsymbol{x})\right]=i\boldsymbol{\nabla}\bar\psi(\boldsymbol{x}) \tag{5.8}$$

For finite translations,

$$U(\boldsymbol{a})\psi(\boldsymbol{x})U^\dagger(\boldsymbol{a}) = \psi(\boldsymbol{x}+\boldsymbol{a}) \tag{5.9}$$

Using (5.8) and $\boldsymbol{\mathcal{P}}\,|0\rangle = 0$ we may verify that the state (5.1) is indeed at rest,

$$\boldsymbol{\mathcal{P}}\,|\mathcal{M};M,\boldsymbol{P}=0\rangle = 0 \tag{5.10}$$

2. Rotations

A rotation $\boldsymbol{x} \to R\,\boldsymbol{x}$, where R is an orthogonal 3×3 matrix, should be represented by an operator $U(R)$ which transforms the quark momentum states accordingly,

$$U(R)b(\boldsymbol{p},\lambda)U^\dagger(R) = b(R\boldsymbol{p},\lambda) \qquad\qquad U(R)d(\boldsymbol{p},\lambda)U^\dagger(R) = d(R\boldsymbol{p},\lambda) \tag{5.11}$$

where the quantization axis for the spin component λ is understood to be rotated. I next verify that this implies

$$U(R)\psi(\boldsymbol{x})U^\dagger(R) = S^{-1}(R)\psi(R\boldsymbol{x}) \tag{5.12}$$

For a rotation by an angle θ around the unit vector $\hat{\boldsymbol{n}}$ the Dirac matrix $S(R)$ is

$$S(R) = \exp\left(i\tfrac{1}{2}\theta\,\hat{\boldsymbol{n}}\cdot\boldsymbol{\Sigma}\right) \qquad \text{where} \qquad \boldsymbol{\Sigma} = \gamma_5\gamma^0\boldsymbol{\gamma} = \begin{pmatrix}\boldsymbol{\sigma} & 0\\ 0 & \boldsymbol{\sigma}\end{pmatrix} \tag{5.13}$$

$S(R)$ has the property

$$S(R)\,\boldsymbol{\gamma}\,S^{-1}(R) = R^{-1}\boldsymbol{\gamma} \tag{5.14}$$

which transforms the u-spinor,

$$S(R)u(\boldsymbol{p},\lambda) = S(R)\frac{E\gamma^0-\boldsymbol{p}\cdot\boldsymbol{\gamma}+m}{\sqrt{E+m}}\begin{pmatrix}\varphi_\lambda\\0\end{pmatrix} = \frac{E\gamma^0-\boldsymbol{p}\cdot R^{-1}\boldsymbol{\gamma}+m}{\sqrt{E+m}}S(R)\begin{pmatrix}\varphi_\lambda\\0\end{pmatrix} \equiv u(R\boldsymbol{p},\lambda) \tag{5.15}$$

In the last step I used $\boldsymbol{p}\cdot R^{-1}\boldsymbol{\gamma} = R\,\boldsymbol{p}\cdot\boldsymbol{\gamma}$ and defined the rotated u-spinor by

$$u(R\boldsymbol{p},\lambda) = \frac{E\gamma^0-R\boldsymbol{p}\cdot\boldsymbol{\gamma}+m}{\sqrt{E+m}}\begin{pmatrix}\exp\left(i\tfrac{1}{2}\theta\,\hat{\boldsymbol{n}}\cdot\boldsymbol{\sigma}\right)\varphi_\lambda\\0\end{pmatrix} \tag{5.16}$$

The v-spinor is rotated in the same way since $\boldsymbol{\Sigma}$ in (5.13) is block diagonal. Using the expression (2.5) for the field,

$$S(R)U(R)\psi(\boldsymbol{x})U^\dagger(R) = \int\frac{d\boldsymbol{p}}{(2\pi)^3 2E}\sum_\lambda\Big[u(R\,\boldsymbol{p},\lambda)e^{iR\boldsymbol{p}\cdot R\boldsymbol{x}}b(R\,\boldsymbol{p},\lambda) + v(R\,\boldsymbol{p},\lambda)e^{-iR\boldsymbol{p}\cdot R\boldsymbol{x}}d^\dagger(R\,\boldsymbol{p},\lambda)\Big] = \psi(R\,\boldsymbol{x}) \tag{5.17}$$

In the last step I changed the integration measure $d\boldsymbol{p} = d(R\,\boldsymbol{p})$. Rotations are generated by the angular momentum operator $\boldsymbol{\mathcal{J}}$,

$$U(R) = \exp[i\theta\,\hat{\boldsymbol{n}}\cdot\boldsymbol{\mathcal{J}}] \tag{5.18}$$

given by

$$\boldsymbol{\mathcal{J}} = \int d\boldsymbol{x}\,\psi^\dagger(\boldsymbol{x})\,\boldsymbol{J}\,\psi(\boldsymbol{x}) \qquad\qquad \boldsymbol{J} = \boldsymbol{x}\times(-i\boldsymbol{\nabla}) + \tfrac{1}{2}\boldsymbol{\Sigma} \tag{5.19}$$

Using

$$[\boldsymbol{\mathcal{J}},\psi(\boldsymbol{x})] = -\big[\boldsymbol{x}\times(-i\overrightarrow{\boldsymbol{\nabla}}) + \tfrac{1}{2}\boldsymbol{\Sigma}\big]\psi(\boldsymbol{x}) \qquad\qquad \big[\boldsymbol{\mathcal{J}},\bar\psi(\boldsymbol{x})\big] = \bar\psi(\boldsymbol{x})\big[\boldsymbol{x}\times(i\overleftarrow{\boldsymbol{\nabla}}) + \tfrac{1}{2}\boldsymbol{\Sigma}\big] \tag{5.20}$$

and $\boldsymbol{\mathcal{J}}\,|0\rangle = 0$ we can determine the condition that the meson state (5.1) is an eigenstate of some component of the angular momentum operator $\boldsymbol{\mathcal{J}}$,

$$\begin{aligned}\boldsymbol{\mathcal{J}}\,|\mathcal{M};M,\boldsymbol{P}=0\rangle \;=\; \int d\boldsymbol{x}_1\,d\boldsymbol{x}_2\,\bar\psi(\boldsymbol{x}_1)\Big\{&\big[\boldsymbol{x}_1\times(-i\overrightarrow{\boldsymbol{\nabla}}_1) + \tfrac{1}{2}\boldsymbol{\Sigma}\big]\Phi_{\mathcal{M}}(\boldsymbol{x}_1-\boldsymbol{x}_2)\\ &-\Phi_{\mathcal{M}}(\boldsymbol{x}_1-\boldsymbol{x}_2)\big[\boldsymbol{x}_2\times(i\overleftarrow{\boldsymbol{\nabla}}_2) + \tfrac{1}{2}\boldsymbol{\Sigma}\big]\Big\}\psi(\boldsymbol{x}_2)\,|0\rangle\end{aligned} \tag{5.21}$$

Thus

$$\mathcal{J}^z\,|\mathcal{M};M,\boldsymbol{P}=0\rangle=\lambda\,|\mathcal{M};M,\boldsymbol{P}=0\rangle\qquad\text{provided}\qquad[J^z,\Phi_{\mathcal{M}}(\boldsymbol{x})]=\lambda\,\Phi_{\mathcal{M}}(\boldsymbol{x})\tag{5.22}$$

A finite rotation transforms the meson state as

$$\begin{aligned}U(R)\,|\mathcal{M};M,\boldsymbol{P}=0\rangle&=\int d\boldsymbol{x}_1\,d\boldsymbol{x}_2\,\bar\psi(R\boldsymbol{x}_1)S(R)\Phi_{\mathcal{M}}(\boldsymbol{x}_1-\boldsymbol{x}_2)S^{-1}(R)\psi(R\boldsymbol{x}_2)\,|0\rangle\\&=\int d\boldsymbol{x}_1\,d\boldsymbol{x}_2\,\bar\psi(\boldsymbol{x}_1)S(R)\Phi_{\mathcal{M}}\big[R^{-1}(\boldsymbol{x}_1-\boldsymbol{x}_2)\big]S^{-1}(R)\psi(\boldsymbol{x}_2)\,|0\rangle\end{aligned}\tag{5.23}$$

The wave function in the rotated coordinate system is thus given by

$$\Phi^{(R)}_{\mathcal{M}}(\boldsymbol{x})=S(R)\Phi_{\mathcal{M}}\big(R^{-1}\boldsymbol{x}\big)S^{-1}(R)\tag{5.24}$$

3. Parity

The parity operator $\mathbb{P}$ reverses 3-momenta $\boldsymbol{p}$ but leaves spins λ invariant:

$$\mathbb{P}b(\boldsymbol{p},\lambda)\mathbb{P}^\dagger=b(-\boldsymbol{p},\lambda)\qquad\qquad\mathbb{P}d(\boldsymbol{p},\lambda)\mathbb{P}^\dagger=-d(-\boldsymbol{p},\lambda)\tag{5.25}$$

We could add an "intrinsic" parity for the quarks, but it is irrelevant for $q\bar q$ states so I omit it. The *relative* intrinsic parity -1 of quarks and antiquarks in (5.25) ensures that the field transforms as

$$\mathbb{P}\psi(t,\boldsymbol{x})\mathbb{P}^\dagger=\gamma^0\psi(t,-\boldsymbol{x})\qquad\qquad\mathbb{P}\bar\psi(t,\boldsymbol{x})\mathbb{P}^\dagger=\bar\psi(t,-\boldsymbol{x})\gamma^0\tag{5.26}$$

That in turn allows to consider the condition for the (rest frame) meson states to be eigenstates of parity,

$$\mathbb{P}\,|\mathcal{M};M,\boldsymbol{P}=0\rangle=\int d\boldsymbol{x}_1\,d\boldsymbol{x}_2\,\bar\psi(\boldsymbol{x}_1)\gamma^0\Phi_{\mathcal{M}}(-\boldsymbol{x}_1+\boldsymbol{x}_2)\gamma^0\psi(\boldsymbol{x}_2)\,|0\rangle=\eta_P\,|\mathcal{M};M,\boldsymbol{P}=0\rangle\tag{5.27}$$

The wave function of a parity eigenstate with eigenvalue $\eta_P=\pm1$ satisfies

$$\gamma^0\Phi_{\mathcal{M}}(-\boldsymbol{x})\gamma^0=\eta_P\Phi_{\mathcal{M}}(\boldsymbol{x})\tag{5.28}$$

4. Charge conjugation

The charge conjugation operator $\mathbb{C}$ transforms particles into antiparticles,

$$\mathbb{C}b(\boldsymbol{p},\lambda)\mathbb{C}^\dagger=d(\boldsymbol{p},\lambda)\qquad\qquad\mathbb{C}d(\boldsymbol{p},\lambda)\mathbb{C}^\dagger=b(\boldsymbol{p},\lambda)\tag{5.29}$$

In the standard Dirac matrix representation this implies (T indicates transpose)

$$\mathbb{C}\psi(t,\boldsymbol{x})\mathbb{C}^\dagger=i\gamma^0\gamma^2\bar\psi^T(t,\boldsymbol{x})\qquad\qquad\mathbb{C}\bar\psi(t,\boldsymbol{x})\mathbb{C}^\dagger=i\psi^T(t,\boldsymbol{x})\gamma^0\gamma^2\tag{5.30}$$

For a meson state to be an eigenstate of charge conjugation with eigenvalue $\eta_C=\pm1$,

$$\mathbb{C}\,|\mathcal{M};M,\boldsymbol{P}=0\rangle=\int d\boldsymbol{x}_1\,d\boldsymbol{x}_2\,\bar\psi(\boldsymbol{x}_1)\gamma^0\gamma^2\Phi^T_{\mathcal{M}}(\boldsymbol{x}_2-\boldsymbol{x}_1)\gamma^0\gamma^2\psi(\boldsymbol{x}_2)\,|0\rangle=\eta_C\,|\mathcal{M};M,\boldsymbol{P}=0\rangle\tag{5.31}$$

its wave function should satisfy

$$\gamma^0\gamma^2\Phi^T_{\mathcal{M}}(-\boldsymbol{x})\gamma^0\gamma^2=\eta_C\Phi_{\mathcal{M}}(\boldsymbol{x})\tag{5.32}$$

C. The confining field $\mathcal{A}^\mu$

1. Requirements on a viable solution

I now consider whether there is a classical field $\mathcal{A}^\mu$ which could be relevant for hadrons. Recall that in Positronium the classical field (1.9) depends on the positions $\boldsymbol{x}_1, \boldsymbol{x}_2$ of the e^- and e^+. In QCD the field will also depend on the quark colors A, B, C. The total color field generated by the hadron (which would be felt by an external color probe, excluding $\mathcal{O}(\alpha_s)$ gluon exchange) is the coherent sum of the fields of all quark color components. The total field vanishes for the meson and baryon states, see (5.45) and (5.55) below. Hence the confining field $\mathcal{A}^\mu$ referred to below concerns only the field between quarks with specific colors.

To make my arguments concerning the confining field transparent I list them as separate items. The outcome is a field with a single dimensionful parameter Λ. Possibly this is the only acceptable scenario.

#1. There is no dimensionful constant Λ_{QCD} in the classical field equations. It can only appear in their solution via a boundary condition.

#2. Rotational symmetry requires that $\mathcal{A}^\mu$ depend on the positions of the quarks, *cf.* the QED case (1.9).

#3. The quark positions determine $\mathcal{A}^0$ for all $\boldsymbol{x}$ at an instant of time. The propagating components $\boldsymbol{\mathcal{A}}$ respond to the quark positions with a delay, which would be infinite at the spatial boundary, $|\boldsymbol{x}| \to \infty$.

#4. I choose $\boldsymbol{\mathcal{A}} = 0$ in the hadron rest frame ($\boldsymbol{P} = 0$), in the gauge with wave functions (5.5), (5.6). The field felt by a moving hadron ($\boldsymbol{P} \neq 0$) is then given by a Lorentz boost of $\mathcal{A}^0$ as in (2.12).

#5. Each quark interacts with the confining field independently of the others. The color structures (5.5), (5.6) are maintained only if $\mathcal{A}^0_a T^{AB}_a \propto \delta^{AB}$. Hence $\mathcal{A}^0_a \neq 0$ only for $a = 3, 8$, in the standard notation where

$$T_3 = \frac{1}{2}\begin{pmatrix} 1 & 0 & 0 \\ 0 & -1 & 0 \\ 0 & 0 & 0 \end{pmatrix} \qquad\qquad T_8 = \frac{1}{2\sqrt{3}}\begin{pmatrix} 1 & 0 & 0 \\ 0 & 1 & 0 \\ 0 & 0 & -2 \end{pmatrix} \tag{5.33}$$

#6. In the rest frame the confining field should be a homogeneous solution of Gauss' law,

$$\boldsymbol{\nabla}^2 \mathcal{A}^0_a = 0 \qquad (a = 3, 8) \tag{5.34}$$

#7. The field energy density is, including a convenient normalization factor,

$$\sum_{a=3,8} \left[\boldsymbol{\nabla}\mathcal{A}^0_a(\boldsymbol{x})\right] \cdot \left[\boldsymbol{\nabla}\mathcal{A}^0_a(\boldsymbol{x})\right] \equiv \Lambda_3^4 + \Lambda_8^4 \equiv 12\Lambda^4 \tag{5.35}$$

Translation invariance requires that Λ be $\boldsymbol{x}$-independent, $\Lambda \neq \Lambda(\boldsymbol{x})$.

#8. The infinite field energy $\int d\boldsymbol{x} \sum_{a=3,8} \left[\boldsymbol{\nabla}\mathcal{A}^0_a(\boldsymbol{x})\right]^2 = 12\Lambda^4 \int d\boldsymbol{x}$ must be universal. Hence Λ is independent of the quark positions and colors.

#9. The simplest field $\mathcal{A}^0_a$ which satisfies the above requirements is linear in $\boldsymbol{x}$. Color and Poincaré invariance imposes a scalar product between $\boldsymbol{x}$ and a vector formed from the quark positions $\boldsymbol{x}_i$ weighted by their color charges. This implies a specific classical field for each quark component of a hadron with the color structure of (5.5), (5.6) (no sum on colors):

$$\bar\psi_A(\boldsymbol{x}_1)\psi_A(\boldsymbol{x}_2)\,|0\rangle: \quad \mathcal{A}^0_a(\boldsymbol{x}) = \boldsymbol{x} \cdot \frac{T^{AA}_a(\boldsymbol{x}_1 - \boldsymbol{x}_2)}{|T^{AA}_a(\boldsymbol{x}_1 - \boldsymbol{x}_2)|}\,\Lambda^2_a(\boldsymbol{x}_i, A) \tag{5.36}$$

$$(a = 3, 8)$$

$$\psi^\dagger_A(\boldsymbol{x}_1)\psi^\dagger_B(\boldsymbol{x}_2)\psi^\dagger_C(\boldsymbol{x}_3)\,|0\rangle: \quad \mathcal{A}^0_a(\boldsymbol{x}) = \boldsymbol{x} \cdot \frac{T^{AA}_a\,\boldsymbol{x}_1 + T^{BB}_a\,\boldsymbol{x}_2 + T^{CC}_a\,\boldsymbol{x}_3}{|T^{AA}_a\,\boldsymbol{x}_1 + T^{BB}_a\,\boldsymbol{x}_2 + T^{CC}_a\,\boldsymbol{x}_3|}\,\Lambda^2_a(\boldsymbol{x}_i, A, B, C) \tag{5.37}$$

As indicated, Λ_3 and Λ_8 may depend on the quark positions and colors, but not on $\boldsymbol{x}$. (5.35) requires that their 4th powers sum to the universal scale $12\Lambda^4$.

#10. The ratio Λ_3/Λ_8 is determined by stationarity of the field energy density (5.35).

The parameter Λ (5.35) is of $\mathcal{O}(g^0)$ and determines the energy scale through the strength of the confining field $\mathcal{A}^0_a$. The quark interactions with the confining field are $\propto g\mathcal{A}^0_a$, *i.e.*, of $\mathcal{O}(g\Lambda^2)$.

2. Field energy of the meson component (5.36)

The field energy $\int d\boldsymbol{x}\,\frac{1}{2}F_{j0}F^{j0}$ has a universal $\mathcal{O}\left(\Lambda^4\right)$ contribution (#8) and an $\mathcal{O}\left(g\Lambda^2\right)$ contribution from the interference of the confining field $\mathcal{A}^0_a$ with the standard Coulomb field A^0_a due to the quark color charges. The field energy needs to be evaluated to the same $\mathcal{O}\left(g\Lambda^2\right)$ as the quark interactions.

The standard Coulomb field A^0 generated by the $q_A(\boldsymbol{x}_1)\bar{q}_A(\boldsymbol{x}_2)$ component of the meson state (no sum on color A) is an inhomogeneous solution of Gauss' law,

$$-\boldsymbol{\nabla}^2 A^0_a(\boldsymbol{x}) = gT^{AA}_a\left[\delta^3(\boldsymbol{x}-\boldsymbol{x}_1)-\delta^3(\boldsymbol{x}-\boldsymbol{x}_2)\right] \tag{5.38}$$

When the quarks move relativistically they will generate also a vector field $\boldsymbol{A}_a$. The vector field does not interfere with $\mathcal{A}^0_a$ and so contributes only at $\mathcal{O}\left(g^2\right)$. To $\mathcal{O}\left(g\Lambda^2\right)$,

$$E^{AA}_{\mathcal{M}}(\boldsymbol{x}_1,\boldsymbol{x}_2) = -\tfrac{1}{2}\sum_{a=3,8}\int d\boldsymbol{x}\,\boldsymbol{\nabla}(\mathcal{A}^0_a+A^0_a)\cdot\boldsymbol{\nabla}(\mathcal{A}^0_a+A^0_a) \to \tfrac{1}{2}\sum_{a=3,8}\int d\boldsymbol{x}\,\mathcal{A}^0_a\,\boldsymbol{\nabla}^2 A^0_a \tag{5.39}$$

In the second step I omitted the $\mathcal{O}\left(\Lambda^4\right)$ and $\mathcal{O}\left(g^2\right)$ contributions, as well as the insertion at spatial infinity from the partial integration. The integral of the $\mathcal{O}\left(g\Lambda^2\right)$ contribution is marginally convergent, its definition affects the coefficient of the result. This scheme dependence is absorbed in the definition of Λ. From (5.36) and (5.38) we have

$$E^{AA}_{\mathcal{M}}(\boldsymbol{x}_1,\boldsymbol{x}_2) = -\tfrac{1}{2}\sum_{a=3,8} gT^{AA}_a\left[\mathcal{A}^0_a(\boldsymbol{x}_1)-\mathcal{A}^0_a(\boldsymbol{x}_2)\right] = -\tfrac{1}{2}\sum_{a=3,8} g\Lambda^2_a\,|T^{AA}_a(\boldsymbol{x}_1-\boldsymbol{x}_2)| \equiv E_{\mathcal{M}}(\boldsymbol{x}_1,\boldsymbol{x}_2) \tag{5.40}$$

Let us verify that the energy is independent of the quark color $A=1,2,3$. Since $\Lambda^4_3+\Lambda^4_8 = 12\Lambda^4$ I parametrize

$$\Lambda^2_3 = 2\sqrt{3}\,\Lambda^2\sin\beta \qquad\qquad \Lambda^2_8 = 2\sqrt{3}\,\Lambda^2\cos\beta \tag{5.41}$$

A=1:

$$E^{11}_{\mathcal{M}}(\boldsymbol{x}_1,\boldsymbol{x}_2) = -\tfrac{1}{4}g\Big(\Lambda^2_3+\frac{1}{\sqrt{3}}\Lambda^2_8\Big)|\boldsymbol{x}_1-\boldsymbol{x}_2| = -\frac{\sqrt{3}}{2}g\Lambda^2\Big(\sin\beta+\frac{1}{\sqrt{3}}\cos\beta\Big)|\boldsymbol{x}_1-\boldsymbol{x}_2| \tag{5.42}$$

From $dE^{11}_{\mathcal{M}}/d\beta = 0$ (#10 above) follows $\sin\beta = \sqrt{3}/2$ and $\cos\beta = 1/2$. Thus

$$E^{11}_{\mathcal{M}}(\boldsymbol{x}_1,\boldsymbol{x}_2) = -g\Lambda^2|\boldsymbol{x}_1-\boldsymbol{x}_2| = E_{\mathcal{M}}(\boldsymbol{x}_1,\boldsymbol{x}_2) \tag{5.43}$$

A=2: $E^{22}_{\mathcal{M}} = E_{\mathcal{M}}$ follows trivially since $|T^{11}_a| = |T^{22}_a|$ implies the same values for Λ^2_3 and Λ^2_8 as for $A=1$.

A=3: Since $T^{33}_3 = 0$ stationarity gives $\Lambda^2_3 = 0$ and $\Lambda^2_8 = 2\sqrt{3}\,\Lambda^2$,

$$E^{33}_{\mathcal{M}}(\boldsymbol{x}_1,\boldsymbol{x}_2) = -g\Lambda^2|\boldsymbol{x}_1-\boldsymbol{x}_2| = E_{\mathcal{M}}(\boldsymbol{x}_1,\boldsymbol{x}_2) \tag{5.44}$$

This completes the demonstration that the meson field energy is independent of the quark color A.

An external probe at $\boldsymbol{x}$ would sense the confinement fields generated by the coherent sum over of all quark colors $A=B$ in the meson state (5.1), with each color equally weighted due to the singlet wave function (5.5). Let us verify that a color singlet meson does not generate a color field for any quark positions $\boldsymbol{x}_1,\boldsymbol{x}_2$. From (5.36),

$$\sum_{A=1,2,3}\mathcal{A}^0_a(\boldsymbol{x};\boldsymbol{x}_1,\boldsymbol{x}_2,A) = \frac{\boldsymbol{x}\cdot(\boldsymbol{x}_1-\boldsymbol{x}_2)}{|\boldsymbol{x}_1-\boldsymbol{x}_2|}\sum_A\frac{T^{AA}_a}{|T^{AA}_a|}\,\Lambda^2_a(\boldsymbol{x}_i,A) = 0 \tag{5.45}$$

The sum vanishes for $a=3$ since $T^{11}_3 = -T^{22}_3$ and $\Lambda^2_3(A=1) = \Lambda^2_3(A=2)$, $\Lambda^2_3(A=3) = 0$. For $a=8$ we had $\Lambda^2_8(A=1,2) = \sqrt{3}\,\Lambda^2$ while $\Lambda^2_8(A=3) = 2\sqrt{3}\,\Lambda^2$. Weighting with the signs of T^{AA}_8 makes (5.45) vanish also for $a=8$.

3. Field energy of the baryon component (5.37)

The color singlet baryon wave function (5.6) assigns the quark colors $1,2,3$ to quarks at $\boldsymbol{x}_1,\boldsymbol{x}_2,\boldsymbol{x}_3$ in all permutations, with even and odd permutations having a opposite signs. Consider first the case where A,B,C in (5.37) is $1,2,3$. Gauss' law is

$$-\boldsymbol{\nabla}^2 A_a^0 = g\big[T_a^{11}\delta^3(\boldsymbol{x}-\boldsymbol{x}_1)+T_a^{22}\delta^3(\boldsymbol{x}-\boldsymbol{x}_2)+T_a^{33}\delta^3(\boldsymbol{x}-\boldsymbol{x}_3)\big] \tag{5.46}$$

As for mesons, the field energy of $\mathcal{O}\left(g\Lambda^2\right)$ arises from the interference between the confining field $\mathcal{A}_a^0$ of (5.37) and the inhomogeneous solution A_a^0 of (5.46),

$$\begin{aligned} E_{\mathcal{B}}^{123}(\boldsymbol{x}_1,\boldsymbol{x}_2,\boldsymbol{x}_3) &= \tfrac{1}{2}\sum_{a=3,8}\int d\boldsymbol{x}\,\mathcal{A}_a^0\,\boldsymbol{\nabla}^2 A_a^0 = -\tfrac{1}{2}\sum_{a=3,8} g\big[T_a^{11}\mathcal{A}_a^0(\boldsymbol{x}_1)+T_a^{22}\mathcal{A}_a^0(\boldsymbol{x}_2)+T_a^{33}\mathcal{A}_a^0(\boldsymbol{x}_3)\big] \\ &= -\tfrac{1}{2}\sum_{a=3,8} g\big|T_a^{11}\boldsymbol{x}_1+T_a^{22}\boldsymbol{x}_2+T_a^{33}\boldsymbol{x}_3\big|\,\Lambda_a^2(\boldsymbol{x}_i,1,2,3)\equiv E_{\mathcal{B}}(\boldsymbol{x}_1,\boldsymbol{x}_2,\boldsymbol{x}_3) \end{aligned} \tag{5.47}$$

Let us verify that the $\mathcal{O}\left(g\Lambda^2\right)$ field energy is independent of the color permutation. With the parametrization (5.41),

$$E_{\mathcal{B}}^{123}(\boldsymbol{x}_1,\boldsymbol{x}_2,\boldsymbol{x}_3) = -\sqrt{3}\,g\Lambda^2\Big[\tfrac{1}{2}\sin\beta\,|\boldsymbol{x}_1-\boldsymbol{x}_2|+\tfrac{1}{2\sqrt{3}}\cos\beta\,|\boldsymbol{x}_1+\boldsymbol{x}_2-2\boldsymbol{x}_3|\Big] \tag{5.48}$$

The stationarity condition $dE_{\mathcal{B}}^{123}/d\beta=0$ gives

$$\sin\beta=\frac{\sqrt{3}\,|\boldsymbol{x}_1-\boldsymbol{x}_2|}{2d(\boldsymbol{x}_1,\boldsymbol{x}_2,\boldsymbol{x}_3)} \qquad\qquad \cos\beta=\frac{|\boldsymbol{x}_1+\boldsymbol{x}_2-2\boldsymbol{x}_3|}{2d(\boldsymbol{x}_1,\boldsymbol{x}_2,\boldsymbol{x}_3)} \tag{5.49}$$

where

$$d(\boldsymbol{x}_1,\boldsymbol{x}_2,\boldsymbol{x}_3)\equiv\frac{1}{\sqrt{2}}\sqrt{(\boldsymbol{x}_1-\boldsymbol{x}_2)^2+(\boldsymbol{x}_2-\boldsymbol{x}_3)^2+(\boldsymbol{x}_3-\boldsymbol{x}_1)^2} \tag{5.50}$$

Using this in (5.48) gives

$$E_{\mathcal{B}}^{123}(\boldsymbol{x}_1,\boldsymbol{x}_2,\boldsymbol{x}_3) = -\,g\Lambda^2\,d(\boldsymbol{x}_1,\boldsymbol{x}_2,\boldsymbol{x}_3) \tag{5.51}$$

The field components (5.37) with any other permutation of the colors A,B,C will give the same field energy since $d(\boldsymbol{x}_1,\boldsymbol{x}_2,\boldsymbol{x}_3)$ is independent of the permutations of $\boldsymbol{x}_1,\boldsymbol{x}_2,\boldsymbol{x}_3$. This justifies the definition of $E_{\mathcal{B}}$ in (5.47).

It remains to consider the total color field of a baryon, given by the sum over colors A,B,C in (5.37) weighted by the color dependence ε^{ABC} of the wave function (5.6). As for mesons, we may keep the quark positions $\boldsymbol{x}_1,\boldsymbol{x}_2,\boldsymbol{x}_3$ fixed. For $a=3$ and $A,B,C=1,2,3$ we have using (5.49),

$$\mathcal{A}_{a=3}^0(\boldsymbol{x};123)=\frac{\boldsymbol{x}\cdot(\boldsymbol{x}_1-\boldsymbol{x}_2)}{|\boldsymbol{x}_1-\boldsymbol{x}_2|}\,\frac{\sqrt{3}\,|\boldsymbol{x}_1-\boldsymbol{x}_2|}{2d(\boldsymbol{x}_1,\boldsymbol{x}_2,\boldsymbol{x}_3)}\,2\sqrt{3}\,\Lambda^2=3\Lambda^2\,\frac{\boldsymbol{x}\cdot(\boldsymbol{x}_1-\boldsymbol{x}_2)}{d(\boldsymbol{x}_1,\boldsymbol{x}_2,\boldsymbol{x}_3)} \tag{5.52}$$

Since $T_3^{11}=-T_3^{22}$ and $\varepsilon^{123}=-\varepsilon^{213}$ we have $\mathcal{A}_{a=3}^0(\boldsymbol{x};123)=\mathcal{A}_{a=3}^0(\boldsymbol{x};213)$. The switch $1\leftrightarrow 2$ will similarly not change the color field for any other permutation of $1,2,3$. Multiplying by a factor 2 we may thus restrict the sum to the even permutations,

$$\sum_{A,B,C}\varepsilon^{ABC}\mathcal{A}_{a=3}^0(\boldsymbol{x};ABC)=\frac{6\Lambda^2}{d(\boldsymbol{x}_1,\boldsymbol{x}_2,\boldsymbol{x}_3)}\,\boldsymbol{x}\cdot\big[(\boldsymbol{x}_1-\boldsymbol{x}_2)+(\boldsymbol{x}_2-\boldsymbol{x}_3)+(\boldsymbol{x}_3-\boldsymbol{x}_1)\big]=0 \tag{5.53}$$

For $a=8$ and $A,B,C=1,2,3$ we have

$$\mathcal{A}_{a=8}^0(\boldsymbol{x};123)=\frac{\boldsymbol{x}\cdot(\boldsymbol{x}_1+\boldsymbol{x}_2-2\boldsymbol{x}_3)}{|\boldsymbol{x}_1+\boldsymbol{x}_2-2\boldsymbol{x}_3|}\,\frac{|\boldsymbol{x}_1+\boldsymbol{x}_2-2\boldsymbol{x}_3|}{2d(\boldsymbol{x}_1,\boldsymbol{x}_2,\boldsymbol{x}_3)}\,2\sqrt{3}\,\Lambda^2=\sqrt{3}\,\Lambda^2\,\frac{\boldsymbol{x}\cdot(\boldsymbol{x}_1+\boldsymbol{x}_2-2\boldsymbol{x}_3)}{d(\boldsymbol{x}_1,\boldsymbol{x}_2,\boldsymbol{x}_3)} \tag{5.54}$$

Since $T_8^{11}=T_8^{22}$ and $\varepsilon^{123}=-\varepsilon^{213}$ the sum $\mathcal{A}_{a=8}^0(\boldsymbol{x};123)+\mathcal{A}_{a=8}^0(\boldsymbol{x};213)=0$. The two amplitudes related by a switch $1\leftrightarrow 2$ will similarly cancel each other for any other permutation of $1,2,3$. Thus an external color probe will not detect the baryon via its confining field,

$$\sum_{A,B,C}\varepsilon^{ABC}\mathcal{A}_a^0(\boldsymbol{x};ABC)=0 \tag{5.55}$$

The vanishing of the total confining field $\mathcal{A}_a^0$ for mesons and baryons means that this field does not transmit interactions between hadrons, only between quarks of specific colors in the same hadron. This is a non-abelian feature. In a $U(1)$ gauge theory the confinement field corresponding to (5.36) would be

$$\mathcal{A}^0(\boldsymbol{x};\boldsymbol{x}_1,\boldsymbol{x}_2)=\frac{\boldsymbol{x}\cdot(\boldsymbol{x}_1-\boldsymbol{x}_2)}{|\boldsymbol{x}_1-\boldsymbol{x}_2|}\,\Lambda^2 \tag{5.56}$$

An external observer would see an electric field of magnitude Λ^2, aligned with $\boldsymbol{x}_1-\boldsymbol{x}_2$. The sum over $\boldsymbol{x}_1,\boldsymbol{x}_2$ weighted by the wave function need not vanish, giving rise to long-range correlations of undiminished strength. The vanishing of the field in non-abelian theories for each $\boldsymbol{x}_1,\boldsymbol{x}_2$ avoids this feature.

Interactions between hadrons can occur through annihilations between a quark in one hadron and an antiquark in another. This is related to string breaking as in Fig. 8(a). There is also $\mathcal{O}(\alpha_s)$ perturbative gluon exchange which is not considered here.

D. The bound state equations ($\boldsymbol{P}=0$)

1. The meson confining potential

The meson state (5.1) should be an eigenstate of the QCD Hamiltonian,

$$H_{QCD}(\mathcal{A})\,|\mathcal{M};M,\boldsymbol{P}=0\rangle=M\,|\mathcal{M};M,\boldsymbol{P}=0\rangle \tag{5.57}$$

At $\mathcal{O}\left(\alpha_s^0\right)$ (more precisely, $\mathcal{O}\left(g\Lambda^2\right)$) only the classical confining field $\mathcal{A}$ determined in section V C 1 appears in the Hamiltonian. Since the field was determined for a system at rest we have $\boldsymbol{P}=0$ and $E=M$ in (5.57). The Hamiltonian is assumed to annihilate the vacuum, $H_{QCD}\,|0\rangle=0$, since the color summed confining field vanishes for each hadron. String breaking effects before color summation is treated iteratively, as discussed in sections I 6 and VIII 6. Quark and gluon production is possible via perturbative contributions which are not considered here.

The classical field $\mathcal{A}_a^0$ is specific for each color and spatial configuration of the quarks. The quark interaction term in H_{QCD} gives for the component (5.36) of the meson state (no sum on A)

$$\begin{aligned}
&\Big[\int d\boldsymbol{x}\sum_{a,C,D}\psi_C^\dagger(\boldsymbol{x})g\mathcal{A}_a^0(\boldsymbol{x})T_a^{CD}\psi_D(\boldsymbol{x})\Big]\bar\psi_A(\boldsymbol{x}_1)\psi_A(\boldsymbol{x}_2)\,|0\rangle\\
&\quad=\Big[\sum_{a,C}\bar\psi_C(\boldsymbol{x}_1)g\mathcal{A}_a^0(\boldsymbol{x}_1)T_a^{CA}\psi_A(\boldsymbol{x}_2)-\sum_{a,D}\bar\psi_A(\boldsymbol{x}_1)g\mathcal{A}_a^0(\boldsymbol{x}_2)T_a^{AD}\psi_D(\boldsymbol{x}_2)\Big]\,|0\rangle\\
&\quad=\sum_{a=3,8}gT_a^{AA}\big[\mathcal{A}_a^0(\boldsymbol{x}_1)-\mathcal{A}_a^0(\boldsymbol{x}_2)\big]\bar\psi_A(\boldsymbol{x}_1)\psi_A(\boldsymbol{x}_2)\,|0\rangle=-2E_{\mathcal{M}}(\boldsymbol{x}_1,\boldsymbol{x}_2)\bar\psi_A(\boldsymbol{x}_1)\psi_A(\boldsymbol{x}_2)\,|0\rangle
\end{aligned} \tag{5.58}$$

In the final equality I noted that the dependence on the confining field is the same as in (5.40). This combination was found to be independent of the quark color A, and given by (5.43).

Since $\bar\psi_A(\boldsymbol{x}_1)\psi_A(\boldsymbol{x}_2)\,|0\rangle$ is an eigenstate of the quark interactions this is also the case for the meson potential, obtained by adding the field energy $E_{\mathcal{M}}$,

$$V_{\mathcal{M}}(\boldsymbol{x}_1-\boldsymbol{x}_2)=-2E_{\mathcal{M}}(\boldsymbol{x}_1,\boldsymbol{x}_2)+E_{\mathcal{M}}(\boldsymbol{x}_1,\boldsymbol{x}_2)=g\Lambda^2\,|\boldsymbol{x}_1-\boldsymbol{x}_2| \tag{5.59}$$

The fact that the potential is linear is obviously welcome from a phenomenological point of view. It appears to be the only alternative in the framework I am describing here.

2. The baryon confining potential

The quark interaction term in H_{QCD} gives, operating on the component (5.37) of the baryon wave function,

$$\begin{aligned}
&\Big[\int d\boldsymbol{x}\sum_{a,D,E}\psi_D^\dagger(\boldsymbol{x})g\mathcal{A}_a^0(\boldsymbol{x})T_a^{DE}\psi_E(\boldsymbol{x})\Big]\psi_A^\dagger(\boldsymbol{x}_1)\psi_B^\dagger(\boldsymbol{x}_2)\psi_C^\dagger(\boldsymbol{x}_3)\,|0\rangle\\
&\quad=\sum_{a=3,8}g\big[T_a^{AA}\mathcal{A}_a^0(\boldsymbol{x}_1)+T_a^{BB}\mathcal{A}_a^0(\boldsymbol{x}_2)+T_a^{CC}\mathcal{A}_a^0(\boldsymbol{x}_3)\big]\psi_A^\dagger(\boldsymbol{x}_1)\psi_B^\dagger(\boldsymbol{x}_2)\psi_C^\dagger(\boldsymbol{x}_3)\,|0\rangle
\end{aligned} \tag{5.60}$$

From (5.47) we see that the eigenvalue is $-2E_{\mathcal{B}}(\boldsymbol{x}_1,\boldsymbol{x}_2,\boldsymbol{x}_3)$. The baryon potential is obtained by adding the field energy to the quark interaction energy,

$$V_{\mathcal{B}}(\boldsymbol{x}_1,\boldsymbol{x}_2,\boldsymbol{x}_3) = -E_{\mathcal{B}}(\boldsymbol{x}_1,\boldsymbol{x}_2,\boldsymbol{x}_3) = g\Lambda^2\, d(\boldsymbol{x}_1,\boldsymbol{x}_2,\boldsymbol{x}_3) \tag{5.61}$$

with $d(\boldsymbol{x}_1,\boldsymbol{x}_2,\boldsymbol{x}_3)$ defined in (5.50). When two quarks in the baryon are at the same position, $\boldsymbol{x}_2 = \boldsymbol{x}_3$, we have $d(\boldsymbol{x}_1,\boldsymbol{x}_2,\boldsymbol{x}_2) = |\boldsymbol{x}_1 - \boldsymbol{x}_2|$. Consequently the baryon potential reduces to the meson potential,

$$V_{\mathcal{B}}(\boldsymbol{x}_1,\boldsymbol{x}_2,\boldsymbol{x}_2) = V_{\mathcal{M}}(\boldsymbol{x}_1 - \boldsymbol{x}_2) \tag{5.62}$$

The translation invariance ($\boldsymbol{x}_i \to \boldsymbol{x}_i + \boldsymbol{a}$) of the meson and baryon potentials (5.59) and (5.61) is a consequence of the states being color singlets. Postulating analogous confining fields for single quark states would break Poincaré invariance.

Furthermore, as may be surmised from the expression (5.48) for the baryon field energy, the three quarks are confined along $|\boldsymbol{x}_1 - \boldsymbol{x}_2|$ by the $\mathcal{A}^0_3$ potential and along $|\boldsymbol{x}_1 + \boldsymbol{x}_2 - 2\boldsymbol{x}_3|$ by the $\mathcal{A}^0_8$ potential. In #5 of section V C 1 I noted that only the $a = 3, 8$ color fields, which have diagonal color generators, preserve the color structure (5.6) of the wave function. These two diagonal generators of $SU(3)$ allow to confine at most three quarks (having two independent separations). Thus an analogous confining potential could not be constructed for, *e.g.*, $(q\bar{q})(q\bar{q})$ states, even if they were color singlets. In the present scenario the XYZ multi-quark states [30] seem best understood as hadron molecules.

3. Meson bound state equation

In section V D 1 we saw that the component (5.36) of the meson state is an eigenstate of the interaction Hamiltonian $H_{int}(\mathcal{A}^0)$, with the potential $V_{\mathcal{M}}$ (5.59) as eigenvalue. For the meson to be an eigenstate of the full Hamiltonian as in (5.57) that component must be an eigenstate also of the free Hamiltonian H_0,

$$\big[H_0 + V_{\mathcal{M}}(\boldsymbol{x}_1 - \boldsymbol{x}_2) - M\big]\, \bar{\psi}^{(1)}_A(\boldsymbol{x}_1)\Phi_{\mathcal{M}}(\boldsymbol{x}_1 - \boldsymbol{x}_2)\psi^{(2)}_A(\boldsymbol{x}_2)\,|0\rangle = 0 \qquad \text{(no sum on } A\text{)} \tag{5.63}$$

The color reduced wave function (5.5) is included in (5.63) to indicate the Dirac matrix structure. A flavor index $f = 1, 2$ is added to the quark field $\psi^{(f)}$ to allow for the case of unequal masses. The free Hamilonian is

$$H_0 = \sum_{f,C} \int d\boldsymbol{x}\, \bar{\psi}^{(f)}_C(\boldsymbol{x})\big(-i\vec{\boldsymbol{\nabla}}\cdot\boldsymbol{\gamma} + m_f\big)\psi^{(f)}_C(\boldsymbol{x}) \tag{5.64}$$

where the arrow on $\boldsymbol{\nabla}$ indicates the direction of differentiation. Recalling that the vacuum $|0\rangle$ is annihilated by H_{QCD} (5.63) becomes

$$\Big\{\bar{\psi}^{(1)}_A(\boldsymbol{x}_1)\big(i\overleftarrow{\boldsymbol{\nabla}}_1\cdot\boldsymbol{\gamma} + m_1\big)\gamma^0\Phi_{\mathcal{M}}(\boldsymbol{x}_1 - \boldsymbol{x}_2)\psi^{(2)}_A(\boldsymbol{x}_2) - \bar{\psi}^{(1)}_A(\boldsymbol{x}_1)\Phi_{\mathcal{M}}(\boldsymbol{x}_1 - \boldsymbol{x}_2)\gamma^0\big(-i\vec{\boldsymbol{\nabla}}_2\cdot\boldsymbol{\gamma} + m_2\big)\psi^{(2)}_A(\boldsymbol{x}_2)\Big]\,|0\rangle$$
$$= \big[M - V_{\mathcal{M}}(\boldsymbol{x}_1 - \boldsymbol{x}_2)\big]\bar{\psi}^{(1)}_A(\boldsymbol{x}_1)\Phi_{\mathcal{M}}(\boldsymbol{x}_1 - \boldsymbol{x}_2)\psi^{(2)}_A(\boldsymbol{x}_2)\,|0\rangle = 0 \tag{5.65}$$

where $\boldsymbol{\nabla}_j \equiv \partial/\partial\boldsymbol{x}_j$. Since the state (5.1) involves an integral over $\boldsymbol{x}_1, \boldsymbol{x}_2$ we may partially integrate $\overleftarrow{\boldsymbol{\nabla}}_1 \to -\vec{\boldsymbol{\nabla}}_1$ so that the derivative acts on the wave function, and similarly $\vec{\boldsymbol{\nabla}}_2 \to -\overleftarrow{\boldsymbol{\nabla}}_2$. Identifying the coefficients of the quark fields gives the bound state equation

$$i\boldsymbol{\nabla}\cdot\big\{\gamma^0\boldsymbol{\gamma}, \Phi(\boldsymbol{x})\big\} + m_1\gamma^0\Phi(\boldsymbol{x}) - m_2\Phi(\boldsymbol{x})\gamma^0 = \big[M - V_{\mathcal{M}}(\boldsymbol{x})\big]\Phi(\boldsymbol{x}) \tag{5.66}$$

where I denoted $\boldsymbol{x}_1 - \boldsymbol{x}_2 = \boldsymbol{x}$.

The separation of angular variables in the rest frame and the derivation of radial equations for the meson wave function may be found in [46] for the equal-mass case ($m_1 = m_2$). I review this in the section VI C.

4. Baryon bound state equation

The derivation of the bound state equation for the baryon wave function $\Phi_{\mathcal{B}}$ (5.6) of the state (5.2) is similar to that for mesons. For generality I shall assume that all three quarks have distinct flavors $f = 1, 2, 3$. The condition

corresponding to (5.63) gives

$$\sum_{j=1}^{3}\big[-i\overrightarrow{\boldsymbol{\nabla}}_j\cdot(\gamma^0\boldsymbol{\gamma})_j+m_j\gamma_j^0\big]\Phi_{\mathcal{B}}(\boldsymbol{x}_1,\boldsymbol{x}_2,\boldsymbol{x}_3)=\big[M-V_{\mathcal{B}}(\boldsymbol{x}_1,\boldsymbol{x}_2,\boldsymbol{x}_3)\big]\Phi_{\mathcal{B}}(\boldsymbol{x}_1,\boldsymbol{x}_2,\boldsymbol{x}_3) \tag{5.67}$$

where $\boldsymbol{\nabla}_j\equiv\partial/\partial\boldsymbol{x}_j$ and the subscript j on the Dirac matrices indicates which (suppressed) index on $\Phi_{\mathcal{B}}$ they are contracted with. The expression for the baryon potential $V_{\mathcal{B}}(\boldsymbol{x}_1,\boldsymbol{x}_2,\boldsymbol{x}_3)$ is given in (5.61).

The separation of variables in the baryon equation (5.67) and the frame dependence of its wave function remain to be addressed.

VI. REST FRAME MESON WAVE FUNCTIONS

In this section I discuss some properties of the solutions of the meson bound state equation (5.66) with the linear potential (5.59). I begin with the case of $D=1+1$ dimensions, which allows to address several of the novel properties in a simple setting with analytical solutions [21]. I then consider $D=2+1$ and $D=3+1$. For simplicity I assume the quark masses to be equal, $m_1=m_2=m$. For $D=1+1$ the solution with unequal masses may be found in [21]. Solutions in frames with non-vanishing bound state momentum $\boldsymbol{P}$ are discussed in section VII.

A. $D=1+1$ dimensions

1. *Analytic solution*

I represent the Dirac matrices with Pauli matrices as in (3.26) for the Dirac equation. The bound state equation (5.66) with $m_1=m_2=m$ then reads

$$i\partial_x\{\sigma_1,\Phi(x)\}+m\,[\sigma_3,\Phi(x)]=[M-V(x)]\Phi(x) \tag{6.1}$$

where[2]

$$V(x)=g\Lambda^2\,|x|\equiv V'\,|x| \tag{6.2}$$

Since $\Phi(x)$ is a 2×2 matrix it can be expanded in Pauli matrices,

$$\Phi(x)=\phi_0(x)\mathbb{1}+\phi_1(x)\,\sigma_1+\phi_2(x)\,i\sigma_2+\phi_3(x)\,\sigma_3 \tag{6.3}$$

The bound state equation (6.1) for the wave function of the $q\bar{q}$ state (5.1) has common features, but also differences, compared to the Dirac equation (3.25) for the single fermion state (3.4).

(a) The Dirac coordinate x refers to the fixed external field $A^0(x)$. For the meson case $x=x_1-x_2$ is the distance between the quark and the antiquark, and $V(x)=V(x_1-x_2)$. Thus the meson equation is translation invariant.

(b) The meson wave function (6.3) has four scalar components *vs.* the Dirac wave function's two components (3.28). However, ϕ_2 and ϕ_3 do not contribute to the anti-commutator in (6.1) and may be solved algebraically:

$$\phi_2(x)=\frac{2m}{M-V(x)}\phi_1(x)\qquad\qquad\phi_3(x)=0 \tag{6.4}$$

(c) The coupled differential equations for ϕ_0 and ϕ_1,

$$2i\partial_x\phi_1(x)\;=\;(M-V)\phi_0(x) \tag{6.5}$$

$$2i\partial_x\phi_0(x)\;=\;(M-V)\Big[1-\frac{4m^2}{(M-V)^2}\Big]\phi_1(x) \tag{6.6}$$

---

[2] For convenience in comparison with earlier results the notation in section III uses $e=1$ in (3.27), corresponding to a scale in which $V'=\frac{1}{2}$. From now on I show the scale V' explicitly.

reduce to the single 2nd order equation

$$\partial_x^2\phi_1(x) + \frac{\varepsilon(x)V'}{M-V}\,\partial_x\phi_1(x) + \big[\tfrac{1}{4}(M-V)^2 - m^2\big]\phi_1(x) = 0 \tag{6.7}$$

where $\varepsilon(x)$ is the sign function. This may be compared with (3.30) in the Dirac case.

(d) A phase convention analogous to the Dirac (3.31) may be imposed at $x = 0$ and then holds for all x,

$$\phi_1^*(x) = \phi_1(x) \qquad\qquad \phi_0^*(x) = -\phi_0(x) \tag{6.8}$$

(e) Solutions of parity $\eta = \pm 1$ may be defined analogously[3] to the Dirac (3.32),

$$\phi_1(-x) = \eta\,\phi_1(x) \qquad\qquad \phi_0(-x) = -\eta\,\phi_0(x) \tag{6.9}$$

Consequently the differential equations may be solved for $x \geq 0$ with the constraint

$$\phi_0(0) = 0 \quad (\eta = +1) \qquad\qquad \phi_1(0) = 0 \quad (\eta = -1) \tag{6.10}$$

(f) The wave functions depend on M and x only through the dimensionless variable[4] $\tau(x)$

$$\tau(x) = (M-V)^2/V' \qquad\qquad \partial_x = -2\,\varepsilon(x)(M-V)\partial_\tau \tag{6.11}$$

The 2nd order equation (6.7) is in terms of τ,

$$16\,\partial_\tau^2\,\phi_1(\tau) + \Big[1 - \frac{4m^2}{V'\tau}\Big]\phi_1(\tau) = 0 \tag{6.12}$$

which has the general solution

$$\phi_1(\tau) = \tau\,\exp(-i\tfrac{1}{4}\tau)\big[a\,{}_1F_1(1 - i\tfrac{1}{2}\,\mathtt{m}^2, 2, i\tfrac{1}{2}\tau) + b\,U(1 - i\tfrac{1}{2}\,\mathtt{m}^2, 2, i\tfrac{1}{2}\tau)\big] \tag{6.13}$$

where ${}_1F_1$ and U are the confluent hypergeometric functions of the first and second kind, respectively. The parameters a and b are constants and the dimensionless mass $\mathtt{m}$ is

$$\mathtt{m}^2 \equiv \frac{m^2}{V'} \tag{6.14}$$

2. Non-relativistic and relativistic limits

(a) $\mathtt{m} \to \infty$: *Non-relativistic limit*

In the non-relativistic limit $M = 2m + E_b$, where the fermion mass m is much larger than the binding energy E_b and the potential $V(x)$. The Schrödinger equation (3.43) specifies the mass dependence $E_b \sim V \propto m^{-1/3}$. Taking $\mathtt{m} \to \infty$ at fixed $\mathtt{m}^{1/3}V(x)$ in (6.13) gives [2, 21]

$$\tau\,e^{-i\tau/4}\,{}_1F_1(1 - i\tfrac{1}{2}\,\mathtt{m}^2, 2, i\tfrac{1}{2}\tau) \;=\; 4\,\mathtt{m}^{-2/3}e^{\pi\mathtt{m}^2/2}\mathrm{Ai}\big[\mathtt{m}^{1/3}(V-E_b)/\sqrt{V'}\,\big]\Big[1 + \mathcal{O}\big(\mathtt{m}^{-4/3}\big)\Big] \tag{6.15}$$

$$\begin{aligned}\tau\,e^{-i\tau/4}\,U(1 - i\tfrac{1}{2}\,\mathtt{m}^2, 2, i\tfrac{1}{2}\tau) \;&=\; -2\,\mathtt{m}^{4/3}\frac{\pi e^{-\pi\mathtt{m}^2/2}}{\Gamma(1 - i\frac{1}{2}\,\mathtt{m}^2)}\Big\{\mathrm{Ai}\big[\mathtt{m}^{1/3}(V-E_b)/\sqrt{V'}\,\big] + i\,\mathrm{Bi}\big[\mathtt{m}^{1/3}(V-E_b)/\sqrt{V'}\,\big]\Big\} \\ &\quad\times\Big[1 + \mathcal{O}\big(\mathtt{m}^{-4/3}\big)\Big]\end{aligned} \tag{6.16}$$

The Airy Ai-solution (6.15) agrees (up to the normalization) with the Schrödinger wave function (3.44). The Airy Bi-function is not normalizable, indicating that we need to take $b = 0$ in (6.13). In the next section VI A 3 I discuss why this is necessary even in the relativistic case.

---

[3] $\eta = -\eta_P$ in (5.28) since I follow the convention of [21]. In $D = 1 + 1$ charge conjugation does not provide an independent constraint.

[4] This corresponds to the variable $\sigma(x)$ in (3.28) for the Dirac equation. Since the expressions in section III assume $V' = \frac{1}{2}$ the definition (6.11) of $\tau(x)$ differs from the definition of $\sigma(x)$ by a factor of 2.

(b) $\tau \to \infty$: *Large M or large $V(x)$*

Substituting the ansatz $\phi_1(\tau \to \infty) = N\,\mathrm{Re}\big[\tau^{i\alpha}\, e^{i\beta\tau+\gamma}\big]$ into the differential equation (6.12) and comparing the terms of $\mathcal{O}\,(\tau^n)$ with $n = 0, -1$ determines the parameters $\alpha = -\frac{1}{2}\mathtt{m}^2$ and $\beta = \frac{1}{4}$. Thus

$$\phi_1(\tau \to \infty) = N \cos\big[\tfrac{1}{4}\tau - \tfrac{1}{2}\mathtt{m}^2 \log(\tfrac{1}{2}\tau) + \gamma\big] \tag{6.17}$$

The analytic solution (6.13) with $b = 0$ specifies

$$N = \frac{4a}{\mathtt{m}\sqrt{\pi}}\sqrt{\exp(\pi\mathtt{m}^2) - 1} \qquad\qquad \gamma = \arg\Gamma(1 + i\tfrac{1}{2}\mathtt{m}^2) - \tfrac{1}{2}\pi \tag{6.18}$$

From (6.5),

$$\phi_0(\tau \to \infty) = -4i\partial_\tau\phi_1(\tau \to \infty) = i\,N \sin\big[\tfrac{1}{4}\tau - \tfrac{1}{2}\mathtt{m}^2 \log(\tfrac{1}{2}\tau) + \gamma\big] \tag{6.19}$$

The result may be summarized as

$$\lim_{\tau\to\infty}\big[\phi_1(\tau) + \phi_0(\tau)\big] = \lim_{\tau\to\infty}\big[\phi_1(\tau) - \phi_0(\tau)\big]^* = N \exp\big[i\tfrac{1}{4}\tau - i\tfrac{1}{2}\mathtt{m}^2 \log(\tfrac{1}{2}\tau) + i\gamma\big] \tag{6.20}$$

The absolute value of (6.20) is independent of τ as in the Dirac case (3.35). There we saw that the wave function at large $|x|$ was due to the positron component of the virtual e^+e^- pairs, since positrons were repulsed by the linear potential. In the present case the constant norm of the wave function might be interpreted as being dual to pair production. The real pairs would be produced when string breaking is taken into account. I discuss this further below.

(c) $m \to 0$: *Massless quarks*

The bound state equation (6.12) is trivial for $m = 0$. The $\tau \to \infty$ solution (6.20) is then exact for all values of τ,

$$\lim_{m\to 0}\big[\phi_1(\tau) + \phi_0(\tau)\big] = \lim_{m\to 0}\big[\phi_1(\tau) - \phi_0(\tau)\big]^* = N \exp\big[i\tfrac{1}{4}\tau + i\gamma\big] \tag{6.21}$$

3. Discrete spectrum

An essential difference between the meson and Dirac equations arises due to the algebraic conditions (6.4): $\phi_2(x)$ is singular at $M - V(x) = 0$ unless $\phi_1(\tau = 0) = 0$. The differential equation (6.12) allows $\phi_1(\tau \to 0) \propto \tau^\alpha$ with $\alpha = 0,\ 1$. In order for $\phi_2(x)$ to be regular we must choose $\phi_1(\tau \to 0) \propto \tau^1$, which implies $b = 0$ in the solution (6.13). The same constraint ensures the normalizability of the wave function in the non-relativistic limit (6.16). The $x = 0$ continuity constraint (6.10) can then be satisfied only for *discrete* bound state masses M.

Meson states with distinct eigenvalues $M_a \neq M_b$ are orthogonal, as seen from

$$\langle M_b|H\,|M_a\rangle = M_a\langle M_b|M_a\rangle = M_b\langle M_b|M_a\rangle \tag{6.22}$$

The bound state equations imply wave function orthogonality [21],

$$\int_{-\infty}^{\infty} dx\,\mathrm{Tr}\,\big[\Phi_b^\dagger(x)\Phi_a(x)\big] = 0 \quad \text{for } M_a \neq M_b \tag{6.23}$$

which is equivalent to the orthogonality of the states,

$$\begin{aligned}\langle M_b|M_a\rangle \;&=\; \int_{-\infty}^{\infty}\Big[\prod_{i=1,2} dx_{bi}dx_{ai}\Big]\langle 0|\psi^\dagger(x_{b2})\Phi_b^\dagger(x_{b1}-x_{b2})\gamma^0\psi(x_{b1})\bar\psi(x_{a1})\Phi_a(x_{a1}-x_{a2})\psi(x_{a1})\,|0\rangle \\ &=\; \int_{-\infty}^{\infty} dx_{a1}dx_{a2}\,\mathrm{Tr}\,\big[\Phi_b^\dagger(x_{a1}-x_{a2})\Phi_a(x_{a1}-x_{a2})\big] = 2\pi\delta(0)\int_{-\infty}^{\infty} dx\,\mathrm{Tr}\,\big[\Phi_b^\dagger(x)\Phi_a(x)\big] = 0\end{aligned} \tag{6.24}$$

where $\delta(0)$ represents momentum conservation: both states are defined in the rest frame. For $a = b$ the normalization integral diverges due to the constant norm (6.20) of the meson wave function at large $|x|$. A normalization to $\delta(M_a - M_b)$ as in (3.39) is not possible when M_a, M_b are discrete.

To illuminate this puzzle, consider the $m \to 0$ analytic solution (6.21). For any finite m, however small, the regularity of $\phi_2(\tau)$ requires $\phi_1(\tau = 0) = 0$. Imposing also the continuity condition (6.10) at $x = 0$ (where $\tau = M^2/V'$) gives for $x \geq 0$,

$$M_n^2(m \to 0) \;=\; 2V'\big[2n - \tfrac{1}{2}(1+\eta)\big]\pi \tag{6.25}$$

$$\phi_1(x) \;=\; N\cos\big[-\tfrac{1}{2}M_n x + \tfrac{1}{4}V'x^2 + \tfrac{1}{4}(1-\eta)\pi\big] \tag{6.26}$$

where the parity η is defined in (6.9) and n is an integer. The trigonometric functions (6.26) do not form a complete functional basis when the masses are restricted to the discrete values (6.25).

These issues do not arise for the Dirac states. The Dirac wave functions (3.34) are regular for all values of σ, allowing a continuous spectrum. This reflects the unconfined positron component of the Dirac state which can have any energy. The continuous mass spectrum ensures orthonormality and completeness, as was verified in (3.59) and (3.60) for the $m \to 0$ wave functions (3.57).

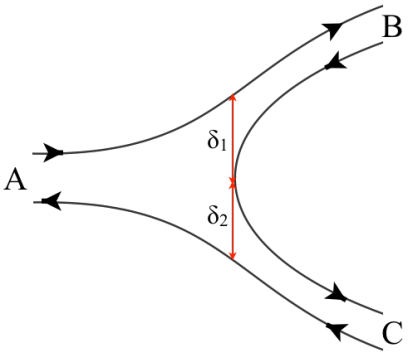

FIG. 11: Dual diagram generated by the annihilation of an antiquark in meson B with a quark in meson C.

The Dirac equation is derived under the assumption that the electron interacts only with the external field, not with any other bound electron nor with the e^+e^- pairs in the higher Fock states. In mesons the $q\bar{q}$ pairs of a given color mutually interact via the classical field (5.36) that they generate. Since the classical field vanishes when summed over quark colors (5.45) the field does not induce interactions between mesons (neglecting $\mathcal{O}(\alpha_s)$ gluon exchange). However, a quark in one meson can annihilate an antiquark in another meson if their space-time coordinates coincide (*cf.* the double annihilation in (6.24)). This gives rise to "string breaking", as depicted by the dual diagram in Fig. 11. The amplitude for this diagram may be calculated in terms of the meson wave wavefunctions obtained from a "tree-level" bound state equation such as (6.1) (more precisely, (7.7) for bound state momentum P). For a linear potential $V(\delta_1 + \delta_2) = V(\delta_1) + V(\delta_2)$, so there is no instantaneous change in the potential energy. The amplitude of Fig. 11 is of $\mathcal{O}\left(1/\sqrt{N_c}\right)$ compared to the tree-level states (5.1), N_c being the number of colors.

The process of Fig. 11 implies that the meson states (5.1) are not orthogonal to two-meson states. The splitting and fusion process can be repeated any number of times, leading to overlaps with multi-meson states and hadron loop corrections to the tree-level wave functions. A new basis of "dressed" states will be obtained by diagonalizing the interactions induced by Fig. 11. Such corrections are necessary, and hopefully also sufficient, to generate a complete orthonormal set of normalizable states with unitary scattering amplitudes at $\mathcal{O}\left(\alpha_s^0\right)$. Verifying this is an import avenue for future research.

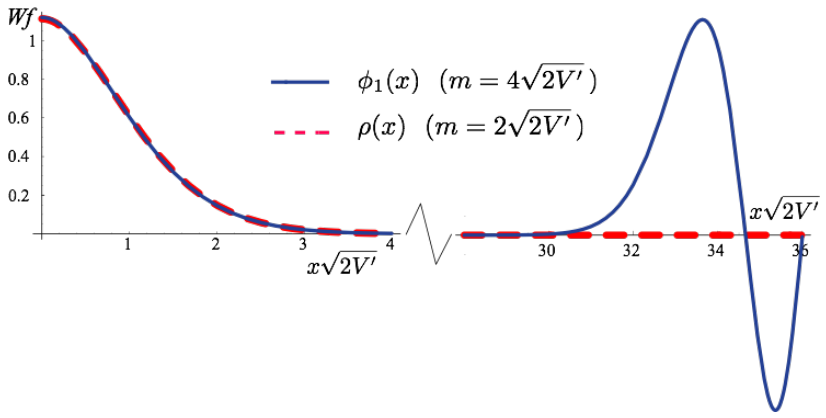

FIG. 12: The $\phi_1(x)$ wave function (6.13) (with $b = 0$) of the ground state meson wave function (solid blue line) compared to the solution $\rho(x)$ of the Schrödinger equation (3.43) with the reduced mass (dashed red line). The meson mass is $8.4100\sqrt{2V'}$ while the binding energy of the Schrödinger solution is $E_b = 0.4043\sqrt{2V'}$. Both wave functions are normalized to unity in the region $0 \leq x\sqrt{2V'} \leq 5$. Figure from [21].

4. Duality

Fig. 12 shows the $\phi_1(x)$ wave function of the ground state ($\eta = +1$) meson. The quark mass $m = 4\sqrt{2V'}$ is large enough to ensure good agreement with the Schrödinger wave function $\rho(x)$ in the non-relativistic region where $V(x) \ll 2m$.

In the region where $V(x) \gg 2m$ the wave function oscillates with constant amplitude (6.20). This behavior may be compared with that of the Dirac wave function in Fig. 4 (where $m = \sqrt{2V'}$). A comparison of Figs. 4a,b shows that the magnitude of the oscillations relative to the wave function at $x = 0$ depends sensitively on the parameter β of the Dirac wave function (3.34). Mesons with non-singular wave functions have $b = 0$ in (6.13), leaving only the overall normalization a as a free parameter: the relative magnitude of the oscillations cannot be adjusted. Since ϕ_1 depends on x via the function $\tau(x) = (M - V)^2/V'$ we have $\phi_1(x = 0) = \phi_1(x = 2M/V')$, as seen in Fig. 12.

The Dirac state (3.20) has a "valence" component $\propto b_p^\dagger$ and a "sea" component $\propto d_p$. The sea reflects the momentum distribution of the positron component in the state. Eq. (3.63) shows that at large momenta (related to the rapid oscillations at large $|x|$ in coordinate space) the wave function has only a sea component. The valence component vanishes for $p \to \infty$, as seen in Fig. 6(a) and Eq. (3.62).

The meson state (5.1) has four components[5], $b^\dagger b$, $b^\dagger d^\dagger$, db and $dd^\dagger$. For high excitations $M \gg V(x)$ and in the region of the oscillations where $V(x) \gg M$ only one component dominates. Both cases correspond to the $\tau \to \infty$ limit given in (6.20). In order to make contact with the parton picture I consider the ultrarelativistic limit where the quark mass m can be neglected.

Expressing the quark fields in the meson state (5.1) in terms of the b and d operators as in (2.5), with the u, v spinors of (3.48) and (3.49) evaluated for $m = 0$, and Fourier transforming the wave function as in (3.8) we get (suppressing colors),

$$|M\rangle = \int_{-\infty}^{\infty} \frac{dp}{2\pi\, 2|p|} \Big\{ \varepsilon(p)\phi_2(p) b_p^\dagger b_p + \big[\phi_1(p) - \varepsilon(p)\phi_0(p)\big] b_p^\dagger d_{-p}^\dagger + \big[\phi_1(p) + \varepsilon(p)\phi_0(p)\big] b_p d_{-p} + \varepsilon(p)\phi_2(p) d_{-p}^\dagger d_{-p} \Big\} |0\rangle \tag{6.27}$$

where the $\phi_i(p)$ are the momentum space versions of the wave function components $\phi_i(x)$ defined in (6.3). According to (6.4) $\phi_2(x) = 2m\phi_1(x)/(M - V)$ vanishes for $m = 0$ (and contributes at non-leading order even for finite m in the $\tau \to \infty$ limit). Using the parity relations (6.9) the Fourier transforms of $\phi_1(x)$ and $\phi_0(x)$ are

$$\begin{aligned} \phi_1(p) &= \int_{-\infty}^{\infty} dx\, \phi_1(x)\, e^{-ipx} = \int_0^{\infty} dx\, \phi_1(x) \big(e^{-ipx} + \eta e^{+ipx} \big) = \eta\, \phi_1(-p) \\ \phi_0(p) &= \int_{-\infty}^{\infty} dx\, \phi_0(x)\, e^{-ipx} = \int_0^{\infty} dx\, \phi_0(x) \big(e^{-ipx} - \eta e^{+ipx} \big) = -\eta\, \phi_0(-p) \end{aligned} \tag{6.28}$$

The combinations appearing in the state (6.27) are thus

$$\phi_1(p) \pm \phi_0(p) = \int_0^{\infty} dx \Big\{ \big[\phi_1(x) \pm \phi_0(x)\big] e^{-ipx} + \eta \big[\phi_1(x) \mp \phi_0(x)\big] e^{ipx} \Big\} \tag{6.29}$$

From (6.26) we find

$$\phi_1(x) + \phi_0(x) = \big[\phi_1(x) - \phi_0(x)\big]^* = N \exp\big[- i\tfrac{1}{2} M x + i\tfrac{1}{4} V' x^2 + i\tfrac{1}{4}(1 - \eta)\pi \big] \tag{6.30}$$

Using $\eta \exp[-i(1 - \eta)\pi/4] = \exp[i(1 - \eta)\pi/4]$ gives

$$\phi_1(p) + \phi_0(p) = N\, e^{i(1-\eta)\pi/4} \int_0^{\infty} dx \Big\{ \exp\big[- ix(p + \tfrac{1}{2}M) + i\tfrac{1}{4} V' x^2 \big] + \exp\big[ix(p + \tfrac{1}{2}M) - i\tfrac{1}{4} V' x^2 \big] \Big\} \tag{6.31}$$

$$\phi_1(p) - \phi_0(p) = N\, e^{-i(1-\eta)\pi/4} \int_0^{\infty} dx \Big\{ \exp\big[- ix(p - \tfrac{1}{2}M) - i\tfrac{1}{4} V' x^2 \big] + \exp\big[ix(p - \tfrac{1}{2}M) + i\tfrac{1}{4} V' x^2 \big] \Big\} \tag{6.32}$$

I now consider the two limits mentioned above.

(a) $M \to \infty$, $V(x)$ fixed

We may drop the $\mathcal{O}\left(x^2\right)$ term in the exponents: $\frac{1}{4} x V(x) \ll \frac{1}{2} x M$. The two terms may be combined into a single

---

[5] The color field causes a Bogoliubov transformation analogous to (3.9), so that b and d do not annihilate the vacuum.

integral,

$$\phi_1(p) + \phi_0(p) \;=\; N\, e^{i(1-\eta)\pi/4} \int_{-\infty}^{\infty} dx\, \exp\big[-ix(p+\tfrac{1}{2}M)\big] = N\, e^{i(1-\eta)\pi/4}\, 2\pi\, \delta(p+\tfrac{1}{2}M)$$

$$\phi_1(p) - \phi_0(p) \;=\; N\, e^{-i(1-\eta)\pi/4} \int_{-\infty}^{\infty} dx\, \exp\big[-ix(p-\tfrac{1}{2}M)\big] = N\, e^{-i(1-\eta)\pi/4}\, 2\pi\, \delta(p-\tfrac{1}{2}M) \tag{6.33}$$

The expression (6.27) for the state reduces to

$$|M \gg V\rangle = \frac{1}{M}\, N\, e^{i(1-\eta)\pi/4} \Big[b^\dagger_{M/2} d^\dagger_{-M/2} + \eta\, b^\dagger_{-M/2} d^\dagger_{M/2} \Big] \tag{6.34}$$

The wave function of a highly excited state (large M), at separations x between the quarks where the potential $V(x)$ is small compared to M, has only the valence $b^\dagger d^\dagger$ quark component, as in the parton picture. The bound state wave function reduces to a plane wave ($p = \pm\frac{1}{2}M$) due to its oscillations at large τ and the linearity of the potential.

Quark-Hadron duality is a remarkable feature of data on hadron scattering (section IV 3). In $e^+e^- \to X$ (with X an inclusive hadron state) direct channel resonances build the cross section at low energies. At high energies the total cross section for hadron production can be calculated in the quark and gluon basis. Even the distribution of individual hadrons (mostly pions) follows the distribution of the partons (mostly gluons).

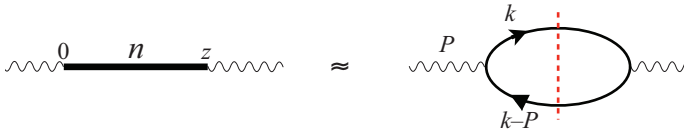

FIG. 13: Duality between a resonance n and a quark-loop contribution to the imaginary part of a current propagator [21].

The Bloom-Gilman duality of Deep Inelastic electron Scattering $e + M \to e + X$ expresses the fact that the resonance contributions to the final state X agree with the scaling parton contribution at high values of M_X. This may be another implication of the valence quark dominance in (6.34).

(b) M fixed, $V(x) \to \infty$

For $p \to +\infty$ the phase in the exponent of (6.31) has a stationary phase at

$$\frac{d}{dx}\big[-x(p+\tfrac{1}{2}M) + \tfrac{1}{4}V'x^2\big] = 0 \qquad\qquad M = V(x) - 2p \tag{6.35}$$

The stationary phase approximation (3.51) gives

$$\lim_{p\to+\infty} \big[\phi_1(p) + \phi_0(p)\big] \;=\; 4N e^{i(1-\eta)\pi/4} \sqrt{\frac{\pi}{V'}}\, \cos\Big[\frac{1}{V'}(p+\tfrac{1}{2}M)^2 - \frac{\pi}{4}\Big] \tag{6.36}$$

$$\lim_{p\to+\infty} \big[\phi_1(p) - \phi_0(p)\big] \;=\; 0 \tag{6.37}$$

where the latter result follows because the stationary phase in the exponent of (6.32) is at $p < 0$. On the other hand, from (6.28)

$$\lim_{p\to+\infty} \big[\phi_1(-p) - \phi_0(-p)\big] = \lim_{p\to+\infty} \eta\, \big[\phi_1(p) + \phi_0(p)\big] \tag{6.38}$$

We may combine the nonvanishing $p \to \pm\infty$ limits as

$$\lim_{p\to\infty} \big[\phi_1(p) + \varepsilon(p)\phi_0(p)\big] = 4N e^{\varepsilon(p) i(1-\eta)\pi/4} \sqrt{\frac{\pi}{V'}}\, \cos\Big[\frac{1}{V'}(|p|+\tfrac{1}{2}M)^2 - \frac{\pi}{4}\Big] \tag{6.39}$$

The stationary phase approximation (6.35) implies that $x \propto p$. Comparing with (6.27) we find

$$|M \ll V\rangle = \int_{|p|\gg M} \frac{dp}{2\pi\, 2|p|} \big[\phi_1(p) + \varepsilon(p)\phi_0(p)\big]\, b_p d_{-p}\, |0\rangle \tag{6.40}$$

Only the $b_p d_{-p}\,|0\rangle$ component of a meson state survives in the region of large $|x|$ where the wave function is oscillating. The rapid oscillations of the coefficient (6.39) will suppress this component when it is convoluted with a function that has a smooth p-dependence. The result (6.34) is analogous to the one for the Dirac state (3.47), where the d_p contribution dominates the $b^\dagger_p$ one at large $|p|$ according to (3.62) and (3.63).

B. Mesons in $D = 2 + 1$ dimensions

1. Bound state equation

In $D = 2 + 1$ dimensions there is one transverse direction, but the Dirac matrices may still be represented using the 2×2 Pauli matrices,

$$\gamma^0 = \sigma_3 \qquad \gamma^0\gamma^1 = \sigma_1 \qquad \gamma^0\gamma^2 = \sigma_2 \tag{6.41}$$

The arguments for the classical confining potential in section V C are independent of the dimension. The bound state equation for mesons at rest has the same form as in (5.66). In the representation (6.41) and assuming $m_1 = m_2 = m$,

$$i\,\{\boldsymbol{\sigma}\cdot\boldsymbol{\nabla}, \Phi(\boldsymbol{x})\} + m\,[\sigma_3, \Phi(\boldsymbol{x})] = \big[M - V(\boldsymbol{x})\big]\Phi(\boldsymbol{x}) \qquad\qquad V(\boldsymbol{x}) = V'|\boldsymbol{x}| \tag{6.42}$$

with $V' = g\Lambda^2$ and the $D = 2+1$ vector notation illustrated by $\boldsymbol{\sigma} = (\sigma_1, \sigma_2)$, Since the potential depends only on $|\boldsymbol{x}|$ there is rotational symmetry in the $(1, 2)$-plane. In terms of the cylindrical (r, φ) coordinates

$$\begin{aligned} x^1 &= r\cos\varphi \qquad & \partial_1 &= \cos\varphi\,\partial_r - \frac{\sin\varphi}{r}\partial_\varphi \\ x^2 &= r\sin\varphi \qquad & \partial_2 &= \sin\varphi\,\partial_r + \frac{\cos\varphi}{r}\partial_\varphi \end{aligned} \tag{6.43}$$

the single "z" component of the angular momentum $\boldsymbol{J}$ defined in (5.19) is

$$J^z = -i(x^1\partial_2 - x^2\partial_1) + \tfrac{i}{2}\gamma^1\gamma^2 = -i\partial_\varphi + \tfrac{1}{2}\sigma_3 \tag{6.44}$$

The 2×2 wave function $\Phi(\boldsymbol{x})$ may be expanded so that each of the four components transforms covariantly under rotations (5.24) in the plane,

$$\Phi^\lambda(\boldsymbol{x}) = \big[F_a^\lambda(r) + \frac{\boldsymbol{\sigma}\cdot\boldsymbol{x}}{r}F_b^\lambda(r) + \frac{\boldsymbol{\sigma}\times\boldsymbol{x}}{r}F_c^\lambda(r) + \sigma_3\,F_d^\lambda(r)\big]e^{i\lambda\varphi} \tag{6.45}$$

The coefficients of the radial functions are invariant under rotations due to (5.14): $S(R)\boldsymbol{\gamma}S^{-1}(R) = R^{-1}\boldsymbol{\gamma}$,

$$S(R)\boldsymbol{\gamma}S^{-1}(R)\cdot R^{-1}\boldsymbol{x} = (R^{-1}\boldsymbol{\gamma})\cdot(R^{-1}\boldsymbol{x}) = \boldsymbol{\gamma}\cdot\boldsymbol{x} \qquad\qquad S(R)\boldsymbol{\gamma}S^{-1}(R)\times R^{-1}\boldsymbol{x} = \boldsymbol{\gamma}\times\boldsymbol{x} \tag{6.46}$$

The cross product has only a z-component, which is preserved by rotations around the z-axis. Consequently a rotation by θ only changes $\varphi \to \varphi - \theta$ in the wave function (6.45).

Equivalently, we may easily check that

$$[J^z, \boldsymbol{\sigma}\cdot\boldsymbol{x}] = [J^z, \boldsymbol{\sigma}\times\boldsymbol{x}] = [J^z, \sigma_3] = 0 \tag{6.47}$$

Hence the wave function (6.45) is an eigenfunction of J^z with eigenvalue λ,

$$\big[J^z, \Phi^\lambda(\boldsymbol{x})\big] = \lambda\,\Phi^\lambda(\boldsymbol{x}) \tag{6.48}$$

which as in (5.22) ensures that the meson state (5.1) is an eigenstate of the angular momentum operator $\mathcal{J}^z$ with eigenvalue λ.

In the parity condition (5.28) $\boldsymbol{x} \to -\boldsymbol{x}$ implies $\varphi \to \varphi + \pi$. From (6.45) we see that

$$\sigma_3\Phi^\lambda(-\boldsymbol{x})\sigma_3 = (-1)^\lambda\Phi^\lambda(\boldsymbol{x}) \tag{6.49}$$

which implies that the parity of the state is $\eta_P = (-1)^\lambda$. The charge conjugation condition (5.32)

$$\sigma_2\Phi^T(-\boldsymbol{x})\sigma_2 = (-1)^\lambda\Phi(\boldsymbol{x}) \tag{6.50}$$

gives the same result since $F_d(r) = 0$ (see (6.54) below). Thus also $\eta_C = (-1)^\lambda$.

Substituting the expansion (6.45) into the bound state equation (6.42) gives the constraints

$$1: \qquad 2i\Big(\frac{F_b^\lambda}{r} + \partial_r F_b^\lambda\Big) + \frac{2\lambda}{r}F_c^\lambda = (M - V)F_a^\lambda \tag{6.51}$$

$$\boldsymbol{\sigma}\cdot\boldsymbol{x}: \qquad 2i\partial_r F_a^\lambda + 2imF_c^\lambda = (M - V)F_b^\lambda \tag{6.52}$$

$$\boldsymbol{\sigma}\times\boldsymbol{x}: \qquad \frac{2\lambda}{r}F_a^\lambda - 2imF_b^\lambda = (M - V)F_c^\lambda \tag{6.53}$$

$$\sigma_3: \qquad 0 = (M - V)F_d^\lambda \tag{6.54}$$

Eliminating F_c^λ we get two coupled first order radial equations,

$$2r(M-V)\partial_r F_a^\lambda = -4m\lambda F_a^\lambda - i\big[(M-V)^2 - 4m^2\big] r F_b^\lambda$$

$$2r(M-V)\partial_r F_b^\lambda = -2\big[(M-V) - 2\lambda m\big] F_b^\lambda - i\big[(M-V)^2 - \frac{4\lambda^2}{r^2}\big] r F_a^\lambda \tag{6.55}$$

2. *Wave function in the $r \to \infty$ limit*

In $D = 1+1$ dimensions the bound state equation (6.12) depends on the coordinate x and the bound state mass M only via the variable τ of (6.11). In $D = 2+1$ this no longer holds, as the radius r appears explicitly. In studying the $r \to \infty$ limit it is nevertheless helpful to introduce

$$\tau(r) = \big[M - V(r)\big]^2 / V' \qquad\qquad \partial_r = -2(M-V)\partial_\tau \tag{6.56}$$

The bound state equations can then be expressed as

$$-4V'\tau\partial_\tau F_a^\lambda = -\frac{4m\lambda}{r} F_a^\lambda - i\big[V'\tau - 4m^2\big] F_b^\lambda \tag{6.57}$$

$$-4V'\tau\partial_\tau F_b^\lambda = -\frac{2}{r}\big[(M-V) - 2\lambda m\big] F_b^\lambda - i\big[V'\tau - \frac{4\lambda^2}{r^2}\big] r F_a^\lambda \tag{6.58}$$

Neglecting terms of $\mathcal{O}\left(r^{-1}\right)$ on the rhs. this simplifies to

$$\partial_\tau i F_a^\lambda = -\frac{1}{4}\Big(1 - \frac{4m^2}{V'\tau}\Big) F_b^\lambda \tag{6.59}$$

$$\partial_\tau F_b^\lambda = -\frac{1}{2\tau} F_b^\lambda + \frac{1}{4} i F_a^\lambda \tag{6.60}$$

Eliminating F_a^λ and neglecting $\mathcal{O}\left(\sigma^{-2}\right)$ leaves

$$\partial_\tau^2 F_b^\lambda + \frac{1}{2\tau}\partial_\tau F_b^\lambda + \frac{1}{16}\Big(1 - \frac{4m^2}{V'\tau}\Big) F_b^\lambda = 0 \qquad\qquad (\tau \to \infty) \tag{6.61}$$

As in section VI A 2(b) (6.61) implies the leading behavor

$$\lim_{r\to\infty} F_a^\lambda = \lim_{r\to\infty} F_b^\lambda \propto \frac{1}{\tau^{1/4}}\, \tau^{-im^2/2V'} e^{i\tau/4} \propto \frac{1}{\sqrt{r}}\, r^{-im^2/V'} \exp\big[i(M-V)^2/4V'\big] \tag{6.62}$$

Apart from the factor $\tau^{-1/4} \simeq 1/\sqrt{r}$ this result is similar to the behavior of the $D = 1+1$ wave function (6.20). From (6.53) follows that F_c^λ is suppressed by a factor $1/r$ compared to $F_{a,b}^\lambda$.

As in (6.24) the normalization integral is proportional to

$$\int d\boldsymbol{x}\, \mathrm{Tr}\left[{\Phi^\lambda}^\dagger(\boldsymbol{x})\Phi^\lambda(\boldsymbol{x})\right] = 4\pi \int_0^\infty dr\, r\big[|F_a^\lambda|^2 + |F_b^\lambda|^2 + |F_c^\lambda|^2\big] \tag{6.63}$$

The norm of the wave function for large r is constant, since the phase space factor r compensates for the $1/\sqrt{r}$ fall-off of the wave function in (6.62). Hence an interpretation of the asymptotic wave function as representing, via duality, the constant density of hadrons produced via string breaking remains viable.

3. *Spectrum in $D = 2+1$*

Eq. (6.53) implies that F_c^λ is singular at $M = V(r)$ unless the combination of $F_{a,b}^\lambda$ appearing on the lhs. of the equation vanishes at this point. This condition, which ensures that the norm (6.63) of the wave function is locally finite, is satisfied only for discrete values of the bound state mass M. The demonstration is quite analogous to the

$D = 1 + 1$ case discussed in section VI A 3. For simplicity I discuss here only two special cases, where the coupled equations (6.55) are easily reduced to a single second order equation.

(a) $m = 0$, $\lambda \neq 0$

Eliminating F_b^λ gives for a second order equation for F_a^λ

$$\partial_r^2 F_a^\lambda + \Big[\frac{1}{r} + \frac{V'}{M-V}\Big]\partial_r F_a^\lambda + \Big[\tfrac{1}{4}(M-V)^2 - \frac{\lambda^2}{r^2}\Big]F_a^\lambda = 0 \qquad (m=0) \tag{6.64}$$

implying $F_a^\lambda(r \to 0) \propto r^{\pm\lambda}$. A finite density at $r = 0$ requires $F_a^\lambda(r \to 0) \propto r^{|\lambda|}$. For $\lambda \neq 0$ this fixes $F_a^\lambda(r = 0) = 0$ and $\partial_r F_a^\lambda(r = 0) \neq 0$, with the slope of the derivative defining the absolute normalization of the wave function.

Similarly at $M - V = 0$, $F_a^\lambda(r \to M/V') \propto (M - V)^\beta$ with $\beta = 0, 2$. As already remarked, (6.53) requires us to choose $F_a^\lambda(r \to M/V') \propto (M - V)^2$ for $F_c^\lambda(r \to M/V')$ to be finite. Since the boundary condition at $r = 0$ already determined the wave function (up to an overall normalization) the condition at $M - V = 0$ can only be fulfilled by adjusting the bound state mass M accordingly.

(b) $\lambda = 0$, any m

Eliminating $F_a^{\lambda=0}$ we get a second order equation for $F_b^{\lambda=0}$,

$$\partial_r^2(rF_b^0) + \Big[-\frac{1}{r} + \frac{V'}{M-V}\Big]\partial_r(rF_b^0) + \big[\tfrac{1}{4}(M-V)^2 - m^2\big](rF_b^0) = 0 \qquad (\lambda=0) \tag{6.65}$$

Now $F_b^0(r \to 0) \propto r^{\pm 1}$, and we need to choose $F_b^0(r \to 0) \propto r$ for a finite density at the origin. This determines the solution up to its overall normalization.

For F_c^0 to be finite at $M - V = 0$ we must have $F_b^0(r \to M/V') \propto (M - V)^2$. This allows only discrete values of M. Note that this condition is absent if $m = 0$, but does persist as $m \to 0$, as long as $m \neq 0$. In $D = 1 + 1$ dimensions the bound state equation (6.12) similarly has singular solutions at $\tau = 0$ only when $m \neq 0$.

(c) Numerical example

The radial bound state equations (6.64), (6.65) can be readily solved numerically, and the value of M determined which makes the wave function vanish at $M - V = 0$. In Fig. 14 I show some examples for the case of vanishing quark mass, $m = 0$. The Chew-Frautshi type plot in Fig. 14(a) demonstrates that the spectrum resembles that of the dual model, with a linear dependence of M^2 on $J^z = \lambda$ for the leading trajectory, and parallel daughter trajectories corresponding to radial excitations. The $\lambda = 0$ states appear to lie on trajectories with smaller slope. The $F_b^{\lambda=0}(r)$ wave function in Fig. 14(b) is seen to vanish at $M = V(r) = 3.91\sqrt{V'}$, and oscillate at larger radii according to (6.62).

The values of the bound states masses plotted in Fig. 14(a) are given in Fig. 15.

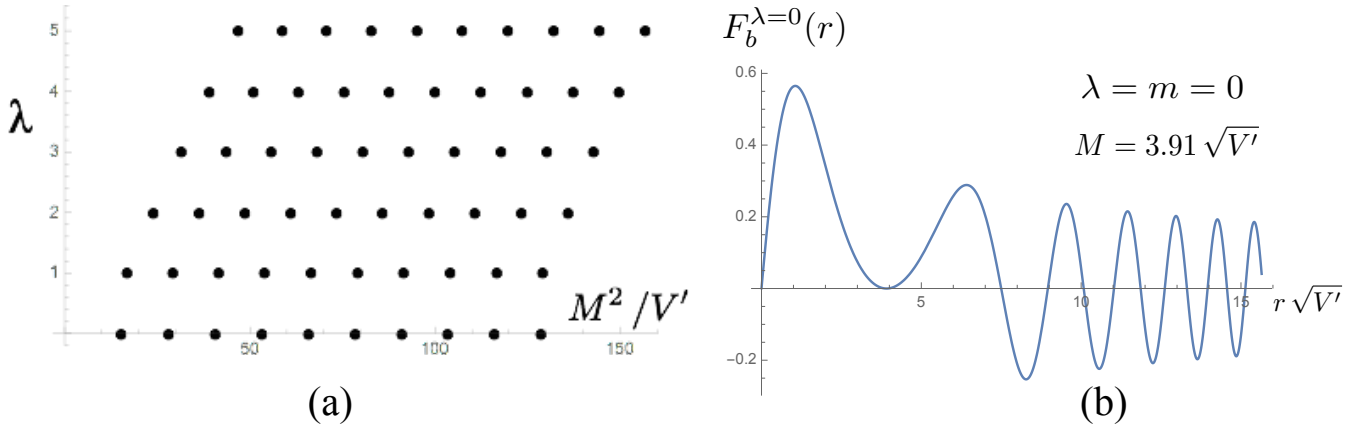

FIG. 14: (a) Mass spectrum of the $D = 2+1$ mesons for $m = 0$, when the only energy scale is $\sqrt{V'}$. (b) Plot of the (arbitrarily normalized) radial wave function $F_b^{\lambda=0}(r)$ of the ground state.

Radial excitation

λ	1	2	3	4	5	6	7	8	9	10
0	3.91	5.29	6.37	7.30	8.11	8.85	9.54	10.18	10.78	11.34
1	4.11	5.40	6.45	7.35	8.16	8.89	9.57	10.20	10.80	11.37
2	4.90	6.02	6.97	7.81	8.57	9.27	9.92	10.53	11.11	11.66
3	5.61	6.60	7.47	8.25	8.97	9.64	10.26	10.85	11.41	11.95
4	6.25	7.15	7.95	8.69	9.37	10.00	10.60	11.17	11.72	12.24
5	6.84	7.66	8.41	9.10	9.75	10.36	10.94	11.49	12.02	12.52

FIG. 15: Masses M of the $D = 2 + 1$ mesons for $m = 0$, in units of $\sqrt{V'}$.

C. Mesons in $D = 3 + 1$ dimensions

1. *Quantum numbers*

The separation of variables in the meson bound state equation (5.66) is less straightforward in $D = 3 + 1$ than in lower dimensions. However, limiting ourselves to the equal mass case $m_1 = m_2 = m$ we can use the results of Geffen and Suura [46], who considered the same equation (multiplied by γ^0 from the left). They studied the spectrum for a phenomenological potential $V(r)$. For future reference I keep $V'' = \partial_r^2 V(r)$ in the radial equations, although $V'' = 0$ for the linear potential (5.59).

Considering the angular momentum $(J, J^z = \lambda)$, parity η_P and charge conjugation η_C, similarly to section V B, the states can be grouped into three "Regge trajectories" [46],

$$\begin{aligned} &\pi\ trajectory: && \eta_P = (-1)^{J+1} && \eta_C = (-1)^J \\ &a_1\ trajectory: && \eta_P = (-1)^{J+1} && \eta_C = (-1)^{J+1} \\ &\rho\ trajectory: && \eta_P = (-1)^J && \eta_C = (-1)^J \end{aligned} \tag{6.66}$$

The names associate to well-known mesons with the corresponding quantum numbers. However, we are considering a single flavor so there is no isospin. It should be easy to added more flavors, whereas the case of $m_1 \neq m_2$ may require more effort. Since we are considering relativistic dynamics, the orbital angular momentum L and spin S are not separately conserved. In the quark model $\eta_P = (-1)^{L+1}$ and $\eta_C = (-1)^{L+S}$, which implies that the combination $\eta_P = (-1)^J$, $\eta_C = (-1)^{J+1}$ should not exist. The quantum numbers (6.66) which are allowed by the meson bound state equation (5.66) agree with the quark model in this respect. Furthermore, the quark model does not allow $J^{PC} = 0^{--}$, and the $J = 0$ state is indeed missing on the a_1 trajectory.

I next quote the results of [46] for each of the above trajectories in terms of the standard spherical coordinates (r, θ, φ) and the spherical harmonics $Y_{J\lambda}$.

2. *π trajectory*

The 4×4 wave functions on the pion trajectory with angular momentum J and $J^z = \lambda$ have the form

$$\Phi_\pi(\boldsymbol{x}) = \Big[-\frac{2im}{M-V}\,\gamma^0\gamma_5 - i\gamma_5 + \frac{2}{M-V}\,\gamma_5\,\boldsymbol{\alpha}\cdot\boldsymbol{\nabla}\Big] F_2(r) Y_{J\lambda}(\theta,\varphi) \tag{6.67}$$

The radial function satisfies the second order differential equation

$$F_2''(r) + \Big(\frac{2}{r} + \frac{V'}{M-V}\Big) F_2'(r) + \Big[\tfrac{1}{4}(M-V)^2 - m^2 - \frac{J(J+1)}{r^2}\Big] F_2(r) = 0 \tag{6.68}$$

which has a structure similar to (6.64) in the $D = 2 + 1$ case and (6.7) in $D = 1 + 1$.

The behavior of $F_2(r)$ at large radii may be found similarly as in section VI A 2(b). For $V(r) = V'r$,

$$\lim_{r\to\infty} F_2(r) = N\,\frac{1}{r}\,r^{-im^2/V'} \exp\Big[i\,\frac{(M-V)^2}{4V'}\Big] \tag{6.69}$$

where N is a constant. The factor $1/r$ compensates for phase space so that the local density is constant,

$$\int d\boldsymbol{x}\,\mathrm{Tr}\left[\Phi^\dagger(\boldsymbol{x})\Phi(\boldsymbol{x})\right] \sim \int dr\, r^2 \frac{8|N|^2}{r^2} \sim 8|N|^2 \int dr \tag{6.70}$$

As in $D = 1+1$ and $D = 2+1$ this allows an interpretation of the constant density as representing a constant rate of string breaking per unit length. The precise meaning and correctness of such an interpretation requires further study.

The radial equation (6.68) allows $F_2(r \to 0) \propto r^\alpha$ with $\alpha = J$ and $\alpha = -J-1$. We must choose $\alpha = J$ for the norm in (6.70) to be integrable at $r = 0$. Similarly $F_2(r \to M/V') \propto (M-V)^\beta$ imposes $\beta = 0,\ 2$ and integrability of the norm at $r = M/V'$ requires $\beta = 2$. Together with the condition at $r = 0$ this can only be satisfied for discrete values of M.

Fig. 16(a) lists the masses $M/\sqrt{V'}$ of the mesons on the π trajectory when the quark mass $m = 0$. The states lie on nearly linear Regge trajectories as shown in (b).

The radial equation (6.68) allows a locally normalizable solution also for $M = 0$, in which case the potentially singular points $r = 0$ and $r = M/V'$ coincide. Massless solutions in the rest frame have four-momenta $P = 0$ in all frames. The $M = 0,\ J^{PC} = 0^{-+}$ state on the pion trajectory might take the role of a Goldstone boson in chiral symmetry breaking. I return to this issue in section VI D 3.

π trajectory, radial excitation

J \	1	2	3	4	5	6	7	8	9	10
0	3.80	5.14	6.23	7.15	7.98	8.72	9.41	10.06	10.67	11.23
1	4.59	5.76	6.74	7.61	8.38	9.10	9.76	10.38	10.96	11.52
2	5.31	6.35	7.25	8.05	8.79	9.47	10.10	10.70	11.27	11.81
3	5.97	6.90	7.73	8.49	9.19	9.84	10.45	11.02	11.57	12.10
4	6.58	7.43	8.20	8.91	9.57	10.20	10.78	11.34	11.88	12.39
5	7.14	7.93	8.65	9.32	9.95	10.55	11.12	11.66	12.18	12.68

(a)

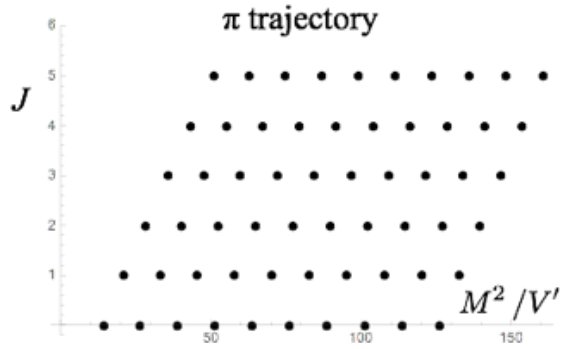

(b)

FIG. 16: (a) Masses M of the mesons on the π trajectory for $m = 0$, in units of $\sqrt{V'}$. (b) Plot of the spin J *vs.* M^2/V' for the states listed in (a).

3. a_1 trajectory

The wave functions on the a_1 trajectory have the form

$$\Phi_{a1}(\boldsymbol{x}) = \Big[\boldsymbol{\gamma}\cdot\boldsymbol{L} + \frac{2m}{M-V}\,\boldsymbol{\alpha}\cdot\boldsymbol{L} - \frac{2}{M-V}\,\gamma_5\,\boldsymbol{\gamma}\cdot\boldsymbol{\nabla}\times\boldsymbol{L}\Big]F_1(r)Y_{J\lambda}(\theta,\varphi) \tag{6.71}$$

Since the orbital angular momentum

$$\boldsymbol{L} = -i\,\boldsymbol{x}\times\boldsymbol{\nabla} \tag{6.72}$$

differentiates only wrt. θ and φ the a_1 wave functions (6.71) are non-vanishing only for $J \geq 1$. The radial function satisfies the second order differential equation

$$F_1''(r) + \Big(\frac{2}{r} + \frac{V'}{M-V}\Big)F_1'(r) + \Big[\tfrac{1}{4}(M-V)^2 - m^2 - \frac{J(J+1)}{r^2} + \frac{V'}{r(M-V)}\Big]F_1(r) = 0 \tag{6.73}$$

The behavior of this equation for large r is the same as the pion equation (6.68). Hence the asymptotic limit $F_1(r \to \infty)$ is the same as that of $F_2(r)$ in (6.69). The leading behaviors at $r = 0$ and $M - V = 0$ are also the same as for the pion trajectory. The numerical results for $m = 0$ are given in Fig. 17.

a_1 trajectory, radial excitation

J	1	2	3	4	5	6	7	8	9	10
1	4.45	5.67	6.68	7.56	8.34	9.06	9.73	10.35	10.94	11.50
2	5.21	6.28	7.20	8.01	8.75	9.44	10.08	10.68	11.25	11.79
3	5.90	6.85	7.69	8.45	9.15	9.81	10.42	11.00	11.56	12.08
4	6.52	7.38	8.16	8.88	9.55	10.17	10.76	11.32	11.86	12.37
5	7.09	7.89	8.62	9.29	9.93	10.53	11.10	11.64	12.16	12.66

(a)

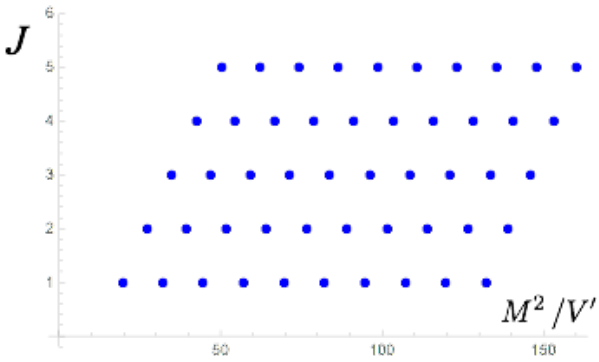

(b)

FIG. 17: (a) Masses M of the mesons on the a_1 trajectory for $m = 0$, in units of $\sqrt{V'}$. (b) Plot of the spin J *vs.* M^2/V' for the states listed in (a).

4. ρ trajectory

The wave functions of states on the ρ trajectory have the form

$$\Phi_\rho(\boldsymbol{x}) \;=\; \boldsymbol{\gamma}\cdot\boldsymbol{\nabla}\left\{\frac{4}{M-V}\Big[-i\tfrac{1}{2}mF_2(r)+\Big(\frac{rG_1(r)}{M-V}\Big)'\Big]Y_{J\lambda}(\theta,\varphi)\right\}+\boldsymbol{\gamma}\cdot\boldsymbol{x}\,G_1(r)\,Y_{J\lambda}(\theta,\varphi)$$

$$-i\boldsymbol{\alpha}\cdot\boldsymbol{\nabla}\big[F_2(r)\,Y_{J\lambda}(\theta,\varphi)\big]+\frac{\boldsymbol{\alpha}\cdot\boldsymbol{x}}{M-V}\Big[\frac{iV'}{r}F_2(r)+2mG_1(r)\Big]Y_{J\lambda}(\theta,\varphi)$$

$$+\not{K}\Big[-\frac{(M-V)^2-4m^2}{2(M-V)}F_2(r)+\frac{4im}{M-V}\Big(\frac{rG_1(r)}{M-V}\Big)'\Big]Y_{J\lambda}(\theta,\varphi)$$

$$+\gamma_5\,\boldsymbol{\gamma}\cdot\boldsymbol{L}\,\frac{2i}{M-V}\,G_1(r)\,Y_{J\lambda}(\theta,\varphi) \tag{6.74}$$

where the radial function $F_2(r)$ is unrelated to the F_2 of the π solution (6.67). The radial functions satisfy coupled second order equations,

$$G_1''(r)+\Big(\frac{2}{r}+\frac{3V'}{M-V}\Big)G_1'(r)+\Big[\tfrac{1}{4}(M-V)^2-m^2-\frac{J(J+1)}{r^2}+\frac{3V'^2}{(M-V)^2}+\frac{3V'}{r(M-V)}+\frac{V''}{M-V}\Big]G_1(r)$$
$$=\frac{imV'}{r}\,F_2(r) \tag{6.75}$$

$$F_2''(r)+\Big(\frac{2}{r}-\frac{V'}{M-V}\Big)F_2'(r)+\Big[\tfrac{1}{4}(M-V)^2-m^2-\frac{J(J+1)}{r^2}-\frac{V'^2}{(M-V)^2}-\frac{2V'}{r(M-V)}-\frac{V''}{M-V}\Big]F_2(r)$$
$$=-\frac{4im}{M-V}\,G_1(r) \tag{6.76}$$

where $V''=0$ for a linear potential. The ρ solutions have twice as many degrees of freedom as the π or a_1 trajectories. The identification of the physical, locally normalizable solutions at $r=0$ and $M-V=0$ requires care due to the coupled equations. I only summarize the discussion in [46].

(a) $r=0$

$$G_1(r\to 0)=\mathcal{O}\left(r^J\right) \qquad\qquad F_2(r\to 0)=\mathcal{O}\left(r^J\right) \tag{6.77}$$

This ensures that the most singular terms of $\mathcal{O}\left(r^{J-2}\right)$ vanish separately in (6.75) and (6.76), and that the norm of the wave function is locally normalizable at $r = 0$. The ratio $\lim_{r\to 0} G_1(r)/F_2(r)$ remains a free parameter (in addition to the overall normalization). Together with the bound state mass M this allows to choose normalizable solutions for G_1 and F_2 at $M - V = 0$.

(b) $M - V(r) = 0$

Assuming $G_1 \sim (M-V)^\alpha$ and $F_2 \sim (M-V)^\beta$ we may first conclude that the terms of $\mathcal{O}\big[(M-V)^{\alpha-2}\big]$ and $\mathcal{O}\big[(M-V)^{\beta-2}\big]$ on the lhs. of (6.75) and (6.76), respectively, must vanish. This allows $\alpha = 1, 3$ and $\beta = \pm 1$. Local normalizability of the norm of Φ_ρ imposes $\beta = 1$. Comparing the powers of $M - V$ on the lhs. and rhs. of (6.75) excludes $\alpha = 3$, leaving $\alpha = \beta = 1$. The normalizability of the G_1 contributions to Φ_ρ imposes a specific behavior of G_1 at $r = R = M/V'$,

$$G_1(r \to R) \;=\; \frac{M-V}{r}\Big[A + B(M-V)^2\Big] + \mathcal{O}\big[(M-V)^4\big] \tag{6.78}$$

$$F_2(r \to R) \;=\; -\frac{F_2'(R)}{V'}(M-V) + \mathcal{O}\big[(M-V)^2\big] \tag{6.79}$$

We may verify that the contributions of $\mathcal{O}\big[(M-V)^0\big]$ to (6.75) vanish. At $\mathcal{O}\big[(M-V)^1\big]$ we find a relation between the coefficient A and $F_2'(R)$,

$$A = \frac{im}{m^2 + J(J+1)/R^2}\, F_2'(R) \tag{6.80}$$

(c) $m \to 0$, $J \geq 1$

The limit $m \to 0$ is interesting because of the chiral invariance of the action when $m = 0$. When $J \geq 1$ we have $A \to 0$ in (6.80), and the rhs. of (6.75) and (6.76) vanish. With the redefinitions

$$\begin{aligned} G_1(r) \;&=\; (M-V)H_1(r) \\ F_2(r) \;&=\; \frac{1}{M-V}\, H_2(r) \end{aligned} \tag{6.81}$$

the equation (6.75) for H_1 becomes the equation (6.73) for the a_1 trajectory (with $m = 0$), and (6.76) for H_2 becomes the equation (6.68) for the pion trajectory. Thus the spectra are parity degenerate in the $m \to 0$ limit when $J \geq 1$ [46].

(d) $J = 0$ state on ρ trajectory

The relation (6.80) is singular when $m \to 0$ and $J = 0$. It is therefore easier to consider the spinless case separately. The $J = 0$ wave functions on the ρ trajectory take the form

$$\Phi_\rho^{J=0}(\boldsymbol{x}) = -\frac{2im}{M-V}\,\boldsymbol{\gamma}\cdot\boldsymbol{x}\, G_2(r) - i\boldsymbol{\alpha}\cdot\boldsymbol{x}\, G_2(r) + \frac{2\big[r^3 G_2(r)\big]'}{r^2(M-V)}\,\mathbb{1} \tag{6.82}$$

The radial function $G_2(r)$ satisfies

$$G_2''(r) + \Big(\frac{4}{r} + \frac{V'}{M-V}\Big)G_2'(r) + \Big[\tfrac{1}{4}(M-V^2) - m^2 + \frac{3V'}{r(M-V)}\Big]G_2(r) = 0 \tag{6.83}$$

Since this equation differs from the $J = 0$ pion equation (6.68) the $J^{PC} = 0^{++}$ and $J^{PC} = 0^{-+}$ mesons do not have the same mass. The absence of parity degeneracy arises from the requirement of local normalizability and implies the breaking of chiral invariance [46]. I return to this issue in section VI D 2.

The behavior of $G_2(r \to \infty)$ may be analyzed as for the pion, giving $|G_2(r \to \infty)| \sim r^{-2}$. It implies a constant asymptotic norm of the wave function, as in (6.70).

The requirement of local normalizability implies

$$G_2(r \to 0) \sim r^0 \qquad\qquad G_2(M - V \to 0) \sim (M-V)^2 \tag{6.84}$$

The numerical values of the masses M for $J = m = 0$ are given in Fig. 18.

ρ trajectory, $J = 0$ radial excitation

	1	**2**	**3**	**4**	**5**	**6**	**7**	**8**	**9**	**10**
$\boldsymbol{J=0}$	4.28	5.57	6.61	7.50	8.30	9.03	9.70	10.33	10.92	11.48

FIG. 18: Masses M of the $J = 0$ mesons on the ρ trajectory for $m = 0$, in units of $\sqrt{V'}$. The ρ trajectory states with $J \geq 1$ are degenerate with those of the same spin but opposite parity on the π and a_1 trajectories.

D. Chiral symmetry

1. *Chiral transformations*

For vanishing quark mass $m = 0$ the QCD action is invariant under (global) chiral transformations[6]. The chiral transformation operator is

$$U_\chi(\alpha) = \exp\left[i\alpha \int d\boldsymbol{x}\, \psi^\dagger(\boldsymbol{x})\gamma_5\psi(\boldsymbol{x})\right] \tag{6.85}$$

where γ_5 anticommutes with all the Dirac matrices. The operator (6.85) transforms the fields as

$$U_\chi(\alpha)\psi(\boldsymbol{x})U_\chi^\dagger(\alpha) = \exp(-i\alpha\gamma_5)\psi(\boldsymbol{x}) \qquad\qquad U_\chi(\alpha)\bar\psi(\boldsymbol{x})U_\chi^\dagger(\alpha) = \bar\psi(\boldsymbol{x})\exp(-i\alpha\gamma_5) \tag{6.86}$$

For a chiral invariant the vacuum, $U_\chi(\alpha)\,|0\rangle = |0\rangle$, the meson state (5.1) is transformed as

$$U_\chi(\alpha)\,|M, \boldsymbol{P} = 0\rangle = \int d\boldsymbol{x}_1\, d\boldsymbol{x}_2\, \bar\psi(\boldsymbol{x}_1)\exp(-i\alpha\gamma_5)\Phi(\boldsymbol{x}_1 - \boldsymbol{x}_2)\exp(-i\alpha\gamma_5)\psi(\boldsymbol{x}_2)\,|0\rangle \tag{6.87}$$

Thus the wave function is transformed into

$$\Phi_\chi(\boldsymbol{x}) \equiv \exp(-i\alpha\gamma_5)\Phi(\boldsymbol{x})\exp(-i\alpha\gamma_5) \tag{6.88}$$

Multiplying the bound state equation (5.66) by $\exp(-i\alpha\gamma_5)$ from both the left and the right we note that if $m_1 = m_2 = 0$ then $\Phi_\chi(\boldsymbol{x})$ is a solution with the same eigenvalue M as $\Phi(\boldsymbol{x})$.

The $m = 0$ states may be classified as chiral even or odd [46] according to the (anti)commutation of their wave function with γ_5,

$$\left\{\gamma_5, \Phi^+\right\} = 0 \qquad\qquad \left[\gamma_5, \Phi^-\right] = 0 \tag{6.89}$$

Chiral invariance implies that $\Phi^\pm$ and $\gamma_5\Phi^\pm$ have the same mass eigenvalues M. If $\Phi^\pm$ has parity η_P and charge conjugation η_C we find from (5.28) and (5.32) that

$$\gamma^0\gamma_5\Phi^\pm(-\boldsymbol{x})\gamma^0 = -\eta_P\,\gamma_5\Phi^\pm(\boldsymbol{x}) \qquad\qquad \gamma^0\gamma^2\left[\gamma_5\Phi^\pm(-\boldsymbol{x})\right]^T\gamma^0\gamma^2 = \mp\eta_C\,\gamma_5\Phi^\pm(\boldsymbol{x}) \tag{6.90}$$

Hence chiral invariance implies the existence of mass degenerate pairs of bound states of opposite parity and opposite (equal) charge conjugation for chiral even (odd) states. Let us see how this is realized for the solutions found above.

2. *Chiral properties of the bound state solutions*

(a) $D = 1 + 1$ dimensions

In the Pauli matrix representation (3.26) of the Dirac matrices $\gamma_5 = \gamma^0\gamma^1 = \sigma_1$, since it anticommutes with both γ^0 and γ^1. In the expansion (6.3) of the wave function $\phi_2 = \phi_3 = 0$ when $m = 0$, according to (6.4). Consequently the chiral even states vanish and

$$\Phi^-(x) = \phi_0(x)\not{k} + \phi_1(x)\,\sigma_1 \qquad\qquad \gamma_5\Phi^-(x) = \phi_1(x)\not{k} + \phi_0(x)\,\sigma_1 \tag{6.91}$$

---

[6] I disregard the $U(1)$ anomaly. The present discussion for a single quark flavor is illustrative and should be easily generalized to the case of two light flavors.

In the limit $m \to 0$ the local integrability of the norm $\mathrm{Tr}\,\Phi^\dagger(x)\Phi(x)$ imposed the discrete spectrum (6.25), with no parity degeneracy. The potential singularity at $M - V = 0$ was due to the contribution $\propto m^2$ in the bound state equation (6.6). Remarkably, chiral symmetry is broken for states with non-singular wave functions in the limit $m \to 0$. When $m = 0$ exactly the norm is regular for any value of the bound state mass M. The continuous spectrum then implies also parity doubling.

(b) $D = 2 + 1$ dimensions

In odd numbers of dimensions there is no "γ_5" matrix that would commute with all the Dirac matrices. This is seen explicitly in the representation (6.41), where we needed all three Pauli matrices to represent γ^0, γ^1 and γ^2. Consequently chiral invariance is not an issue.

(c) $D = 3 + 1$ dimensions

For $m = 0$ the chiral partners of the states on the pion trajectory have wave functions[7]

$$\gamma_5\Phi_\pi(\boldsymbol{x}) = \Big[-i\not{\boldsymbol{x}} + \frac{2}{M-V}\,\boldsymbol{\alpha}\cdot\boldsymbol{\nabla}\Big] F_2^\pi(r) Y_{J\lambda}(\theta,\varphi) \qquad\qquad [\gamma_5, \Phi_\pi] = 0 \tag{6.92}$$

Since the pion trajectory has only chiral odd states their parity partners have $\eta_P = \eta_C = (-1)^J$, *i.e.*, they belong to the ρ trajectory in (6.66). The chiral odd component of the ρ wave function (6.74) is for $m = 0$,

$$\Phi_\rho^- = \Big[-i\boldsymbol{\alpha}\cdot\boldsymbol{\nabla} + \boldsymbol{\alpha}\cdot\boldsymbol{x}\,\frac{iV'}{r(M-V)} - \tfrac{1}{2}(M-V)\not{\boldsymbol{x}}\Big] F_2^\rho\, Y_{J\lambda} = \gamma_5\Phi_\pi \quad \text{for} \quad F_2^\rho(r) = \frac{2i}{M-V}\,F_2^\pi(r) \;\; (J \neq 0) \tag{6.93}$$

The relation between the wave functions of the parity partners is compatible with (6.81). The case $J = 0$ needs to be considered separately because $G_1/F_2^\rho \propto 1/m$ according to (6.80), so that terms $\propto mG_1$ in (6.74) cannot be neglected.

For $m = 0$ the $J = 0$ ρ wave function (6.82) has only a chiral odd component,

$$\Phi_\rho^{J=0,-}(\boldsymbol{x}) = -i\boldsymbol{\alpha}\cdot\boldsymbol{x}\,G_2(r) + \frac{2\big[r^3 G_2(r)\big]'}{r^2(M-V)}\not{\boldsymbol{x}} \tag{6.94}$$

Its chiral 0^{-+} partner on the pion trajectory has the radial wave function

$$\overline{F_2^\pi} = \frac{2i}{M-V}(rG_2' + 3G_2) \tag{6.95}$$

This gives a singular pion wave function since $\overline{F_2^\pi}(r \to M/V') \sim (M-V)^0$. Thus requiring a locally finite norm implies the breaking of chiral invariance in the $m \to 0$ limit: The 0^{++} and 0^{-+} states have distinct masses, as seen also by comparing Fig. 16 with Fig. 18.

The chiral odd states on the a_1 trajectory (6.71) vanish when $m = 0$. The chiral even partners on the a_1 and ρ trajectories have wave functions

$$\gamma_5\Phi_{a1}(\boldsymbol{x}) \;=\; \Big[\gamma_5\,\boldsymbol{\gamma}\cdot\boldsymbol{L} - \frac{2}{M-V}\,\boldsymbol{\gamma}\cdot\boldsymbol{\nabla}\times\boldsymbol{L}\Big] F_1\, Y_{J\lambda} \tag{6.96}$$

$$\Phi_\rho^+(\boldsymbol{x}) \;=\; \Big[\gamma_5\,\boldsymbol{\gamma}\cdot\boldsymbol{L}\,\frac{2i}{M-V} + \boldsymbol{\gamma}\cdot\boldsymbol{x}\Big] G_1\, Y_{J\lambda} + \boldsymbol{\gamma}\cdot\boldsymbol{\nabla}\Big[\frac{4}{M-V}\Big(\frac{rG_1}{M-V}\Big)' Y_{J\lambda}\Big] \tag{6.97}$$

Comparing the coefficients of $\gamma_5\,\boldsymbol{\gamma}\cdot\boldsymbol{L}$ gives

$$G_1 = -\frac{i}{2}(M-V)F_1 \tag{6.98}$$

The differential equation (6.73) ensures that also the other terms agree, $\gamma_5\Phi_{a1} = \Phi_\rho^+$. Both wave functions are non-vanishing only for $J \geq 1$.

---

[7] I add a superscript π (ρ) to distinguish the radial functions $F_2(r)$ of the π (ρ) wave functions.

There is clear evidence that the u and d quarks have small but non-vanishing masses, and that the approximate chiral symmetry is spontaneously broken (CSB) in QCD [47]. An important consequence of CSB is the appearance of a nearly massless Goldstone boson, the pion, with $M_\pi^2 \propto m_u, m_d$. The pion cannot be even approximately described using non-relativistic potential models – the "hyperfine splitting" $M_\rho - M_\pi \simeq 630$ MeV is much larger than $M_\pi \simeq 140$ MeV.

The states discussed above have a regular wave function at the two potentially singular points $r = 0$ and $r = M/V'$. There are also regular solutions with $M = 0$, for which the two points coincide [21]. These states have four-momenta $P^\mu = 0$ in all reference frames. The $J^{PC} = 0^{++}$ state σ on the ρ trajectory discussed in section VI C 4(d) is of particular interest. Since σ has vacuum quantum numbers and vanishing energy when $M = 0$ it can mix with the chiral invariant vacuum to form a ground state that breaks chiral symmetry.

According to (6.82) the wave function of the σ is for $M = 0$, denoting $\hat{\boldsymbol{x}} = \boldsymbol{x}/r$,

$$\Phi_\sigma(\boldsymbol{x}) = -\frac{2}{V'}\,\frac{\left[r^3 G_2(r)\right]'}{r^3}\,\not{x} - irG_2(r)\,\gamma^0\boldsymbol{\gamma}\cdot\hat{\boldsymbol{x}} + \frac{2im}{V'}\,G_2(r)\,\boldsymbol{\gamma}\cdot\hat{\boldsymbol{x}} \tag{6.99}$$

The radial wave function satisfies (6.83),

$$G_2''(r) + \frac{3}{r}\,G_2'(r) + \Big[\tfrac{1}{4}(V'r)^2 - m^2 - \frac{3}{r^2}\Big]G_2(r) = 0 \tag{6.100}$$

The locally normalizable solution at $r = 0$ is

$$G_2(r) = \frac{N}{r^3}\,\exp\big(-i\tfrac{1}{4}V'r^2\big)L^{-2}_{\frac{1}{2}+im^2/2V'}\big(i\tfrac{1}{2}V'r^2\big) \qquad (M=0) \tag{6.101}$$

where L_n^a is a generalized Laguerre function and N an arbitrary normalization constant. Fig. 19 shows a plot of $G_2(r)$ for three values of the quark mass m. The slope $G_2'(r=0) = -N/8$ is independent of m, while the amplitude of the oscillations at large r are $\propto \exp(\pi m^2/2V')/(mr^2)$, increasing exponentially with quark mass. For massless quarks,

$$G_2(r) = \frac{N}{r}\,J_1(\tfrac{1}{4}V'r^2) \qquad (M=m=0) \tag{6.102}$$

where J_1 is a Bessel function.

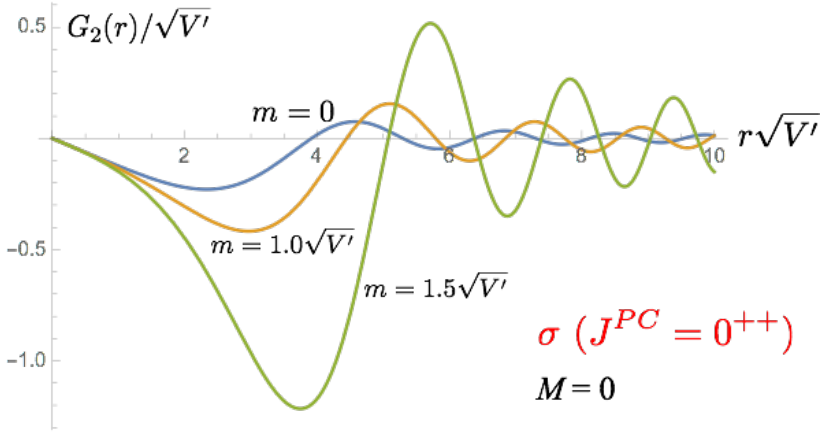

FIG. 19: The radial function $G_2(r)$ (6.101) for the $J^{PC} = 0^{++}$ σ state with $M = 0$ on the ρ trajectory, for three values of the quark mass m and $N = 1$.

The $J^{PC} = 0^{-+}$ state with $M = 0$ on the pion trajectory has the quantum numbers of the Goldstone boson. Its wave function (6.67) is

$$\Phi_\pi(\boldsymbol{x}) = -i\gamma_5\,F_2(r) - \frac{2}{V'r}\,\gamma_5\,\boldsymbol{\alpha}\cdot\hat{\boldsymbol{x}}\,F_2'(r) + \gamma^0\gamma_5\,\frac{2im}{V'r}\,F_2(r) \tag{6.103}$$

The radial function satisfies

$$F_2''(r) + \frac{1}{r}F_2'(r) + \left[\tfrac{1}{4}(V'r)^2 - m^2\right]F_2(r) = 0 \tag{6.104}$$

with the regular solution

$$F_2(r) = N\, e^{-iV'r^2/4}\, {}_1F_1(\tfrac{1}{2} - i\tfrac{m^2}{2V'}, 1, i\tfrac{1}{2}V'r^2) \qquad (M=0) \tag{6.105}$$

where N is an arbitrary normalization constant. In the limits of small and large r,

$$F_2(r\to 0) \;=\; N\left[1 + \tfrac{1}{4}(mr)^2 + \tfrac{1}{64}(m^4 - V'^2)\, r^4 + \mathcal{O}\left(r^6\right)\right] \tag{6.106}$$

$$F_2(r\to\infty) \;=\; N\,\frac{2\sqrt{2}\, e^{\pi m^2/4V'}}{r\sqrt{V'}}\mathrm{Re}\left\{(\tfrac{1}{2}V'r^2)^{-im^2/2V'}\,\frac{e^{i(V'r^2-\pi)/4}}{\Gamma\left[\frac{1}{2}(1-im^2/V')\right]}\right\}\left[1+\mathcal{O}\left(r^{-2}\right)\right] \tag{6.107}$$

For massless quarks,

$$F_2(r) = N\, J_0(\tfrac{1}{4}V'r^2) \qquad (M=m=0) \tag{6.108}$$

Fig. 20 shows a plot of $F_2(r)$ for three values of the quark mass m.

The existence of $M=0$ solutions is interesting, considering the features of spontaneous chiral symmetry breaking. Further studies of bound state interactions (via quark annihilation/creation such as in Fig. 11) are required to understand the properties of these solutions.

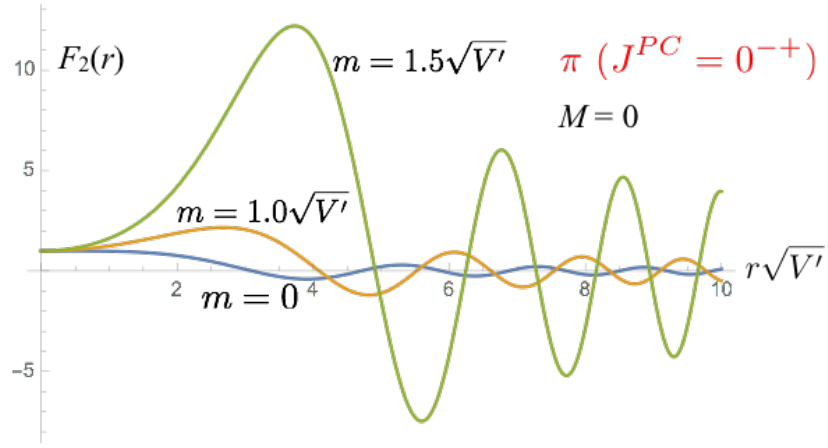

FIG. 20: The radial function $F_2(r)$ (6.105) for the $J^{PC} = 0^{-+}$ π state with $M=0$, for three values of the quark mass m and $N=1$.

VII. FRAME DEPENDENCE

The QCD action is invariant under Poincaré transformations. To address dynamics beyond the mass spectrum, such as form factors or scattering amplitudes, it is necessary to know how bound states transform under boosts, *i.e.*, to know their frame dependence. This is a challenge for spatially extended states because the quantization surface is not invariant under all transformations. An equal time surface is shifted under time translations generated by the Hamiltonian, whereas boosts change the very definition of simultaneity. Consequently part of the Poincaré symmetry of bound states is realized dynamically, through interactions that rearrange their Fock expansion.

In approximations that rely on a power expansion in a fundamental parameter each order of the expansion must have the symmetry of the exact result. The Lorentz invariance of scattering amplitudes at each order in α is a well-known example. Similarly the Born term of an $\hbar$ expansion must be Poincaré symmetric. Demonstrating the symmetry provides a non-trivial check that the Born term is correctly evaluated.

The bound states considered here are not interacting with external forces. Thus the generator $\boldsymbol{\mathcal{P}}$ (2.9) of space translations has no interaction term, and its meson eigenstates with eigenvalue $\boldsymbol{P}$ take the form[8]

$$|E,\boldsymbol{P}\rangle = \int d\boldsymbol{x}_1 d\boldsymbol{x}_2\, e^{i\boldsymbol{P}\cdot(\boldsymbol{x}_1+\boldsymbol{x}_2)/2}\bar{\psi}(\boldsymbol{x}_1)\Phi(\boldsymbol{x}_1-\boldsymbol{x}_2)\psi_\beta(\boldsymbol{x}_2)\,|0\rangle \tag{7.1}$$

In the present approach the generator $\mathcal{H}$ of time translations has a frame-dependent interaction term, given by the classical gauge field boosted from the rest frame similarly as for Positronium in (2.12). The $\boldsymbol{P}$-dependence of the wave function $\Phi(\boldsymbol{x}_1-\boldsymbol{x}_2)$ is determined by the requirement that (7.1) be an eigenstate of the Hamiltonian. Poincaré invariance implies that the energy eigenvalue is $E=\sqrt{\boldsymbol{P}^2+M^2}$, where M is the rest mass of the bound state.

It is useful to gain experience by first considering $D=1+1$ dimensions. The single space dimension allows to solve the bound state equation explicitly for any P. A direct solution is more challenging in higher dimensions, where the absence of rotational symmetry for $\boldsymbol{P}\neq 0$ prevents a separation of variables as in section VI C.

A. Mesons with $\boldsymbol{P}\neq 0$ in $D=1+1$ dimensions

In $D=1+1$ the perturbative $\mathcal{O}(\alpha_s)$ potential is linear, as is the confining potential (5.59). This allows comparing two approaches: (i) the gauge field is treated as an operator with the gauge choice $A^1=0$ (section VII A 1, [48]) and (ii) the classical A^0 potential is boosted analogously to the Positronium case (2.12) (section VII A 2). The gauge choice has a striking effect on the boosted wave function, but both approaches give the same mass spectrum.

1. QED$_2$ bound states with $A^1=0$

The operator version of Gauss' law in QED$_2$

$$-\partial_x^2 A^0(t,x) = e\psi^\dagger(t,x)\psi(t,x) \tag{7.2}$$

allows to express A^0 in terms of the fermion fields. In $A^1=0$ gauge the action then depends on the fermion fields only,

$$S=\int dtdx\,\psi^\dagger\gamma^0\big(i\partial\!\!\!/-m\big)\psi+\frac{e^2}{4}\int dtdxdy\,\psi^\dagger\psi(t,x)|x-y|\psi^\dagger\psi(t,y) \tag{7.3}$$

The action is invariant under Poincaré transformations generated by

$$\begin{aligned}
\mathcal{P}(t) &= \int dx\,\psi^\dagger(t,x)(-i\partial_x)\psi(t,x)\\
\mathcal{H}(t) &= \int dx\,\psi^\dagger(-i\sigma_1\partial_x+m\sigma_3)\psi-\frac{e^2}{4}\int dxdy\,\psi^\dagger\psi(t,x)|x-y|\psi^\dagger\psi(t,y)\\
\mathcal{K}(t) &= t\,\mathcal{P}+\int dx\,\psi^\dagger\big[x(i\sigma_1\partial_x-m\sigma_3)+i\tfrac{1}{2}\sigma_1\big]\psi+\frac{e^2}{8}\int dxdy\,\psi^\dagger\psi(t,x)(x+y)|x-y|\psi^\dagger\psi(t,y)
\end{aligned} \tag{7.4}$$

where the Dirac matrices are represented as in (3.26). These generators satisfy the Lie algebra

$$[\mathcal{P},\mathcal{H}]=0 \qquad\qquad [\mathcal{P},\mathcal{K}]=i\mathcal{H} \qquad\qquad [\mathcal{H},\mathcal{K}]=i\mathcal{P} \tag{7.5}$$

A boost of A^0 gives rise to $A^1\propto A^0$. In order to maintain $A^1=0$ the boost must be combined with a gauge transformation, which is in fact included in the definition of the generator $\mathcal{K}$ in (7.4). The gauge parameter is itself an operator [48],

$$\theta(t,x)=-\frac{e^2}{4}\int dy\,(x-y)|x-y|\psi^\dagger\psi(t,y) \tag{7.6}$$

---

[8] The color algebra is frame independent, so the meson wave function has the (implicit) color structure (5.5) at any $\boldsymbol{P}$.

Since the A^0 potential depends on the separation of the e^+e^- pair, so must the gauge parameter θ.

The bound state (7.1) is an energy eigenstate, $\mathcal{H}\,|E,P\rangle = E\,|E,P\rangle$, provided the wave function satisfies the bound state equation

$$i\partial_x\,\{\sigma_1,\Phi(x)\} - \tfrac{1}{2}P\,[\sigma_1,\Phi(x)] + m\,[\sigma_3,\Phi(x)] = \big[E - V(x)\big]\Phi(x) \tag{7.7}$$

where $V(x) = \frac{1}{2}e^2\,|x| \equiv V'|x|$. The P-dependence of $\Phi(x)$ implied by this equation is consistent with that given by a boost generated by $\mathcal{K}$ [48]. The Lie algebra ensures the correct P-dependence of the energy, $E = \sqrt{P^2+M^2}$.

When $\Phi(x)$ is expanded in a Pauli matrix basis as in (6.3) the coefficients $\phi_2(x)$ of $i\sigma_2$ and $\phi_3(x)$ of σ_3 are not differentiated in (7.7). Expressing them in terms of ϕ_0 and ϕ_1 the 2×2 wave function takes the form

$$\Phi(x) = \phi_0 + \phi_1\sigma_1 - \frac{2m\phi_1}{\tau V'}\sigma_1 \not{\Pi}^\dagger \qquad \Pi = (E - V(x), P) \qquad \tau \equiv \Pi^2/V' = \big[(E-V)^2 - P^2\big]/V' \tag{7.8}$$

where the 2-vector Π is the kinetic momentum ($V = eA^0,\ eA^1 = 0$). The two remaining components of the BSE (7.7) give coupled differential equations for ϕ_0 and ϕ_1. With a change of variables $x \to \tau(x)$ they become (for $x \geq 0$)

$$-4i\partial_\tau\phi_0 = \Big[1 - \frac{4m^2}{\tau V'}\Big]\phi_1 \qquad\qquad -4i\partial_\tau\phi_1 = \phi_0 \tag{7.9}$$

Since these equations are frame independent (*i.e.*, they do not depend explicitly on P), so are $\phi_0(\tau)$ and $\phi_1(\tau)$. The differential equation (6.12) obtained in the rest frame is indeed compatible with (7.9), and the solution is given by (6.13). However, the functional dependence of $\tau(x)$ on x does depend on P. Thus the wave function components $\phi_0(x)$ and $\phi_1(x)$ are frame dependent when expressed as functions of x. In the expression (7.8) for the 2×2 wave function $\Phi(x)$ the kinetic momentum $\Pi(x)$ is explicitly P-dependent.

In section VI A 3 we saw that requiring the rest frame wave function to be locally normalizable at $\tau = 0$ implied $\phi_1(\tau \to 0) \propto \tau$. The same condition ensures that $\Phi(x)$ in (7.8) is regular at $\tau = 0$ in a general frame.

The continuity condition (6.10) requires that either $\phi_0(x=0)$ or $\phi_1(x=0)$ vanishes, depending on the parity η. Since $\phi_0(\tau)$ and $\phi_1(\tau)$ are frame independent, so are the values of τ where they vanish. According to (7.8) $\tau(x=0) = (E^2 - P^2)/V'$, hence we must have $E^2 - P^2 = M^2$ in all frames. The discrete values of the energy E for which the wave function is regular at $\tau = 0$ and continuous at $x = 0$ therefore has the correct dependence on the momentum P.

2. QED$_2$ bound states with a boosted classical gauge field

The Hamiltonian with a classical gauge field (A^0, A^1) is

$$\mathcal{H} = \int dx\,\psi^\dagger\big[-i\sigma_1\partial_x + m\sigma_3 + g(A^0 - \sigma_1 A^1)\big]\psi \tag{7.10}$$

Operating on a state of the form (7.1) we get

$$\begin{aligned}\mathcal{H}\,|E,P\rangle \;&=\; \int dx_1dx_2\,\psi^\dagger(x_1)\Big\{\big[i\sigma_1\overleftarrow{\partial}_1 + m\sigma_3 + gA^0(x_1) - \sigma_1 gA^1(x_1)\big]\sigma_3\,e^{iP(x_1+x_2)/2}\Phi(x_1-x_2)\\ &\qquad -\sigma_3\,e^{iP(x_1+x_2)/2}\Phi(x_1-x_2)\big[-i\sigma_1\overrightarrow{\partial}_2 + m\sigma_3 + gA^0(x_2) - \sigma_1 gA^1(x_2)\big]\Big\}\psi(x_2)\,|0\rangle\\ &=\; E\,|E,P\rangle\end{aligned} \tag{7.11}$$

where $\partial_j = \partial/\partial x_j$. The potentials A^0, A^1 should transform like in (2.12) under the boost from the rest frame (we are boosting the state rather than the field). In the rest frame the (symmetrized) interaction potential is

$$gA^0_R(x_{1R}) = \tfrac{1}{2}V(x_{1R} - x_{2R}) = \tfrac{1}{2}V'|x_1 - x_2|_R = -gA^0_R(x_{2R}) \qquad\qquad gA^1_R(x_{1R}) = gA^1_R(x_{2R}) = 0 \tag{7.12}$$

Lengths are Lorentz contracted in equal-time wave functions. As in (2.13),

$$x_1 - x_2 = \frac{(x_1-x_2)_R}{\cosh\xi} \qquad\qquad \cosh\xi = \frac{E}{M} \tag{7.13}$$

Consequently the potentials in (7.11) are

$$\begin{aligned} gA^0(x_1) &= \cosh\xi\, gA^0_R(x_{1R}) = \tfrac{1}{2}V'\cosh^2\xi\,|x_1-x_2| = -gA^0(x_2) \equiv \tfrac{1}{2}gA^0 \\ gA^1(x_1) &= \sinh\xi\, gA^0_R(x_{1R}) = \tfrac{1}{2}V'\sinh\xi\,\cosh\xi\,|x_1-x_2| = -gA^1(x_2) \equiv \tfrac{1}{2}gA^1 \end{aligned} \tag{7.14}$$

In terms of these potentials and $x = x_1 - x_2$ the bound state condition implied by (7.11) is,

$$i\partial_x\{\sigma_1, \Phi(x)\} = (E - gA^0)\Phi(x) + \tfrac{1}{2}(P - gA^1)[\sigma_1, \Phi(x)] - m[\sigma_3, \Phi(x)] \tag{7.15}$$

The kinetic energy and momentum are

$$\begin{aligned} \Pi^0 \equiv E - gA^0 &= E - V'\cosh^2\xi\,|x| = E\Big(1 - \frac{V'}{M}\cosh\xi\,|x|\Big) \equiv \sqrt{\tau V'}\,\frac{E}{M} \\ \Pi^1 \equiv P - gA^1 &= P - V'\sinh\xi\cosh\xi\,|x| = P\Big(1 - \frac{V'}{M}\cosh\xi\,|x|\Big) = \sqrt{\tau V'}\,\frac{P}{M} \end{aligned} \tag{7.16}$$

This variable τ is related in the same way to the square of the kinetic 2-momentum as its namesake in (7.8),

$$\Pi^2 \equiv (E - gA^0)^2 - (P - gA^1)^2 = V'\tau \tag{7.17}$$

Nevertheless, this function $\tau(x)$ differs from the function $\tau(x)$ defined above in $A^1 = 0$ gauge. For $P = 0$ both reduce to the rest frame function in (6.11).

Expanding $\Phi(x)$ in the basis of Pauli matrices as in (6.3) we find

$$\Phi(x) = \phi_0 + \phi_1\sigma_1 - \frac{2m\phi_1}{\tau V'}\sigma_1 \not{\Pi}^\dagger \tag{7.18}$$

which is identical in form to the expression in (7.8). However, the kinetic 2-momentum $\Pi = (\Pi^0, \Pi^1)$ given in (7.16) as well as τ (7.17) differ from the corresponding variables in $A^1 = 0$ gauge.

The differential equations for ϕ_0 and ϕ_1 are identical in form to those in (7.9). Consequently the solution for $\phi_1(\tau)$ is again given by (6.13), with $b = 0$ for a wave function that is regular at $\tau = 0$. Since $V'\tau(x = 0) = E^2 - P^2$ as in $A^1 = 0$ gauge the energy eigenvalues E have the correct dependence on P.

Fig. 21 compares the x-dependence of the the wave function $\phi_1[\tau(x)]$ (6.13) (with $b = 0$) calculated using the function $\tau(x)$ given by (7.16) (solid blue) and (7.8) (dashed red). The two curves describe the same function, plotted at displaced values of x. The difference between the two expressions for $\tau(x)$ increases with x, since the gauge transformation to $A^1 = 0$ is $\propto x$. This illustrates the gauge dependence of the wave function, corresponding to the same energy eigenvalue (here $M = 3.19\sqrt{V'}$).

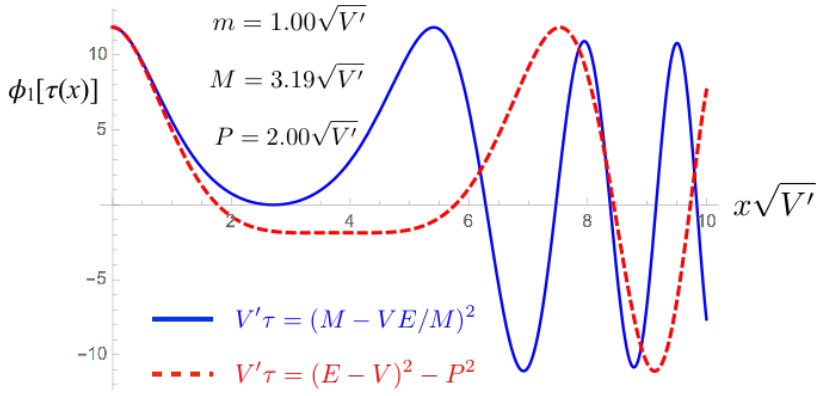

FIG. 21: The wave function $\phi_1[\tau(x)]$ (6.13) ($a = 1,\ b = 0$) for the positive parity ground state in $D = 1+1$, using the function $\tau(x)$ given by (7.16) (solid blue curve) and (7.8) (dashed red curve).

As I noted above, the components $\phi_0(\tau)$ and $\phi_1(\tau)$ of the 2×2 wave function Φ are frame-independent functions of τ (7.16). However, the kinetic momentum $\not{\Pi}^\dagger(P)$ in (7.18) depends explicitly on P. In the rest frame

$$\not{\Pi}^\dagger(P = 0) = \sqrt{V'\tau}\,\sigma_3 \tag{7.19}$$

Using the definition (7.16) of τ it is readily verified that

$$\not{M}^\dagger(P) = (E\sigma_3 + P\, i\sigma_2)\frac{\sqrt{V'\tau}}{M} = e^{-\sigma_1\xi/2}\,\not{M}^\dagger(P=0)\,e^{\sigma_1\xi/2} \tag{7.20}$$

Consequently the explicit dependence of the full wave function $\Phi^{(\xi)}$ on $P = M\sinh\xi$ is

$$\Phi^{(\xi)}(\tau) = e^{-\sigma_1\xi/2}\,\Phi^{(\xi=0)}(\tau)\,e^{\sigma_1\xi/2} \tag{7.21}$$

Since the wave functions are related at the same value of τ their x-dependence Lorentz contracts in the standard way when τ is defined as in (7.16).

The transformation (7.21) of the wave function in finite boosts emerged from the explicit solution of the bound state equation (7.15). In higher dimensions it is less straightforward to solve the bound state equation when $P \neq 0$. It is therefore interesting to ask whether a relation analogous to (7.21) is valid in other dimensions as well. In the next section I show that this transformation is correct in $D = 2+1$, and holds in $D = 3+1$ for some (but not all) states.

B. Mesons with $\boldsymbol{P} \neq 0$ in $D = 2+1$ and $D = 3+1$ dimensions

1. *The bound state equation*

In $D = 3+1$ I choose the z-axis along the bound state momentum,

$$\boldsymbol{P} = (M\cosh\xi, 0, 0, M\sinh\xi) \tag{7.22}$$

The boost of the rest frame field $gA^0_R(\boldsymbol{x}_{1R}) = -gA^0(\boldsymbol{x}_{2R}) = \frac{1}{2}V'|\boldsymbol{x}_1 - \boldsymbol{x}_2|_R$ leaves $A^1 = A^2 = 0$ and

$$\begin{aligned} gA^0(\boldsymbol{x}_1) &= -gA^0(\boldsymbol{x}_2) = \tfrac{1}{2}\cosh\xi\, V'|\boldsymbol{x}_1 - \boldsymbol{x}_2|_\xi \equiv \tfrac{1}{2}gA^0 \\ gA^3(\boldsymbol{x}_1) &= -gA^3(\boldsymbol{x}_2) = \tfrac{1}{2}\sinh\xi\, V'|\boldsymbol{x}_1 - \boldsymbol{x}_2|_\xi \equiv \tfrac{1}{2}gA^3 \end{aligned} \tag{7.23}$$

As in (2.13) the rest frame separation $\boldsymbol{x}_\xi$ is

$$\boldsymbol{x}_\xi = (x, y, z\cosh\xi) \tag{7.24}$$

Requiring that the state (7.1) be an eigenstate of the Hamiltonian

$$\mathcal{H} = \int d\boldsymbol{x}\,\psi^\dagger(\boldsymbol{x})\Big\{ -i\gamma^0\boldsymbol{\gamma}\cdot\boldsymbol{\nabla} + m\gamma^0 + g\big[A^0(\boldsymbol{x}) - \gamma^0\gamma^3 A^3(\boldsymbol{x})\big]\Big\}\psi(\boldsymbol{x}) \tag{7.25}$$

gives the bound state equation for the wave function $\Phi^{(\xi)}(\boldsymbol{x}_1 - \boldsymbol{x}_2)$,

$$i\boldsymbol{\nabla}\cdot\big\{\gamma^0\boldsymbol{\gamma}, \Phi^{(\xi)}(\boldsymbol{x})\big\} = (E - gA^0)\Phi^{(\xi)}(\boldsymbol{x}) + \tfrac{1}{2}(P - gA^3)\big[\gamma^0\gamma^3, \Phi^{(\xi)}(\boldsymbol{x})\big] - m\big[\gamma^0, \Phi^{(\xi)}(\boldsymbol{x})\big] \tag{7.26}$$

where gA^0 and gA^3 are given by (7.23). The absence of spherical symmetry when $\boldsymbol{P} \neq 0$ means that the radial and angular variables cannot be separated similarly as in the rest frame (section VI C). Even in $D = 2+1$ where the Dirac matrices can be represented in terms of the 2×2 Pauli matrices (6.41) the solution of the coupled partial differential equations (7.26) is not obvious.

2. *An ansatz for the boost property of meson wave functions*

Here I shall study only a simple guess of the boost dependence of the wave function, based on the assumption that the quark separation $\boldsymbol{x}$ Lorentz transforms as in classical relativity. The longitudinal direction (denoted $\|$, z or 3) contracts by $\cosh\xi$ whereas the directions transverse to $\boldsymbol{P}$ ($\perp$ or x, y) are invariant. It is then convenient to introduce the boost-invariant longitudinal distance s

$$s = \frac{E}{M}\,z = \cosh\xi\, z \qquad\qquad \partial_z = \cosh\xi\,\partial_s \qquad\qquad \boldsymbol{x}_\xi = (\boldsymbol{x}^\perp, s) \tag{7.27}$$

The boost invariance of $|\boldsymbol{x}_\xi|$ ensures the boost invariance of the variable τ defined by

$$E - gA^0 = E\Big(1 - \frac{V'}{M}|\boldsymbol{x}_\xi|\Big) \equiv \sqrt{V'\tau}\,\cosh\xi \qquad\qquad P - gA^3 = P\Big(1 - \frac{V'}{M}|\boldsymbol{x}_\xi|\Big) = \sqrt{V'\tau}\,\sinh\xi \tag{7.28}$$

The bound state equation (7.26) can be expressed in terms of s, τ and $\boldsymbol{\alpha} \equiv \gamma^0\boldsymbol{\gamma}$, writing $\Phi^{(\xi)}(\boldsymbol{x}^\perp, z(s))$ as $\Phi^{(\xi)}(\boldsymbol{x}^\perp, s)$,

$$\frac{E}{M}\, i\partial_s\big\{\alpha^\parallel, \Phi^{(\xi)}(\boldsymbol{x}^\perp, s)\big\} = \tag{7.29}$$

$$\frac{E}{M}\sqrt{V'\tau}\,\Phi^{(\xi)}(\boldsymbol{x}^\perp, s) + \frac{P}{2M}\sqrt{V'\tau}\big[\alpha^\parallel, \Phi^{(\xi)}(\boldsymbol{x}^\perp, s)\big] - m\big[\gamma^0, \Phi^{(\xi)}(\boldsymbol{x}^\perp, s)\big] - i\boldsymbol{\nabla}^\perp\cdot\big\{\boldsymbol{\alpha}^\perp, \Phi^{(\xi)}(\boldsymbol{x}^\perp, s)\big\}$$

The simplest *Ansatz* for the relation between the boosted and rest frame wave functions is the generalization of (7.21),

$$\Phi^{(\xi)}(\boldsymbol{x}^\perp, s) = \exp(-\tfrac{1}{2}\alpha^\parallel\xi)\Phi^{(0)}(\boldsymbol{x}^\perp, s)\exp(\tfrac{1}{2}\alpha^\parallel\xi) \tag{7.30}$$

The derivative of the wave function wrt. ξ at constant $\boldsymbol{x}_\xi = (\boldsymbol{x}^\perp, s)$ is then given by

$$\partial_\xi\Phi^{(\xi)}(\boldsymbol{x}^\perp, s) = -\tfrac{1}{2}\big[\alpha^\parallel, \Phi^{(\xi)}(\boldsymbol{x}^\perp, s)\big] \tag{7.31}$$

This allows to differentiate the BSE (7.29) wrt. ξ at constant $\boldsymbol{x}_\xi$. Noting that $\big\{\alpha^\parallel, \big[\alpha^\parallel, \Phi^{(\xi)}\big]\big\} = 0$ one gets,

$$\frac{P}{M}i\partial_s\big\{\alpha^\parallel, \Phi^{(\xi)}\big\} = \frac{P}{M}\sqrt{V'\tau}\,\Phi^{(\xi)} - \frac{P}{4M}\sqrt{V'\tau}\big[\alpha^\parallel, \big[\alpha^\parallel, \Phi^{(\xi)}\big]\big] + \tfrac{1}{2}m\big[\gamma^0, \big[\alpha^\parallel, \Phi^{(\xi)}\big]\big] + \tfrac{1}{2}i\boldsymbol{\nabla}^\perp\cdot\big\{\boldsymbol{\alpha}^\perp, \big[\alpha^\parallel, \Phi^{(\xi)}\big]\big\} \tag{7.32}$$

where $\Phi^{(\xi)} = \Phi^{(\xi)}(\boldsymbol{x}^\perp, s)$.

It is straightforward to check whether the ξ-dependence of $\Phi^{(\xi)}(\boldsymbol{x}^\perp, s)$ given by (7.30) is correct near $\xi = 0$. Setting $\xi = 0$ in (7.32) we find a constraint on the rest frame wave function,

$$\Delta \equiv m\big[\gamma^0, \big[\alpha^\parallel, \Phi^{(0)}\big]\big] + i\boldsymbol{\nabla}^\perp\cdot\big\{\boldsymbol{\alpha}^\perp, \big[\alpha^\parallel, \Phi^{(0)}\big]\big\} = 0 \tag{7.33}$$

Check of $\Delta = 0$ in $D = 2+1$ dimensions

Inserting the Pauli matrix expansion (6.45) of $\Phi^{(0)}$ in $D = 2+1$ dimensions it is readily seen that the condition $\Delta = 0$ is satisfied because the coefficient of σ_3 vanishes according to (6.54). The correctness of the boost dependence (7.30) for finite ξ was verified numerically by solving the radial equations (6.55) numerically, thus determining $\Phi^{(0)}$. The transformed wave function (7.30) satisfied the bound state equation (7.29) for general ξ.

Check of $\Delta = 0$ in $D = 3+1$ dimensions

The necessary condition (7.33) for the Ansatz (7.30) to be correct turns out to be satisfied for all values of the angular momentum J, under the following conditions on the quark mass m and $J^z = \lambda$:

- π trajectory: $m = 0$ and $\lambda = 0$.
- a_1 trajectory: $m = 0$.
- ρ trajectory: $\lambda = 0$.

In each case a numerical check similar to the one in $D = 2+1$ showed that the Ansatz (7.30) is correct for general ξ when the $\xi = 0$ condition (7.33) is satisfied. A more systematic study is needed to identify the correct boost dependence of the wave function for the states with $m, \lambda \neq 0$ in $D = 3+1$ dimensions.

VIII. WHAT'S NEW – AND WHAT'S NEXT?

In this concluding section I briefly remark on the novel aspects of the issues discussed in these lectures, and mention some of the (many) opportunities for further studies.

1. QED bound states of lowest order in ħ

The similarity of atomic and quarkonium spectra (Fig. 7) was a main motivation for the bound state studies presented above. The similarity suggests that the QCD description of quarkonia is related to the QED description of atoms. Could perturbative QCD really provide a first principles approach to hadron physics – including confinement? Perturbation theory is our main analytic tool for the Standard Model, so this question merits serious thought.

The perturbative expansion for bound states is less straightforward than for scattering processes (section I 1). Since no single Feynman diagram has a bound state pole we sum a infinite number of ladder diagrams (Fig. 1). The geometric sum builds the classical QED potential $V(r) = -\alpha/r$, which is missing in the $\mathcal{O}\left(\alpha^0\right)$ *in* and *out* states of the perturbative S-matrix.

Positronium at the Born (Schrödinger equation) level is an eigenstate of H_{QED} when the classical A^0 (Coulomb) field of the e^-e^+ pair is used in the Hamiltonian. Since the formulation is based on the relativistic Hamiltonian also bound states in motion can be addressed (section II 4).

This method for deriving the Schrödinger equation as a Born approximation of QED bound states appears to be new. Higher order (loop) corrections in $\hbar$ are calculable in the rest frame using the known methods of NRQED [5, 6]. In an arbitrary frame the expression (1.6) for the S-matrix should be applicable, using the bound states of lowest order in $\hbar$ as asymptotic states. This remains to be demonstrated.

2. Dirac states vs. wave functions

The Dirac equation for an electron bound in an external field specifies a wave function with both positive and negative energy components ($\propto \not{p} \pm m$). The structure of the *state* described by this wave function is rarely discussed. The Klein paradox [9] demonstrates that the Dirac state is composed not only of a single e^-, but also has e^+e^- pairs.

In section III the Dirac bound states were expanded in the basis of free electron and positron Fock states [18]. The Dirac wave function determines the Bogoliubov transform (3.9) of the free creation and annihilation operators. The distribution of the e^+e^- pairs in the ground state (vacuum) depends on the complete set of wave functions.

The energy spectrum specified by the Dirac equation is continuous when the potential $V(r)$ is polynomial in r [10, 49]. This contrasts with the discrete spectrum of the Schrödinger equation and is caused by the presence of positrons in the Dirac states. Potentials that confine electrons repulse positrons. The positrons appear at large r, with kinetic energies that match their (negative) potential energy.

It would be interesting to study the distribution of the e^+e^- pairs in, *e.g.*, the Dirac states of the Hydrogen atom.

3. Confinement from an $\mathcal{O}\left(\alpha_s^0\right)$ classical gluon field

The scale $\Lambda_{QCD} \sim 200$ MeV is central to hadron physics but does not appear in the QCD action. At the level of the classical field equations such a scale can arise only via a boundary condition. The QED potential $V(r) = -\alpha/r$ is given by Gauss' law (1.8) with the boundary condition $\lim_{|\boldsymbol{x}|\to\infty} A^0(\boldsymbol{x}) = 0$. The requirement of Poincaré invariance appears to select a unique homogeneous solution of $\mathcal{O}\left(\alpha_s^0\right)$ (section V C). It is characterized by the strength $\propto \Lambda^2$ of the asymptotic color electric field. Only color singlet $q\bar{q}$ and qqq states are allowed. The $A_a^0(\boldsymbol{x})$ field for each color component of mesons and baryons is given in (5.36) and (5.37), respectively.

The coherent sum of the gauge fields in a color singlet hadron vanishes for all $\boldsymbol{x}$. This non-abelian feature means that the $\mathcal{O}\left(\alpha_s^0\right)$ color field of one hadron does not induce interactions with the quarks of another hadron. Two hadrons interact only when their quark constituents coincide, causing $q\bar{q}$ annihilation/creation as in dual diagrams (Fig. 11).

As in Positronium there is also a Born level, $\mathcal{O}(\alpha_s)$ gluon exchange contribution. Its inclusion with the $\mathcal{O}(\alpha_s^0)$ confining field remains to be addressed. This may be done in the framework of the expression (1.6) for the perturbative S-matrix, with the $\mathcal{O}(\alpha_s^0)$ solutions as *in* and *out* states. A further step would be to consider perturbative loop corrections.

4. Hadron spectra

The meson eigenstates of H_{QCD} with the classical color field (5.36) are readily found when string breaking is neglected. The light $q\bar{q}$ states lie on straight Regge and daughter trajectories (Fig. 16a). Heavy quarkonia have spectra given by the Schrödinger equation with a linear potential.

The states have features of quark-hadron duality (Fig. 13). This may allow to describe the average features of particle production processes even when string breaking is neglected. The wave functions of single hadrons are sensitive to string breaking effects at large color separations. These aspects require further study.

There are $q\bar{q}$ bound states with vanishing mass, $M = 0$ (section VI D 3). They may be relevant for chiral symmetry breaking.

The spectra of mesons with quarks of unequal mass was so far studied only in $D = 1+1$ dimensions [21]. The solutions of the baryon (qqq) bound state equation (5.67) have not been addressed.

5. Boost covariance

The frame dependence of equal-time Positronium states was first given in [8], using the Bethe-Salpeter equation. The present, equivalent formulation is based on boosting the classical gauge field (section II 4). For relativistically bound states I am not aware of any other framework where the transformation of equal-time bound state wave functions under boosts would be explicitly known. The fact that some (albeit not all) wave functions transform according to (7.30) in $D = 3+1$ dimensions is published here for the first time. It is important to identify the correct transformation law for all states.

6. String breaking and hadron loops

The $\mathcal{O}(\hbar^0)$ dynamics must be unitary. The non-linear unitarity conditions cannot be satisfied exactly, only order by order in some expansion. In the absence of string-breaking all states have zero width like in dual models [14, 50]. The string breaking effects described by Fig. 11 can be calculated and is of order $1/\sqrt{N_C}$, where N_C is the number of colors. The square of this diagram gives rise to an $\mathcal{O}(1/N_C)$ hadron loop.

This suggests that unitarity may be satisfied analogously to standard perturbation theory. The expansion parameter would be $1/N_C$ and the loops would be made of hadrons rather than quarks and gluons. For QCD $N_C = 3$ is a moderate number. Nevertheless, the data on hadron dynamics generally supports an approximation scheme based on narrow resonance widths.

7. Scattering amplitudes

The Lorentz covariant expressions for hadron states allows the evaluation of scattering amplitudes, including electromagnetic form factors and parton distributions. So far Deep inelastic scattering was studied only in $D = 1 + 1$ dimensions [21]. The quark distributions were found to be enhanced for $x_B \to 0$, suggesting the contribution of sea quarks. This supports the notion that the relativistic wave functions implicitly describe multiparticle Fock states, similarly as in the Dirac case (section III).

Acknowledgments

I have benefitted from many discussions, particularly with Jean-Paul Blaizot, Stan Brodsky, Dennis D. Dietrich, Matti Järvinen, Jörn Knoll and Stephane Peigné. During the preparation of this material I enjoyed visits of 1-2 months at NIKHEF (Amsterdam), IPhT (Saclay), CP^3 (Odense), GSI (Darmstadt) and ECT* (Trento). I am very grateful for their hospitality, and to the Department of Physics at Helsinki University for my privileges of Professor Emeritus. Travel grants from the Magnus Ehrnrooth Foundation have allowed me to maintain contacts and present my research to colleagues.

---

[1] G. P. Lepage, *"Two-body Bound States In Quantum Electrodynamics"* (PhD thesis), SLAC-R-0212 (1978).
[2] P. Hoyer, arXiv:1402.5005 [hep-ph].
[3] C. D. Roberts, arXiv:1509.02925 [nucl-th].
[4] V. A. Karmanov, Few Body Syst. **55** (2014) 545 doi:10.1007/s00601-014-0846-y [arXiv:1312.2220 [hep-ph]].
[5] T. Kinoshita and G. P. Lepage, *"Quantum Electrodynamics for Nonrelativistic Systems and High Precision Determinations of alpha",* in *Quantum Electrodynamics,* edited by T. Kinoshita (World Scientific, Singapore, 1990), p. 81;
T. Kinoshita, hep-ph/9808351.
[6] M. Baker, P. Marquard, A. Penin, J. Piclum and M. Steinhauser, Phys. Rev. Lett. **112** (2014) no.12, 120407 doi:10.1103/PhysRevLett.112.120407 [arXiv:1402.0876 [hep-ph]];
A. A. Penin, PoS LL **2014** (2014) 074.
[7] S. J. Brodsky and P. Hoyer, Phys. Rev. D **83** (2011) 045026 [arXiv:1009.2313 [hep-ph]].
[8] M. Järvinen, Phys. Rev. D **71** (2005) 085006 [arXiv:hep-ph/0411208].
[9] O. Klein, Z. Phys. **53** (1929) 157. doi:10.1007/BF01339716
[10] M. S. Plesset, Phys. Rev. **41** (1932) 278;
E. C. Titchmarsh, Proc. London Math. Soc. (3) 11 (1961) 159 and 169; Quart. J. Math. Oxford (2), 12 (1961), 227.
[11] G. Zweig, Int. J. Mod. Phys. A **30** (2015) 01, 1430073. doi:10.1142/S0217751X14300737
[12] H. Harari, Phys. Rev. Lett. **22** (1969) 562. doi:10.1103/PhysRevLett.22.562;
J. L. Rosner, Phys. Rev. Lett. **22** (1969) 689. doi:10.1103/PhysRevLett.22.689
[13] S. R. Coleman, Annals Phys. **101** (1976) 239. doi:10.1016/0003-4916(76)90280-3
[14] G. Veneziano, Nuovo Cim. A **57** (1968) 190. doi:10.1007/BF02824451
[15] C. Lovelace, Phys. Lett. B **28** (1968) 264. doi:10.1016/0370-2693(68)90255-4
[16] S. J. Brodsky, In *Brandeis Univ 1969, Proceedings, Atomic Physics and Astrophysics, Vol.1*, New York 1971, p. 91-169;
F. Gross, Phys. Rev. C **26** (1982) 2203;
A. R. Neghabian and W. Gloeckle, Can. J. Phys. **61** (1983) 85.
[17] A. Hansen and F. Ravndal, Phys. Scripta **23** (1981) 1036.
[18] J.-P. Blaizot and P. Hoyer, unpublished.
[19] J. P. Blaizot and G. Ripka, Quantum Theory of Finite Systems (MIT Press, Cambridge, MA, 1986).
[20] F. Sauter, Z. Physik **69** (1931) 742.
[21] D. D. Dietrich, P. Hoyer and M. Järvinen, Phys. Rev. D **87** (2013) 6, 065021 [arXiv:1212.4747 [hep-ph]].
[22] J. S. Schwinger, Phys. Rev. **82** (1951) 664.
[23] M. R. Pennington, J. Phys. G **43** (2016) no.5, 054001 doi:10.1088/0954-3899/43/5/054001 [arXiv:1604.01441 [hep-ph]].
[24] A. S. Kronfeld and C. Quigg, Am. J. Phys. **78** (2010) 1081 doi:10.1119/1.3454865 [arXiv:1002.5032 [hep-ph]].
[25] Y. L. Dokshitzer, In *Vancouver 1998, High energy physics, vol. 1* 305-324 [hep-ph/9812252].
[26] Y. L. Dokshitzer, hep-ph/0306287.
[27] Y. Dokshitzer, PoS CERP **2010** (2010) 001.
[28] F. Siringo, arXiv:1507.05543 [hep-ph].
[29] E. Eichten, S. Godfrey, H. Mahlke and J. L. Rosner, Rev. Mod. Phys. **80** (2008) 1161 doi:10.1103/RevModPhys.80.1161 [hep-ph/0701208].
[30] H. X. Chen, W. Chen, X. Liu and S. L. Zhu, arXiv:1601.02092 [hep-ph].
[31] M. B. Voloshin and L. B. Okun, JETP Lett. **23** (1976) 333 [Pisma Zh. Eksp. Teor. Fiz. **23** (1976) 369];
M. B. Voloshin, arXiv:1601.02540 [hep-ph].
[32] S. Godfrey and N. Isgur, Phys. Rev. D **32** (1985) 189. doi:10.1103/PhysRevD.32.189
[33] A. Selem and F. Wilczek, hep-ph/0602128.
[34] A. M. Cooper-Sarkar, doi:10.3204/DESY-PROC-2009-01/110-2, arXiv:0901.4001 [hep-ph].
[35] S. Okubo, Phys. Lett. **5** (1963) 165;
G. Zweig, CERN-TH-412 (1964);
J. Iizuka, Prog. Theor. Phys. Suppl. **37** (1966) 21.
[36] V. P. Nomokonov and M. G. Sapozhnikov, Phys. Part. Nucl. **34** (2003) 94 [Fiz. Elem. Chast. Atom. Yadra **34** (2003) 189] [hep-ph/0204259].
[37] E. D. Bloom and F. J. Gilman, Phys. Rev. Lett. **25** (1970) 1140;
E. D. Bloom and F. J. Gilman, Phys. Rev. D **4** (1971) 2901.

[38] I. Niculescu, arXiv:1509.07795 [nucl-ex].
[39] K. A. Olive *et al.* [Particle Data Group Collaboration], Chin. Phys. C **38** (2014) 090001.
[40] S. Bethke *et al.*, arXiv:1110.0016 [hep-ph].
[41] V. N. Gribov, Eur. Phys. J. C **10** (1999) 91 [hep-ph/9902279].
[42] Y. L. Dokshitzer, G. Marchesini and G. P. Salam, Eur. Phys. J. direct C **1** (1999) 3 [hep-ph/9812487].
[43] T. Gehrmann, M. Jaquier, G. Luisoni, Eur. Phys. J. **C67** (2010) 57-72. [arXiv:0911.2422 [hep-ph]].
[44] A. C. Aguilar, D. Binosi, J. Papavassiliou and J. Rodriguez-Quintero, Phys. Rev. D **80** (2009) 085018 [arXiv:0906.2633 [hep-ph]].
[45] S. J. Brodsky, S. Menke, C. Merino and J. Rathsman, Phys. Rev. D **67** (2003) 055008 [arXiv:hep-ph/0212078];
G. Grunberg, Phys. Rev. D **73** (2006) 091901 [arXiv:hep-ph/0603135];
C. S. Fischer, J. Phys. G **32** (2006) R253 [arXiv:hep-ph/0605173];
A. Deur, V. Burkert, J. P. Chen and W. Korsch, Phys. Lett. B **665** (2008) 349 [arXiv:0803.4119 [hep-ph]];
A. Courtoy and S. Liuti, Phys. Lett. B **726** (2013) 320 [arXiv:1302.4439 [hep-ph]];
A. Maas, Phys. Rev. D **91** (2015) 3, 034502 doi:10.1103/PhysRevD.91.034502 [arXiv:1402.5050 [hep-lat]].
[46] D. A. Geffen and H. Suura, Phys. Rev. D **16** (1977) 3305.
[47] S. Weinberg, *"The quantum theory of fields. Vol. 2: Modern applications"*. Cambridge University Press (1996);
H. Leutwyler, In *Shifman, M. (ed.): At the frontier of particle physics, vol. 1* 271-316 [hep-ph/0008124].
[48] D. D. Dietrich, P. Hoyer and M. Järvinen, Phys. Rev. D **85** (2012) 105016 doi:10.1103/PhysRevD.85.105016 [arXiv:1202.0826 [hep-ph]].
[49] R. Giachetti and E. Sorace, Phys. Rev. Lett. **101** (2008) 190401 doi:10.1103/PhysRevLett.101.190401 [arXiv:0706.0127 [hep-th]].
[50] S. Mandelstam, Phys. Rept. **13** (1974) 259. doi:10.1016/0370-1573(74)90034-9